Synthesis and characterization of

UiO-67-BNDC MOF

Master Thesis in Chemistry

Lianpao Wu

Department of Chemistry

UNIVERSTITY OF OSLO

[May 2015]

Always strive for truth and wisdom

2015

Synthesis and characterization of UiO-67-BNDC MOF

Lianpao Wu

http://www.duo.uio.no/

Trykk: Reprosentralen, Universitetet i Oslo

Abstract

Metal organic framework is an inorganic-organic hybrid porous material. These materials have attracted many research groups' attentions in the world due to its potential application in gas storage, catalysts and environmental control.

The catalysis group at University of Oslo has discovered a new thermal stable zirconium (IV) MOF UiO-66 (UiO=University of Oslo) since 2008. This MOF was designed based on using the inorganic brick $Zr_6O_4(OH)_4$ and the organic linker 1, 4-benzene-dicarboxylate (**BDC**). Since then, other UiO series MOFs (UiO-67, UiO-68) have been discovered by using different organic linkers (4, 4'-biphenyldicarboxylate (**BPDC**) linker for UiO-67 and 4, 4', 4"-triphenyldicarboxylate (**TPDC**) linker for UiO-68). To find a good MOF material in catalyst and gas adsorption, new organic linkers are demanded.

In this study, the 1,1'-binaphthyl-4,4'-dicarboxylic acid (**BNDC**) linker has been synthesized by six-step synthesis route in five gram level. Meanwhile, a four-step synthesis route was also explored in a milligram scale.

Then a new Zr-MOF with the BNDC linker was prepared by the conventional method. The synthesis of this MOF single crystal was also tested.This new Zr-MOF was characterized by a various methods including powder X-ray diffraction (PXRD), thermogravimetric analysis (TGA), N_2 adsorption, CO_2 and methane adsorption, optical microscope and nuclear magnetic resonance (NMR) spectroscopy, water stability test, pH stability test, and scanning electron microscope (SEM).

This MOF was found to have a well crystallinity, and PXRD study revealed it has a similar structure features as UiO-67. Hence, in this study this MOF will be named as UiO-67-BNDC.

Forword

I would like to thank my supervisor Mats Tilset and co-supervisor Karl Petter Lillerud for giving me an exciting and challenging project to work with. Thanks for give me a great freedom

Furthermore, I want to thank the other members of Mats Group and the Catalysis Group. Especially, I thank Sigurd Øien for help me do the MOF synthesis and characterization. Thank Sharmala, Greag, and Boris help me during the characterization work.

I would like to thank Knut Hylland for the kind suggestion during my study and for invaluable discussion on every Friday meeting.

I would also like to thank Frode Rise, Dirk Petersen and thank Osamu Sekiguchi.

I thank my brother and my parents give me many supports and encourages all this years.

Abbreviations

UiO= University of Oslo

MOF= Porous metal-organic framework

BNDC=1,1'-binaphthyl-4,4'-dicarboxylic acid

PXRD =Powder X-ray Diffraction

TGA=Thermogravimetric Analysis

SEM= Scanning Electron Microscope

NMR= Nuclear Magnetic Resonance

HMBC= Heteronuclear Multiple-bond Correlation

HSQC=Heteronuclear Single-quantum Correlation

COSY=Correlated Spectroscopy

DMF=N,N-dimethylformamide

DMSO =dimethyl sulfoxide

dppf =1,3-bis(diphenylphosphino)ferrocene

NBS= *N*-bromosuccinimide

BPO= benzoyl peroxide

AIBN= azobisisobutyronitrile

TLC= Thin Layer Chromatography

Et=ethyl

eq.=equivalents

h= hour(s)

min=miutes

ppm= parts per million

s= singlet

t= triplet

T= temperature

THF= tetrahydrofuran

Hz=Hertz

J =coupling constant

MS=Mass Spectrometry

Table of Contents

Chapter 1

Introduction

In this chapter, important aspects of Metal organic frameworks (MOFs) are reviewed. A brief introduction of MOFs will be followed by definitions and classifications. Then, the UiO MOFs will be mentioned in particulars. General methods of MOFs synthesis and modification of MOFs are discussed. The emphasis will be on synthesis methods of UiO-67. Common characterization methods of MOF materials are briefly reviewed. The potential applications of various MOF materials will be presented and main focus will be on gas storage. Finally, the aim and outline of the thesis will be presented.

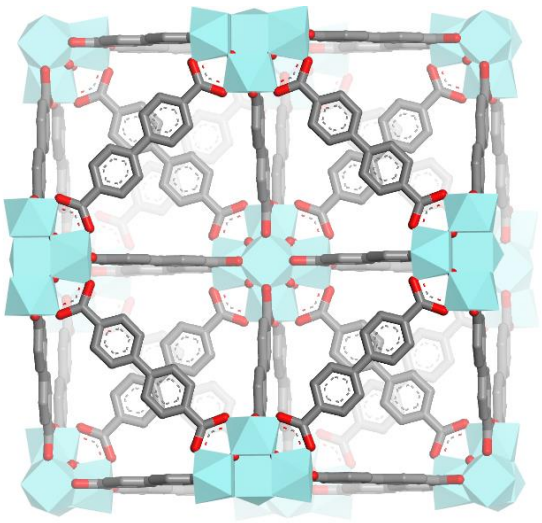

UiO-67

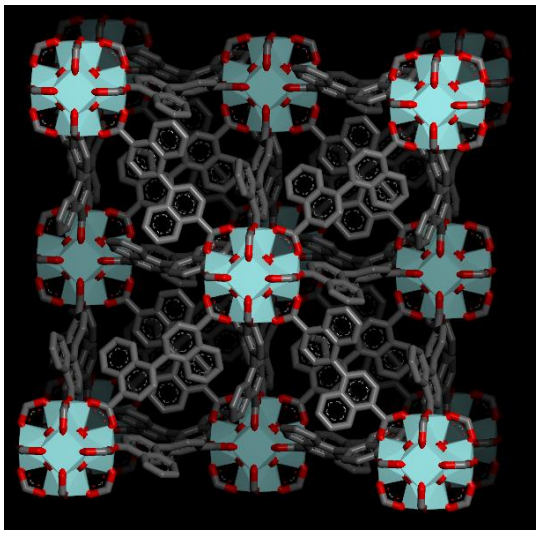

UiO-67-BNDC

1.1 Introduction of Metal Organic Frameworks (MOFs)

1.1.1 Discovery of MOF-5

In modern chemistry, the discovery of MOFs shows the power of combining organic and inorganic chemistry.[1] One of the most important discoveries in the MOF research history is the discovery of MOF-5.Yaghi a scientist from University of Michigan and his coworkers established the first stable Metal organic framework (MOF-5 also called IRMOF-1, **Figure1.1**) with large porosity and this finding proves the MOF structure can still be stable after removal of the guest molecule (solvent). Before that time some scientists thought the MOF structure will collapse after removal of the guest molecule.[2] MOF-5 consists of tetrahedral Zn_4O units as connector and 1, 4-benzenedicarboxylate (**BDC**) as the organic linker. It has a remarkable surface area (up to 2900 m^2/g), stability and porosity at all exceptionally high in 1999. The structure is stable when the solvent is completely removed and temperature up to 300 ℃. Since then these fascinating materials (MOFs) have been investigated by researchers worldwide.[1,3]

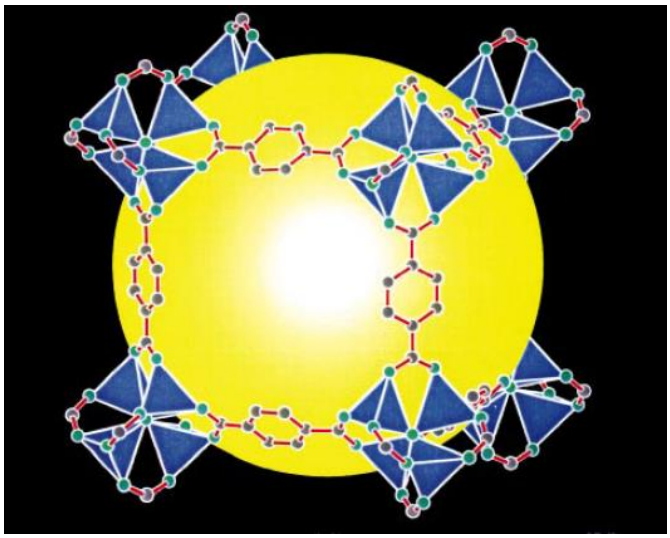

Figure 1.1 View of the structure of MOF-5 (Zn, blue; O, green; C, grey). The yellow sphere indicates a large cavity formed by eight $Zn_4(O)O_{12}C_6$ clusters, and is in contact with the 72 carbon atoms of 12 benzene rings.[3]

1.1.2 Definition of MOF

So what is MOF? According to the IUPAC (International Union of Pure and Applied Chemistry), the definition of MOF is "a Metal-Organic Framework, abbreviated to MOF, is a **Coordination Polymer** (or alternatively **coordination network**) with an open framework containing potential voids." **Coordination networks** are a subset of **coordination polymers**, and MOFs a further subset of **coordination networks**.[4]

A coordination compound continuously extending in 1, 2, or 3 dimensions through coordination bonds is called a **coordination polymer**. One classical example of a1D coordination polymer is the (4,4'-bypyridine-*N*,*N*)-bridged cobalt(II) compound (**Figure 1.2**).[4]

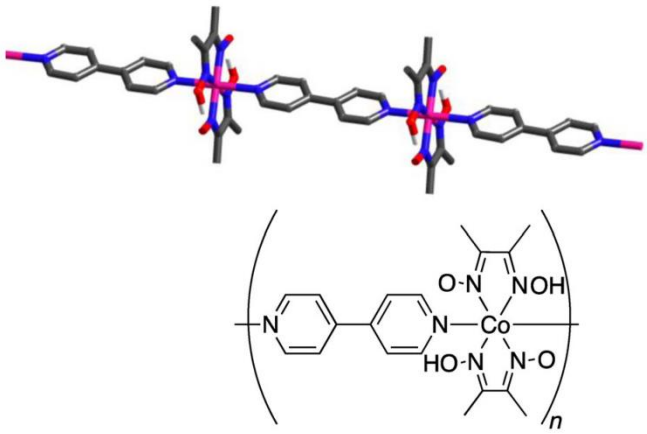

Figure 1.2 An example of a single-chain coordination polymer. Mauve: Co; blue: N; red: O; grey: C; white: H.[4]

A **coordination network** is "a coordination compound extending, through coordination bonds, in 1 dimension, but with cross-links between two or more individual chains, loops or spiro-links, or a coordination compound extending through coordination bonds in 2 or 3 dimensions."[4] One example of a 3D-coordination polymer is the $Cd(CN)_2$•pyz (pyz = pyrazine) polymer (**Figure 1.3**) from Robson's group.[5]

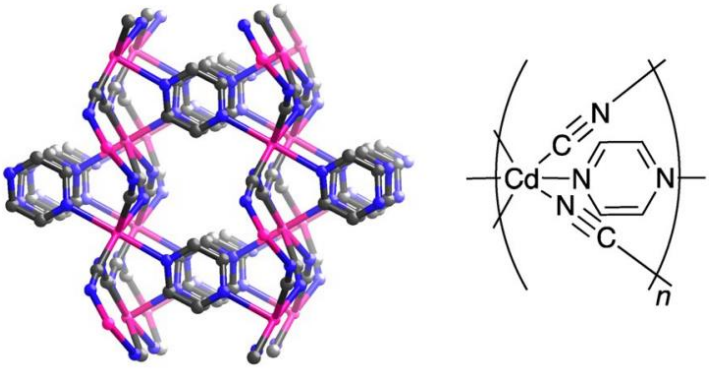

Figure 1.3 The structure of $Cd(CN)_2$•pyz (pyz = pyrazine) polymer. Mauve: Cd; blue: N; grey: C.[4,5]

A MOF is a porous, crystalline material which contains an organic component and an inorganic component. The porosity is one of the important criteria that a material needs to fulfill to be called as a MOF. The organic component is organic molecules which act as linkers in the structure and the inorganic component is metal ions or clusters of metal ions which act as connecters. The structure of the MOF is formed through the formation of coordination bonds between organic linker and metal ions.[4]

There are three generations of MOFs: The first generation MOFs are only stable with the present of the guest molecules in the structures. In other words, they collapse irreversibly when the guest molecules are removed. The second generation MOFs (such as MOF-5) can be stable without guest molecule and they show permanent porosity in the absence of guest molecule. The third generation MOFs that are flexible, dynamic frameworks which respond to

external stimuli (pressure, light, guests, electric field etc.) and change their pores or channels size reversibly.[6]

1.1.3 UiO MOFs

Recently (in 2008), the catalysis group at University of Oslo discovered a new thermal stable zirconium (IV) MOF UiO-66 (UiO=University of Oslo). This MOF was designed based on using the inorganic brick Zr_6O_4 $(OH)_4$ and the organic linker 1, 4-benzene-dicarboxylate (**BDC**). Later, two analogues (UiO-67 and UiO-68) of UiO-66 were prepared by changing the length of the organic linker. The UiO-67 was prepared from the 4, 4'-biphenyldicarboxylate (**BPDC**) linker and UiO-68 from, the 4, 4', 4''-triphenyldicarboxylate (**TPDC**) linker (**Figure 1.4**). The surface area increases as the length of linkers extends. While the thermal stability of the MOFs do not reduce.[7]

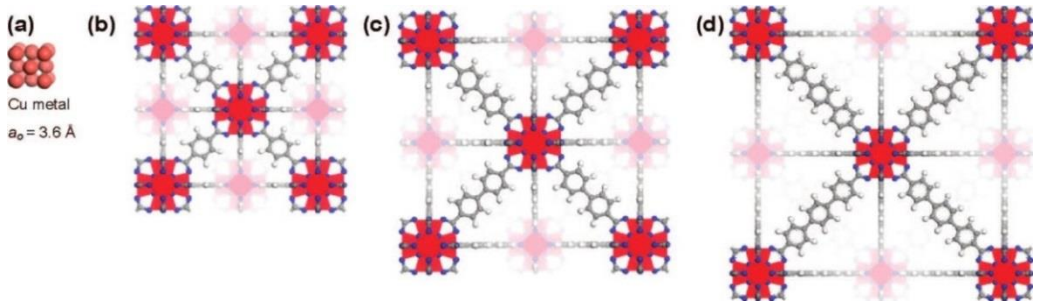

Figure 1.4 Structures of UiO-66 (b), UiO-67 (c) and UiO-68 (d). Zirconium, oxygen, carbon, and hydrogen atoms are red, blue, gray, and white, respectively.[7]

The inorganic brick of UiO MOFs exists two reversibly forms namely, hydrate and dehydrate (**Figure 1.5**). It has been reported that the dehydration of the cluster happens when the temperature arises to 250 ^oC and the full conversion of the hydrated form is obtained at 300 ^oC. Two of the four hydroxyl groups leave together with the hydrogen from the remaining hydroxyl groups to give the Zr_6O_6 inner cluster which is 7-coordinated zirconium.[7]

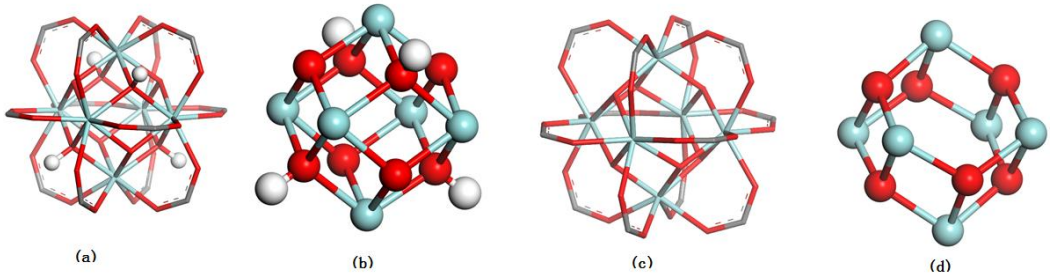

Figure 1.5 Structures of Zr cluster. (a) Hydrated with showing carboxylates, $Zr_6O_4(OH)_4(COO)_{12}$. (b) Hydrated inner core Zr_6- cluster alone, $Zr_6O_4(OH)_4$. (c) Dehydrated with showing carboxylates, $Zr_6O_6(COO)_{12}$. (d) Dehydrated inner core Zr_6- cluster alone, Zr_6O_6. Zirconium, oxygen, carbon and hydrogen atoms are blue, red, gray, and white, respectively.

UiO-66 was found to have high thermal and chemical stability. This high thermal stability of the UiO-66 MOF is due to its inorganic brick. Compared with the previous other MOFs, the UiO MOFs are the highest coordinated MOFs which are 12 coordinated. In the UiO-66

structure, there are two types of pores namely, octahedral cage and tetrahedral cage (**Figure 1.6**).[8]

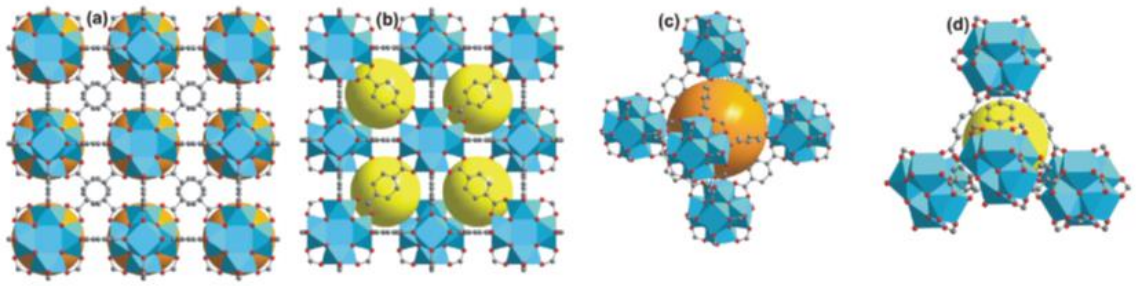

Figure 1.6 Three dimension cubic framework structure of UiO-66 octahedral and tetrahedral cages in the UiO 66 structure (a, b). The octahedral (orange, c) and the tetrahedral (yellow, d) cages. Zr, blue; C, gray; O, red.[8]

1.2 Strategies of MOF synthesis

1.2.1 Building blocks of MOFs

Usually, the inorganic component, also called the secondary building unit (**SBU**), in the MOF synthesis is using well-soluble salts e.g. metal sulfates, nitrate or acetates. To date, there are diverse metal clusters used in the MOF synthesis. Among the most studied MOFs, the inorganic components used are including Zn, Zr, Al, Fe and Cu clusters. The organic linkers commonly are di-, tri-, and tetra- carboxylic acid and azoles (**Figure 1.7**).The reaction usually is performed in a polar organic solvent such as amine (triethylamine) or amide (dimethylformamide, diethylformamide).[9]

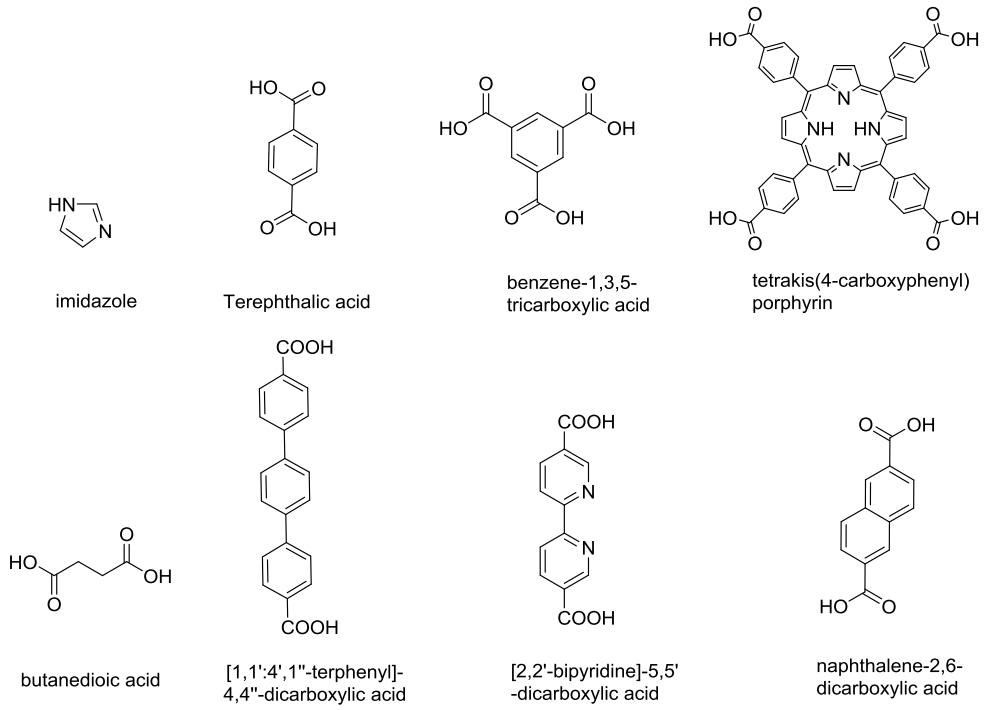

Figure 1.7 Examples of organic linkers used in MOFs synthesis.

1.2.2 Parameters related to the MOFs formation

The construction of MOF is a self-assembly of its building blocks (metal ion and organic linkers). In the early stage of MOF synthesis the methods known to grow high-quality crystal of simple inorganic salts were used. Methods such as slow evaporation of solvents, slow diffusion of one component into the solution of another can reduce the crystal nucleation rate and increase the possibility to get ordered networks.[10]

There are many parameters relate to the MOFs formation such as process parameters (temperature, pressure and reaction time) and compositional parameters (pH, solvents, the ratios of reactants etc.). By adjusting these parameters, the shape and size of MOFs can be manipulated.[11]

1.2.3 Conventional synthesis of MOFs

The reaction carried out by using conventional electric heating is called conventional synthesis (**Figure1.8**).[12] When considering the temperature for MOF synthesis, there are two temperature ranges: solvothermal and nonsolvothermal. The solvothermal reaction is a reaction carried out in a closed vessel under pressure that is above the boiling point of the solvent and the nonsolvothermal reaction is a reaction carried out under normal pressure at or below boiling point of the solvent.[11] After the MOF material was formed, the solvents which were trapped in the pores were removed through exchanging with a low boiling point solvent and heat/vacuum treatment.[12]

There are several advantages of solvothermal method. It is easy to perform and no high requirements on the equipment. Moreover, it is a good method to solve the different solubility issue of inorganic and organic components.

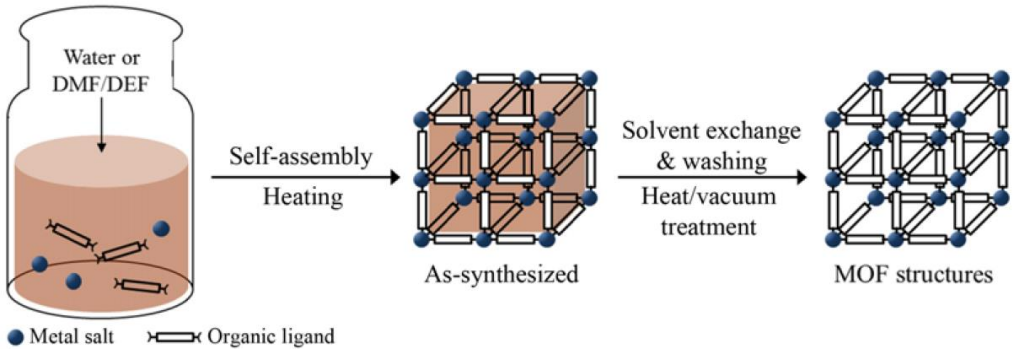

Figure 1.8 Conventional solvothermal synthesis of MOF.[12]

1.2.4 Other methods of MOF synthesis

Except the conventional synthesis, there are many other different synthesis methods for the MOF synthesis such as electrochemical synthesis, microwave-assisted synthesis, mechanochemical synthesis and sonochemical synthesis. By using the different synthesis methods many MOFs with different particle sizes and size distributions were obtained.[11]

1.2.5 UiO-67 synthesis

The UiO series MOFs are usually synthesized by solvothermal synthesis methods.[13] The solvothermal conditions facilitate formation of ordered structure through control the equilibration of bonds formation between inorganic connectors and organic linkers. This is enabled by the weaker coordinative bonds that detach from incoherently assembled build block and reattach the ligands to metal centers to form the thermodynamically more favorable structures.[10]

In order to control the rate of MOF crystal growth, a competing ligand (single-coordinated ligand) also called modulator[14] can be introduced in the synthesis. One early reported work was done by using acetic acid as a modulator in the synthesis of $[Cu_2(ndc)_2(dabco)]$ MOF (ndc^{2-} =1,4-naphthalene dicarboxylyate, dabco =1,4-diazabicyclo[2.2.2]octane).They obtained needle-shaped crystals which were able to be used in the single crystal X-ray diffraction. While the synthesis without modulator gives cubic crystals.[14]

Schaate et al. have reported the first single crystal synthesis of UiO-67 using benzoic acid as a modulator in 2011.They investigated the effect of various amount (from 0 equiv to 30 equiv respect to $ZrCl_4$) of benzoic acid as a modulator in the UiO-67 synthesis. The results indicated with the increasing benzoic acid the crystallinity of MOF gradually improved. They obtained individual microcrystals with edge lengths around 2 μm when 30 equivalents benzoic acid were used in the synthesis. In their study, they also found the addition of modulator could give a high reproducibility of UiO-67.[15]

The proposed mechanism of UiO-66 synthesis has been studied by Nilsen et al., the results revealed the MOF formation experiences three steps (**Figure 1.9**).[16] It starts with the coordination between $ZrCl_4$ and DMF during solvation, follows by exchange of chlorides with carboxylate groups from the linker/ modulator and the hydroxides from water to form the intermediate complexes. Three of these intermediate complexes aggregate to give a triangular intermediate. These triangular intermediates then convert to the connectors, $Zr_6O_4(OH)_4(COO)_{12}$.[13,16]

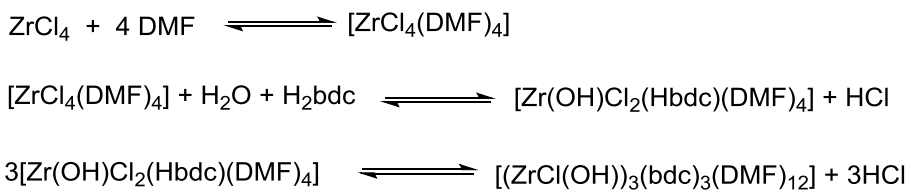

Figure 1.9 Proposed mechanism of UiO-66 synthesis.[13,16]

1.3 Characterization of MOF materials

There are many methods (such as powder X-ray diffraction (PXRD), thermogravimetric analysis (TGA), N_2 adsorption, scanning electron microscope (SEM) and nuclear magnetic resonance (NMR) etc.) can be used in MOF characterization.[14] The general properties of MOF have been studied in this work. The powder X-ray diffraction gives the crystallinity information of MOF material. This method can be applied in qualitative evaluating the

stability of the MOF after different stability tests (such as acid and base stability tests and water stability test).

The porosity, one of the most important properties of MOF, can be checked by sorption measurement through computationally and experimentally. Generally, N_2 adsorption is a typical measurement can be used to obtain the surface area information. Other properties of MOF such as thermal stability and morphology can also be investigated by TGA and SEM respectively. In addition, the ratio between the inorganic clusters and the organic linkers can be achieved by combining the information from TGA and NMR measurements. The theory of each method used in this work will be discussed in the second part of the thesis.

1.4 Potential applications of various MOF materials

The potential application of MOFs is one of the main driving forces for MOF research. Though there are still many challenges in commercialization, great efforts have been devoted to the discovery of potential applications.[17]

Due to the three main properties of MOFs: surface areas, thermal stability and chemical tunability, these materials have a quite broad range applications in gas storage, separation, chemical sensor, catalysis and drug deliver.[1,18-20] Some MOFs shows good thermal stability such as UiO-66 (up to 450 ℃) and MIL-53 (MIL= Materials of Institut Lavoisier, up to 500℃).[7,21] The chemical tunability is reflected in the extraordinary degree variability of both the inorganic building blocks and the organic linkers of their structures.[1]

1.4.1 Gas storage and separation

Up until now, the global warming is still a big problem in the world. Due to the daily global consumption of fossil fuels for transportation, a huge amount of greenhouse gas (carbon dioxide) was release into the atmosphere. Many new technologies have been developed to replace the fossil fuels based energy system. Hydrogen is an attractive clean energy carrier because it is carbon free and abundantly available from water. Moreover, its exceptional mass energy density makes it a good candidate for the new energy system.[22]

However, there is still a challenge to use this gas because of its volatile property under ambient condition. For on-board use, the hydrogen must be compressed which requires very high pressures or store cryogenically. Both of them cost energy and increase the vehicles weights which limit the practical usage of hydrogen as a fuel for vehicles. Therefore, to design low-cost, light-weight materials which can reversibly and rapidly store hydrogen near ambient conditions at a density equal to or even better than liquid Hydrogen will bring some light for practical application.[23]

The remarkable high surface area and chemical tunability of MOFs make them to be some of the most promising candidate materials in the hydrogen storage. The surface area of MOFs around 1500-3000 $m^2 g^{-1}$ is common and that value even higher than 5000 $m^2 g^{-1}$ has also been reported.[24-26] For instance, Yaghi and his coworker reported the MOF-177, which is constructed from a $[Zn_4O_6]^{6+}$ cluster and the organic linker 1,3,5-benzenetribenzoate (BTB), has surface area is close to 6000 $m^2 g^{-1}$. It gives H_2 adsorption capacity of 7.5 wt % at 77 K and 70 bar. [26] Recently year, UiO-66 and UiO-67 have been reported for the hydrogen storage

at high pressure and at liquid nitrogen temperature. The H_2 uptake value at 38 bar and 77 K for UiO-66 is 2.4 mass % and for UiO-67 the value is almost doubled (4.6 mass %) under the same condition. This value is a bit lower than the DOE (Department of Energy USA) target (6 mass %).[23,27]

Not only MOF can be used in hydrogen storage but also can be used in other gases such as CO_2 and methane adsorption. It can be used in removing CO_2 from natural gas and many studies have been reported,[28] such as amine-functionalized MIL-53 (Al) shows high adsorption of CO_2 with respect to CH_4.[29] There are four strategies have been proposed for nature gas adsorption (methane) namely, Liquefied Natural Gas (LNG), Compressed Nature Gas (CNG), Adsorbed Natural Gas (ANG) and Natural Gas Hydrate (NGH). Lower pressures requirement, possibly be operated at room temperature and accessibility to practical application make the ANG technique a more promising method than the other three methods. MOFs materials which have high surface area and structural tunability are ideal potential methane storage media. Kitagawa and coworkers first time reported methane adsorption on Co_2 (4,4'-bipyridine)$_3$(NO_3)$_4$) MOF under pressure in 1997. Later, Yaghi also studied the methane storage capacities of series of isoreticular MOFs. After this early study, various MOF materials were investigated on methane adsorption by various groups.[30]

1.4.2 MOF as catalysts

As mentioned above (**1.1.2**), MOF can also be used in catalysis. Recently years, great efforts have been devoted to artificial photosynthesis. Inspired by the natural photosynthesis, scientists have developed mimic photosynthesis systems and devices to perform the photochemical reactions. MOFs have become potential photocatalysts since late 1990's and early 2000's. The structure of MOFs can promote the diffusion of substrates and products through MOF channels and it makes MOFs an ideal platform to perform artificial photosynthesis.[31] Simple MOFs such as MOF-5,[3] MIL-100 (Fe)[32] or MIL-53 (Fe)[33] have also been studied on photocatalytic oxidative degradation of organic molecules.[31]

The applications of MOF on heterogeneous catalysis in our group have also been studied. Øien et al. reported Pt-functionalized UiO-67 materials (UiO-67-Pt (II), UiO-67-Pt (IV)) which were synthesized through three different methods and tested their reactivity with small-(H_2), medium-(Br_2) and large-size (Toluene-3, 4-dithiol) molecules. They found that these functionalized MOFs have highly accessibility and reactivity to the three above-mentioned molecules.[34]

1.4.3 Other applications

Except the potential applications mentioned above, MOFs materials have other diverse potential applications. Many literatures have been reported the potential usage in luminescent material,[35] biomedicine,[36] heat pump,[37] environmental control, etc..[38]

1.5 The objective and outline of the thesis

There are two main tasks in this project: one is synthesis the organic linker with a sufficient amount (several grams) for the MOF synthesis. The other is synthesis a new Zr-MOF with this new linker and characterized this material with various methods.

In Chapter 2, the principle of various characterization methods will be explained in details. The methods include powder X-ray diffraction (PXRD), thermogravimetric analysis (TGA), N_2 adsorption, CO_2 and methane adsorption, scanning electron microscope (SEM), optical microscope and nuclear magnetic resonance (NMR).

In Chapter 3, the motivation of the organic linkers synthesis and the synthetic strategies of organic linkers will be discussed. The limitations as well as the safety aspect of preparing organic linker for MOF study will also be mentioned (the numbering of each compound will not be shown in this chapter, and only compounds related to the experiments in this work will be numbered in the further chapters).

In Chapter 4, the synthesis routes of organic linkers will be discussed and the main focus is put on the **BNDC** linker synthesis. Three synthetic routes of **BNDC** will be presented and compared. Some reaction mechanisms will also be discussed.

In Chapter 5, the synthesis, structure and thermal stability, N_2 adsorption, CO_2 and methane adsorption of this UiO-67-**BNDC** MOF will be presented. The impacts of modulator in the synthesis of this MOF single crystal will be discussed.

In Chapter 6, the conclusions and outlook of this work will be presented.

In Chapter 7, the experimental details of organic linker synthesis and MOF synthesis together with all the experimental data will be presented.

Chapter 2

Theory of MOF characterization methods

In the preceding chapter, methods include PXRD, TGA, Gas adsorption, SEM, Optical microscope, NMR etc. have been mentioned in the characterization of MOF materials. This chapter will continue to elucidate the principles of these different methods. The main focus will be put on elucidating the first four methods. It will end up with a summary of applications of these methods in this work.

2.1 Powder X-ray diffraction (PXRD)

2.1.1 Diffraction of X-ray

Powder X-ray diffraction is a technique using X-ray diffraction on specimen to give structures information of materials. Powder X-ray diffraction can be used in two main areas: determination of the structure and fingerprint characterization of crystalline materials.[39]

There are two different methods to generate X-rays. One is X-ray tube, which is a conventional X-ray source in a laboratory of any size. The second is a much more expensive and advanced X- ray source-the synchrotron. The former usually has a low efficiency, and their brightness. The latter is extremely bright nearly ten times than that of conventional X-ray source. The brightness can be measure as a photon flux which expressed as a number of photons per second per unit area. The intensity of beam means the total number of photons leaving the target. Usually, the diffraction phenomena are no principal difference by using either of two sources, except for the highly intense peaks in the conventionally X-ray spectrum are absent in synchrotron X-ray spectrum. Because of the photon energy in synchrotron X-ray distributes continuously.[40]

The information in the powder X-ray diffraction can be achieved via the well-known Bragg' law: $n\lambda = 2d\sin\theta$ (**Figure 2.1**). Where λ is the wave length of the X-ray, d is the interplanar spacing of parallel lattice planes (also called Miller planes and the d is noted as $d_{h, k, l}$). The angle between incident beam and lattice plane is θ, and the angle 2θ which is called the diffraction angle is the angle between incident and scattered X-ray beams. In order to have diffraction, the Bragg' law must be fulfilled. PN+NQ=n λ is the condition to satisfy the Bragg's Law.[39] The n is called the order of reflection, which is an integer number. It means the Bragg condition with the same d-spacing and 2θ angle can be satisfied by integer times of X-ray wavelengths (energy).[41]

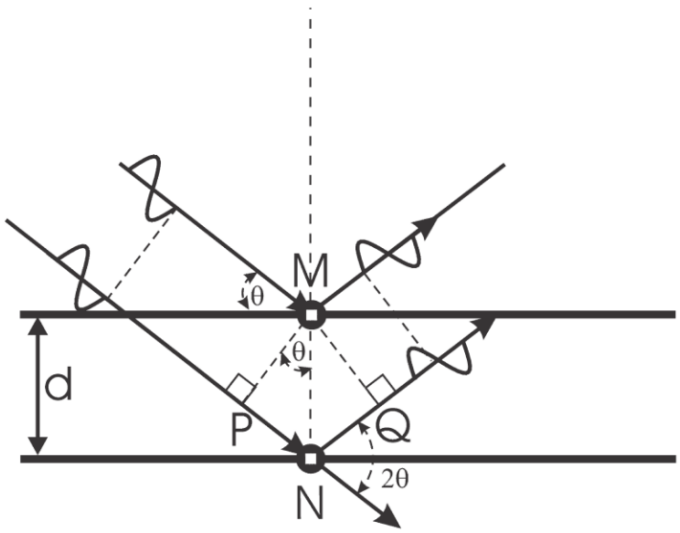

Figure 2.1 Geometrical description of Bragg' law.[39]

In a X-ray diffraction there are three main parameters (**Figure 2.2**) namely intensity *I*, the width of a diffraction peak which is measured by its full width at half maximum (FWHM), and Bragg angle θ where the peak is observed. For perfect crystals with prefect instrumentation gives a peak as the dark straight vertical line in **Figure 2.2**. Usually, a diffraction peak is a broadened peak as shown in **Figure 2.2**. The broadening can be caused by many effects, including imperfect crystal conditions (strain, finite size etc.); instrumental conditions, such as X-ray beam size, detector resolution etc.; and ambient conditions such as atomic thermal vibration. The highest point of the peak gives the maximum intensity of the peak I_{max}. The total diffraction energy of a diffracted beam for a peak is the area under the curve of the peak.[41]

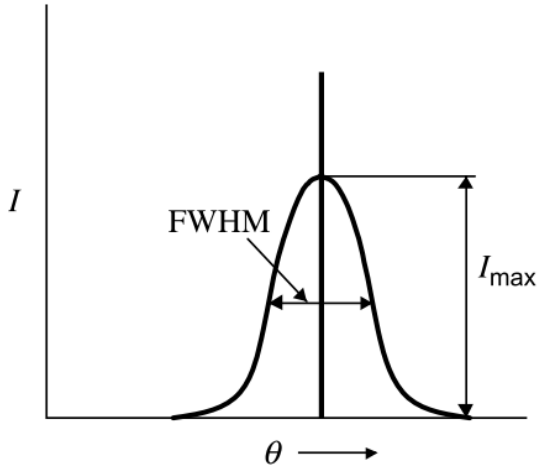

Figure 2.2 The diffraction peak at the θ angle.[41]

2.1.2 Interpretation of PXRD pattern

Each crystalline phase has a unique powder diffraction pattern which can act as a fingerprint for the phase. It can be used to distinguish the same compound with different structure (such as TiO_2) and different compounds with the same structure (such as NaCl and KCl). Hence, phase identification is a quite useful application of PXRD in the sample qualitative analysis.[39]

The Powder X-ray diffraction is a common methods used in MOF to check if the desire phase was present. The X-ray diffraction can provide about the atomic arrangement information in materials with long-range order, short-range order, or no order at all, such as gases, liquids and amorphous materials. The crystalline material gives a set of discrete intensity peaks (called Bragg reflections) each of which has a specific intensity and location in the spectrum (**Figure 2.3**) corresponding to various lattice planes based on the Bragg law: $n\lambda = 2d\sin\theta$. While the amorphous materials (such as glass) and liquid materials do not have long range-order as crystal does, but has a narrow distribution of atomic distance due to the tightly packing of the atoms. Each of them usually gives a broad background peak in the spectrum. A monatomic gas has no order at all. Its PXRD pattern is a curve with the intensity drops continuously with the increase of the 2 θ angle.[41]

As the PXRD patterns shown in **Figure 2.3**, the amorphous solid with crystallinity gives a PXRD pattern with sharp peaks from crystalline phase and a broad background from the

amorphous phase. Similarly, the crystal with air scattering sample gives sharp peaks together with an air-scattering background.[41]

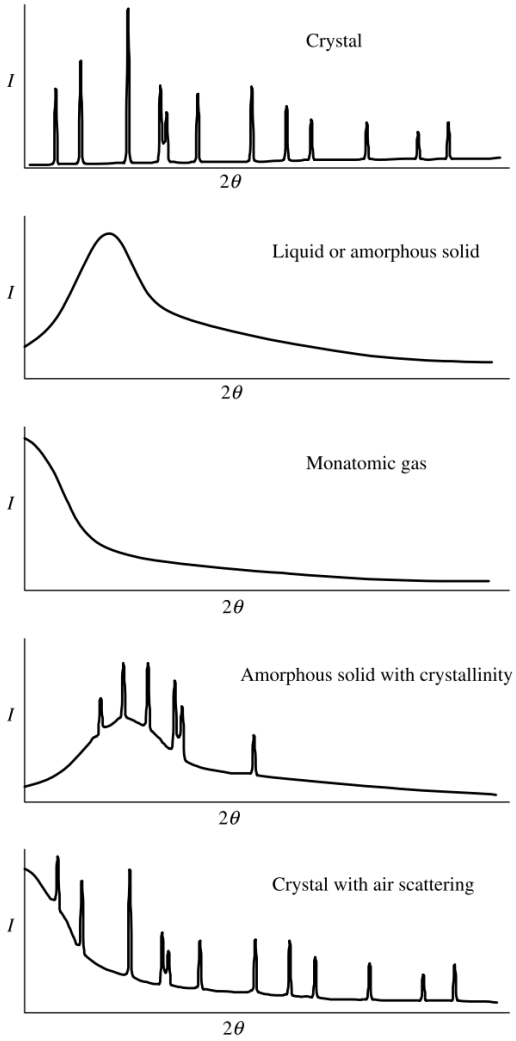

Figure 2.3 Powder X-Ray diffractions of crystalline material, amorphous solid, monatomic gas and their mixtures.[41]

The powder X-ray diffraction obtained from powder sample which is crystalline is an analogous to its single crystal pattern with the incident beam coming from every possible angle. The single crystal X-ray diffraction can be used for analysis the structure by mapping electron density of the structure. But for PXRD it is hard to quantitatively evaluate the samples.[13]

In a PXRD pattern, the number of counts per second, full widths at half maximum (FWHM) and signal-to-noise ratio values can be used to qualitatively evaluate the samples. The **Figure 2.4** gives a PXRD pattern of pure UiO-67. From Bragg equation, this pattern has discernible peaks from all allowed reflection. The peaks are corresponding to Miller planes (see 2.1.1) where h, k, l are all odd or even. While diffraction from other lattice planes are cancelled out due to the destructive interference. The peaks at high 2 θ angles are related to the lattice planes of small d (see 2.1.1) and vice versa at low 2 θ angle. [13]

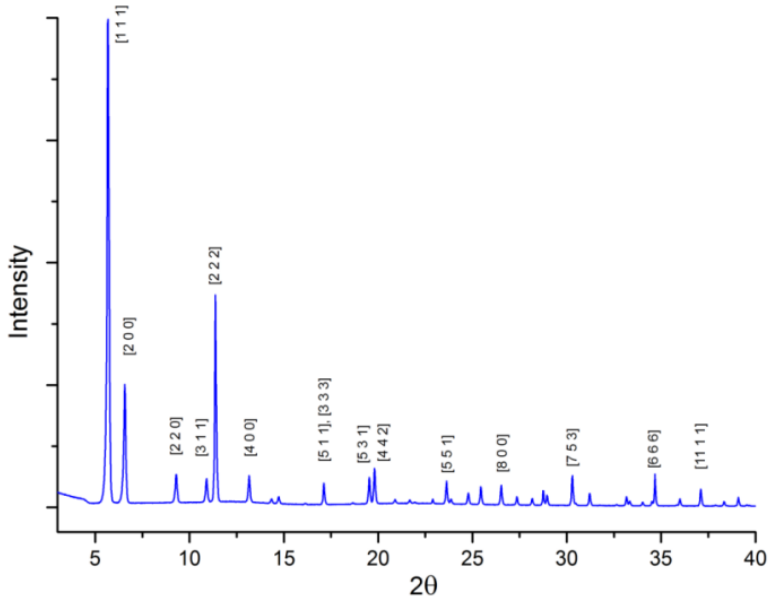

Figure 2.4 A Powder X-ray diffraction spectrum of UiO-67.[13]

2.2 Thermogravimetric analysis (TGA)

2.2.1 Definition and Instrumentation

Thermogravimetric analysis (TGA) or thermogravimetry (TG) is a thermal analysis technique in which studies the mass change (gain or loss) of materials as a function of increasing of temperature (heating rate is constant) in scanning mode, or as a function of time (mass loss is constant and/or temperature is constant) in isothermal mode.[42]

Normally, the thermogravimetric analysis instruments are consisted of a precision balance and a furnace which is programmed for a linear rise of temperature with time. It can provide information about both physical (crystalline transition, absorption, adsorption, desorption, etc.) and chemical (chemisorption, decomposition, oxidative degradation, solid-gas reactions etc.) phenomena of the samples during the measurements.[42] TGA can be coupled with other analysis instruments such as mass spectrometers (TG-MS), Fourier transform infrared spectrometers (TG-FTIR) and gas chromatographs (TG-GC). When TGA combines Differential Scanning Calorimetry (DSC) – Heat Flow in the sample measurement, it can give information about the process (endothermic or exothermic).[43]

2.2.2 Interpretation of TGA curve

TGA curves are recorded using a thermobalance (which typically includes an electronic microbalance, a furnace, a temperature programmer and an instrument for simultaneously recording the outputs from these devices) and they are usually plotted as the mass change against temperature (T) or time (t). A TGA curve of a one-stage reaction process in the scanning mode is shown in **Figure 2.5**.[43] There are two temperature T_i (procedural decomposition temperature) and T_f (final temperature) in this curve. T_i is the lowest

temperature at which the onset of mass change can be detected under given experimental conditions. T_f is the lowest temperature by which there is no weight change of the sample can be detected. The reaction interval is the temperature difference between T_f and T_i. A plateau is the region of the TG curve where the weight is constant. This gives the thermal stability information of the sample under given conditions. Thermal stability means when the temperature arises to a certain degree, the property of the sample will have no change which means no decomposition happens.

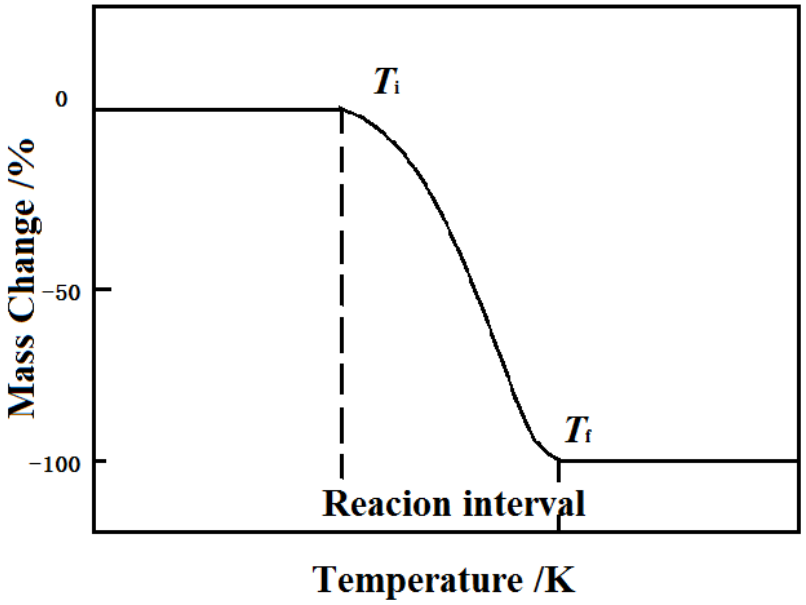

Figure 2.5 Schematic of one-stage reaction process TG curve. [43]

There are 7 different types of TG curves according to their shapes (**Figure 2.6**).[43] Type A curve shows no mass change over the entire range of temperature. This means the decomposition temperature for the sample is greater than the maximum temperature of the instrument under the experimental conditions. Type B curve shows a large initial mass loss followed by mass plateau. It means the sample is volatile and evaporation happens under the given condition. Type C is a single-stage decomposition reaction curves. Type D is a multi-stage decomposition process curve in which the reaction steps are clearly resolved. Type E is a multi-stage decomposition process curve in which the reaction steps are not well resolved. Type F curve shows the mass increase may due to the materials interact with atmosphere (such as surface oxidation). Type G is a curve shows multiple reactions one after another. For example, surface oxidation followed by decomposition of the reaction products.[43]

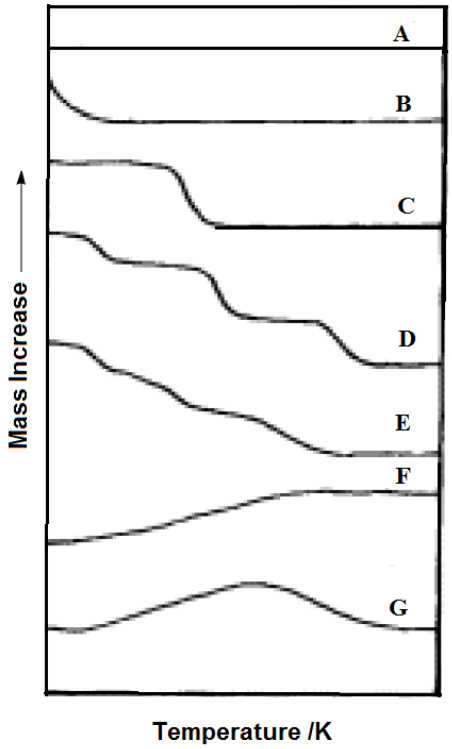

Figure 2.6 Classification of TG curves.[43]

In addition, many parameters (i.e. heating rate, sample weight, geometry of the crucible, atmosphere, etc.) may affect the shape of a correct thermogravimetric curve for a sample.[42]

TGA is a very useful tool in characterizing MOF materials. It can be used to characterize the decomposition and thermal stability of MOFs under a various conditions and to study the thermodynamic processes occurring in the MOFs.

The weight/mass loss in TG can be used to help determine the composition of sample. In the MOF characterization, the weight/ mass loss gives the information of the linker occupancy in the MOF structure by comparing the experimental data and theoretical value. It can also give the information about the amount of solvent in the MOF. For example, the TGA plots of UiO-66 (**Figure 2.7**) shows by using different modulator in the synthesis can have different the missing linker in the structure. In the perfect UiO-66 MOF structure the Zr: BDC linker is 1:1. Weights were normalized with respect to the ZrO_2 residue left after the heating treatment.[44]

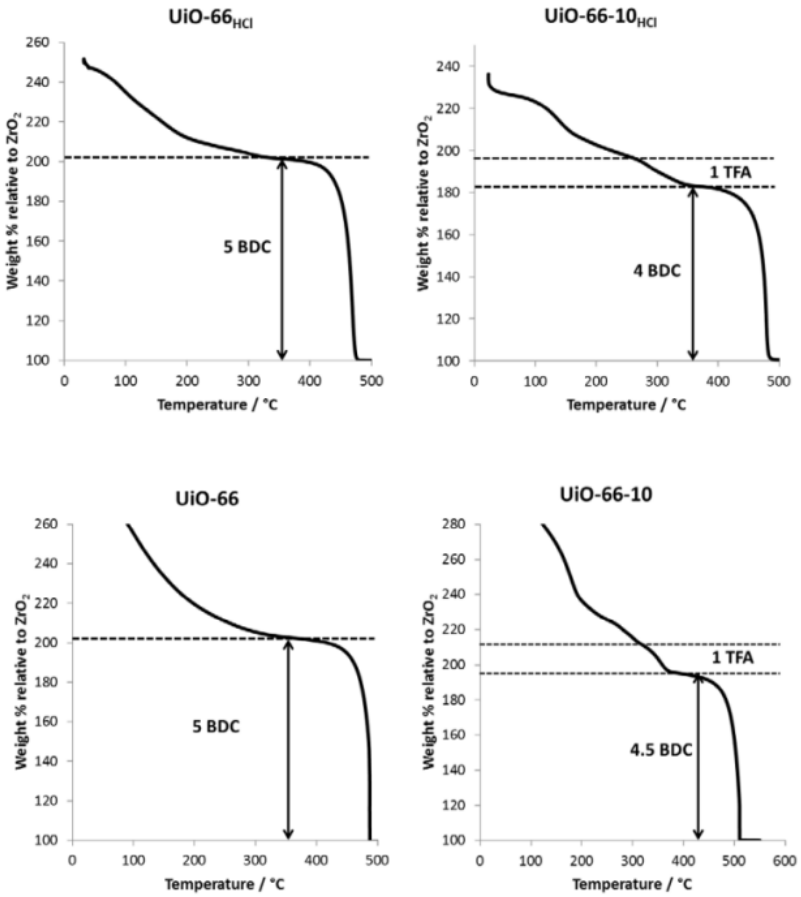

Figure 2.7 TGA of UiO-66_{HCl} (1 equiv HCl), UiO-66-10_{HCl} (1 equiv HCl and 10 equiv TFA), UiO-66, UiO-66-10 (10 equiv TFA), indicating the weight loss corresponding to different amounts of linkers.[44]

2.3 Gas adsorption

2.3.1 Adsorption Isotherms

Adsorption is the enrichment of atoms, ions or molecules in the vicinity of an interface (i.e. the interfacial layer or the adsorption space). There are two types of adsorptions: physical adsorptions and chemical adsorption. The former also called physisorption involves weak interaction (eg.Van der Waals- interaction) between the adsorate and adsorbent, the latter called chemisorption is an adsorption that the adsorate forms one or more chemical bond (s) with adsorbent. The absorbent is the substance on which has an adsorption phenomenon. Adsorate is the substance in the adsorbed state and adsorptive is adsorbable substance in the fluid phase. [45]

Adsorption is usually described through isotherms, which is the relationship between the amount adsorbed and the equilibrium pressure, or concentration. The isotherm is usually plotted as absorbed volume of adsorate (gas) per mass of absorbent (solid) against relative pressure (p/p_0) at given temperature of measurement. The pressure of the gas is p and the

saturation vapor pressure of adsorptive at the given temperature of measurement. When an absorbent is exposed to gas with some definite pressure in a closed space, it begins to adsorb the gas. During this process the pressure of the gas decreases and the weight of the absorbent increase. After a time, the pressure becomes a constant and correspondingly, the weight of absorbent stops increasing. Thus, the amount of gas in the absorbent can be calculated.[46] For example, the N_2 adsorption and desorption isotherm of UiO-67 were shown in **Figure 2.8**. In this isotherm the adsorbed volume of standard state nitrogen (0 ^oC, 1.0 atm) per mass of sample (V_a ($cm^3(STP)g^{-1}$)) is plotted against relative pressure (p/p_0). This isotherm can be used to estimate the internal volume and surface area of UiO-67.[13]

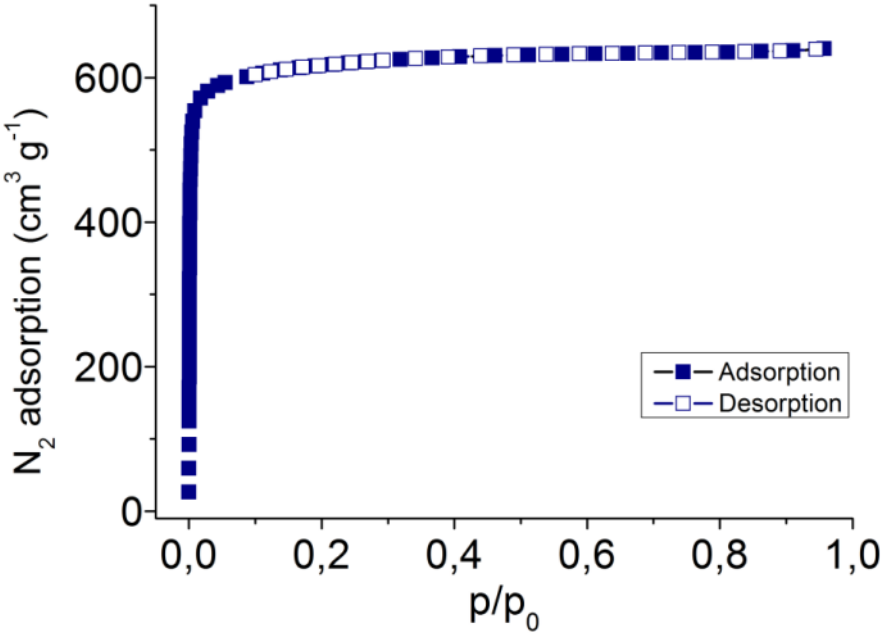

Figure 2.8 N_2 adsorption and desorption isotherm of UiO-67.[13]

The majority of physical adsorption isotherms recorded in the literature may be divided into nine groups (**Figure 2.9**). [45] They have various characteristic shapes which can give useful preliminary information about the pore structure of the absorbent before precise data have been calculated.

The absorbent has narrow micropores (micropore is a pore size < 2 nm) exhibits the type I (a) shape and the absorbent has wider micropores shows type I (b) shape. Type II is corresponds to a non-porous or a macroporous (macroporous is a pore size > 50 nm) adsorbent. Type II (a) is a complete reversible desorption-adsorption isotherm (i.e. no adsorption hysteresis which happens when adsorption and desorption deviate from one another). It indicates monolayer-multilayer adsorption on an open and stable surface. Type II (b) shows a narrow hysteresis loop due to the inter-particle capillary condensation. Type III is the shape of a non-pours or macroporous adsorbent on which is a weak adsorbent-absorbate interactions. Type IV is related to mesoporous (pore size between 2 nm and 50 nm) adsorbents. Type IV (a) which has a hysteresis loops, the lower branch is adsorption and the upper branch is desorption. Type IV (b) is completely reversible which is related to a few ordered mesoporous structures. Type V is associated with a microporous or mesoporous adsorbent on which is a weak adsorbent-absorbate interactions. Type VI is indicative of layer-by-layer adsorption on a highly uniform

surface. Except the adsorption isotherm mentioned above, other shapes (called composite) are sometimes found as a combination of these shapes. [45]

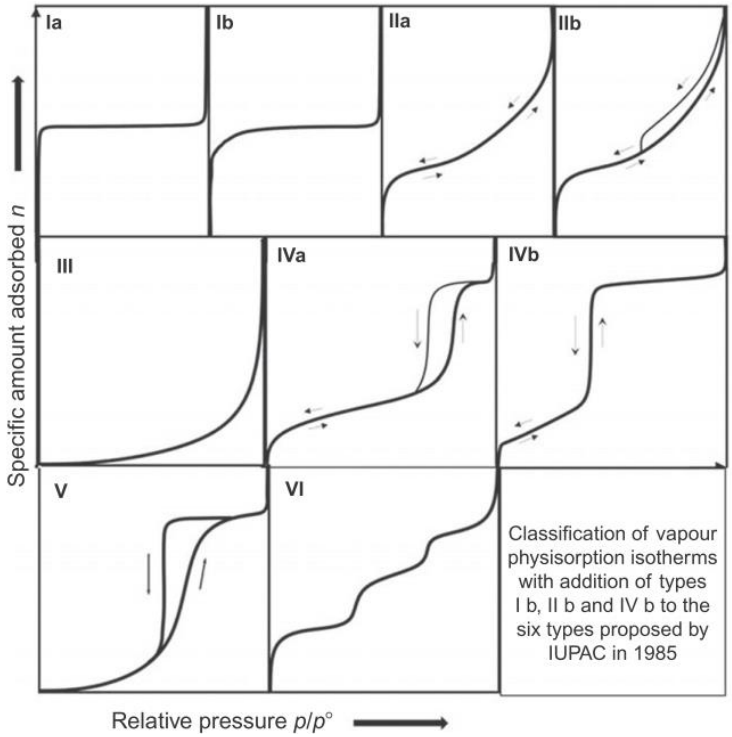

Figure 2.9 Classification of physisorption isotherms.[45]

However, chemical adsorption only gives one simple type of adsorption isotherm, which is similar to type I (a). The plateau is formed due to the completion of a chemically bound monolayer.

2.3.2 Langmuir equation

One of the most widely used isotherms for adsorption is the Langmuir isotherm, which is the type I isotherm mentioned above. The Langmuir mode is one of the initial models used for describing the adsorption of adsorate molecule on bare surfaces.[47,48] In order to use the Langmuir equation some assumptions need to be fulfilled: molecules are adsorbed at equivalent adsorption sites without dissociation, only mono-layer adsorption occurs, no interaction between adsorate on adjacent site.[49]

Because the pore in UiO-MOF is not flat the Langmuir isotherm may give incorrect estimate of the surface area for the material.

2.3.3 Brunauer Emmett Teller (BET) Theory

Another most widely used isotherm in the MOF research is BET isotherm, which is corresponds to the Type II (a) isotherm. It is a model extended from Langmuir equation. It deals with a multilayer adsorption on the absorbent. The BET equation is $\frac{P}{v_a(P^0-P)} = \frac{1}{v_m c} + \frac{c-1}{v_m c} \cdot \frac{P}{P^0}$, where p^0 is saturation vapour pressure (kPa), v_a is the amount

adsorbed at pressure p (cm^3(STP) g^{-1}), v_m is the amount monolayer of adsorbent. The parameter c is equal to $e^{\frac{E_{ads,1}-E_l}{RT}}$, $E_{ads,1}$ is the heat of adsorption of the first layer and E_l is the heat of adsorption of liquefaction. There is a linear ship between $\frac{P}{v_a(P^0-P)}$ and $\frac{P}{P^0}$ in the BET equation, the slope is $\frac{c-1}{v_m c}$ and intercept is $\frac{1}{v_m c}$ (**Figure 2.10**).[13] Surface area can be calculated from $A = v_m \sigma_0 N_{av}$, where σ_0 is the cross-sectional area of nitrogen at liquid density (16.2 Å), N_{av} is Avogadro's number. The pressure range for BET analysis is $0.05 < \frac{P}{P^0} < 0.3$, in which the formation of monolayer is assumed to occur. [50]

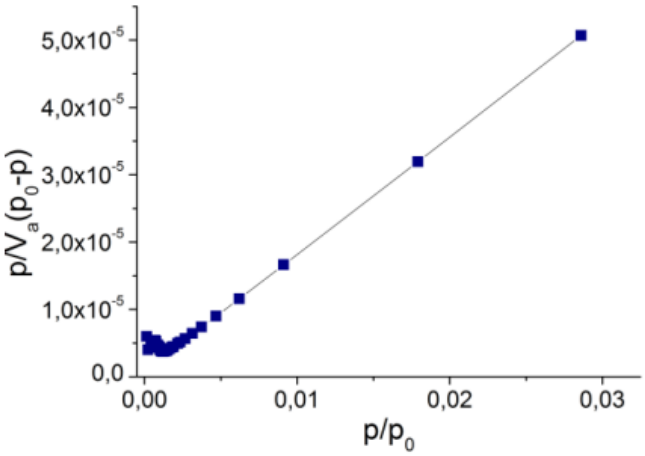

Figure 2.10 A linear ship between $\frac{P}{v_a(P^0-P)}$ and $\frac{P}{P^0}$ in the BET isotherm of UiO-67.[13]

There are two major criteria were used to aid find the pressure rang for the BET analysis. One is the values of $v_a(P^0 - P)$ increase with $\frac{P}{P^0}$ values in the range (**Figure 2.11**)[13], and the other is the value of c which is $e^{\frac{E_{ads,1}-E_l}{RT}}$ should be positive (**Figure 2.10**).[51]

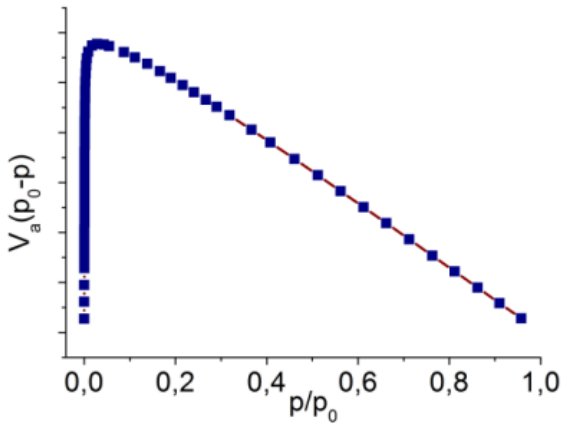

Figure 2.11 The relationship between $v_a(P^0 - P)$ and $\frac{P}{P^0}$ values in UiO-67 adsorption isotherm.[13]

The MOFs materials have surfaces which are far from flat and in some MOFs adsorption occurs through a pore-filling mechanisms rather than layer formation. Thus, there is a suspicion of the truly meaningful of the reported MOFs BET surface areas.[50]

Walton and his coworkers reported the simulated BET surface areas of several MOF materials from N_2 adsorption at 77k by the Grand canonical Monte Carlo (GCMC) simulation. The simulations were carried out from crystal structures and the simulated results highly agree with experimental results.[50] These results demonstrate that the surface areas of MOFs can be obtained by the BET theory with a good accuracy.

2.4 Scanning electron microscope (SEM)

Scanning Electron Microscopy (SEM) is the most versatile technique for material science. Because it is a high resolution imaging technique that can be used to study topography and morphology, chemistry composition, orientation of grains in crystallography and some in-situ experiments. Furthermore, it has good depth of focus and the sample preparation is easy, various specimens (large or small, conductors or insulators) can be analyzed.

Scanning Electron Microscope (SEM) is a high-resolution technique to imaging of surface. Compare with optical microscopy which use visible light as signal, SEM uses electrons as imaging signal. When the electron beam hits the specimen a variety of electron emissions are generated. Among these electron emissions, the secondary electrons (SE), backscattered electrons (BSE), X-rays are analyzed in the SEM through different detectors. By using energy dispersive X-ray spectrometer (EDS) the X-rays signal can be converted to the qualitative and quantitative elemental analysis information of sample. [52]

Energy dispersive spectroscopy (EDS) can provide a quantitative estimate the ratios of the elements in a specimen (Atomic %). EDS detector is a detector is a semiconductor diode, which can absorb the energy of incoming x-ray by ionization. When the electron beam hits the atoms of specimen, characteristic X-rays are formed by excitation of inner shell electrons. The inner shell electron is ejected and an outer shell electron replaces it while energy difference is released as an X-ray. If beam energy If beam energy $E > E_K$ then a K-electron may be excited. Another sequence of events is also possible when the ionization of the specimen atom happens. The hole in the K shell is filled by an electron from the outer shell. The superfluous energy is transferred to another electron which is subsequently ejected as auger electron. And the Auger electron can be used to analyze the true surface. [52]

Within normal accelerating voltage range (15-20 kev) used for EDS analysis, the light elements will emit x-rays of the K series, intermediate elements will emit X-rays of the L or K series, heavy elements will emit X-rays of the M or L series and M series. The intensity of an x-ray line is determined by the transition probability of electrons from the outer to inner shell. These values are fixed for the lines of one series.

The energy of characteristic peaks is defined by element. And the higher the atomic number Z the higher the peak energy (according to Moseley's Law). Ideally, each peak in the EDS spectrum represents an element present within a known region of the specimen.[52]

The SEM is used to analyze the morphology and size of MOF material which is hard to be obtained by optical microscopy. The EDS is used to determine the presence of metal and other heavy elements. In this work, the EDS was used to detect the Zirconium element.

2.5 Optical microscope

The optical microscope is one of the useful tools in the MOF research. It employs visible light to detect small objects such as single crystal of MOF materials. It is convenient to use optical microscope to check the crystal growth due to its reasonable resolution, easy sample preparation and simple measurement.

2.6 Nuclear magnetic resonance (NMR)

NMR is a powerful tool for characterization of organic compounds as well as identification of their purity. In this work, ^{1}H-NMR together with TGA was used to analyze the ratio between Zr and organic linker in the MOF. NMR digest experiment of MOF material was performed by dipping the sample in 1M NaOH (D_2O) overnight. This sample then measured by ^{1}H-NMR can give information about the presence of solvents and modulator and organic linker of MOF material. Through the comparison of theoretical Zr and linker ratio the linker occupancy of MOF material then can be determined by TGA.

2.7 Summary

This chapter gives information about the principle of PXRD, TGA, Gas adsorption, SEM, Optical microscope, NMR, etc. Different applications of these methods in this work are summarized in **Table 2.1**.

Table 2.1 Different applications of characterization method in this work.

Characterization method	Application
PXRD	Phase identification
TGA	Thermal stability, linker occupancy analysis
Gas adsorption	BET surface area
SEM and EDS	Morphology and elements analysis
Optical microscope	Check single crystal
NMR	linker occupancy and purity analysis

Chapter 3

Linker design and synthesis

This chapter is dedicated to the motivation of organic linker synthesis and the strategies of organic linker synthesis. It begins with an overview of organic linkers used for Zr-MOFs in our group. Here, gives information about what kinds of linker are mainly interests for Zr-MOF research in our group. Next, the basic requirements of organic linkers used for MOF synthesis are mentioned. After that, the motivation and synthesis strategies of target organic linker will be introduced. The chapter ends up with a discussion of limitations and safety aspects of preparation of organic linker and a summary of this chapter.

3.1 Organic linkers used in Zr-MOFs

After the discovery of UiO-66 MOF, the catalysis group at University of Oslo continued to investigate other organic linkers in order to find out the most promising Zr-MOF materials for gas (especially CO_2 and methane) adsorption and catalysis applications. Several organic di-carboxylic acids, which are listed in **Figure 3.1**[13,27,53-59] have been mostly studied before this project started.

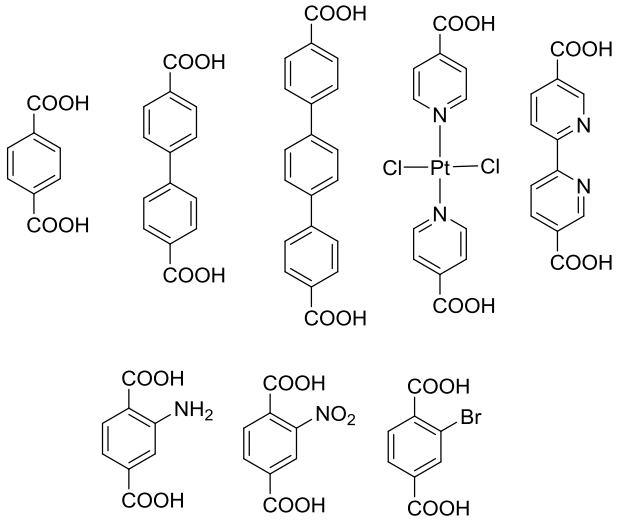

Figure 3.1 Organic dicarboxylic acids used for Zr-MOF at the catalysis group at University of Oslo. [13,27,53-59]

These UiO series of MOFs have a constant structural feature which is the inorganic building unite $Zr_6O_4(OH)_4$. Just by changing the linker molecules used in the MOF synthesis affords different materials. The final properties of material can be tuning by changing the structural properties of the linker using in the MOF synthesis. This strategy is called reticular synthesis.[60] The UiO-66 and UiO-67 were found to have adsorption towards CO_2 and methane. [61,62]The UiO-67 has a higher internal surface area than UiO-66 and it has similar thermal stability as UiO-66.[27]

Hence, if the new MOF has similar size as UiO-67 but with improved adsorption ability and water stability, it could have a potential useful application in gas adsorption.

3.2 Requirements of the organic linkers for MOF synthesis

Because certain amount (more than 5 grams) of organic linker is needed for the MOF synthesis and characterization, the reactions for linker synthesis should be scalable, inexpensive and efficient. The scalable here means the reaction can be scale up to synthesis five grams final target compounds should not have serious problems. The inexpensive means the reagent used in the reaction should be as low cost as possible. The efficient means the synthesis route should be as short as possible and the workup for the synthesis should be as simple as possible to get enough pure compounds.

Furthermore, the Zr-MOF synthesis will be synthesized under strong acid condition, the linker should not decompose during synthesis.

3.3 Motivation and synthesis strategies of target organic linker

1,1'-binaphthyl-2,2'-diol (BINOL) is one of the most popular ligands for both stoichiometric and catalytic asymmetric reactions. The BINOL ligand can coordinate with different metals (such as Ti, Al, lanthanide etc.) as catalysts. For example, the chiral BINOL (**Figure 3.2**) has been extensively studied in enantioselective epoxidation (Ln-BINOL complexes) and asymmetric C-C bond forming (Al-BINOL complexes).[63]

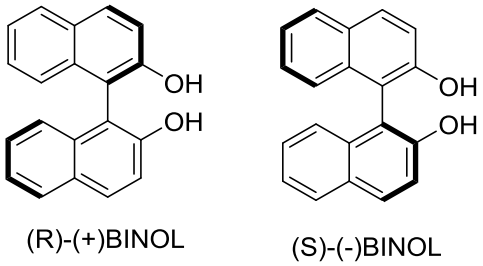

Figure 3.2 The enantiomers of BINOL.[63]

Based on a preliminary survey of the organic linkers have been used for Zr-MOF in the international MOF environment, there is only one papers published by Wenbin Li et al is related to the BINOL system (**Figure 3.3**).[64] In their studies, they used these BINOL linkers to form Zr-phosphonate coordination polymers and then combined catalytically active metal ions to generate asymmetric catalytic sites.

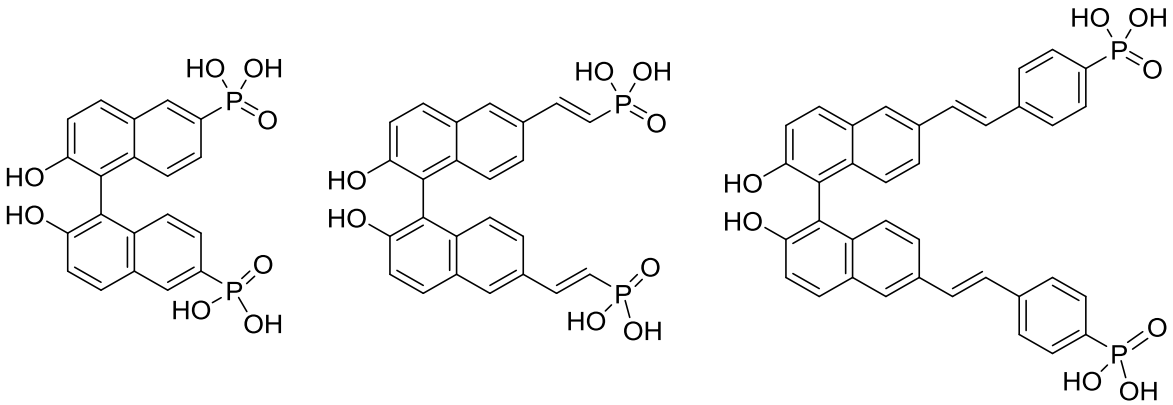

Figure 3.3 BINOL linkers used in chiral Zr-phosphonate coordination polymers.[64]

Therefore, to synthesis BINOL linker which is close to the UiO-67 linker (4, 4'-biphenyldicarboxylate) but without any other substitutions (**Figure 3.4**) becomes an interesting target compound for this project.

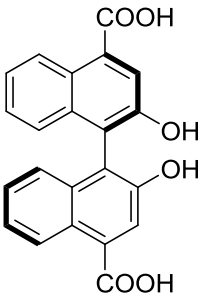

Figure 3.4 One potential target for synthesis Zr-MOF.

For the Zr- MOF synthesis, only a small number of such potential linkers that is commercially available with relative low price and close to the structure of 4,4'-biphenyl-dicarboxylate (**BPDC**) linker. There are still great needs for new organic linkers for the Zr-MOF research in the group. Furthermore, there is no chiral linker has been investigated yet in our group. Thus, it is interesting to synthesis Zr-MOF with this chiral linker and to investigate its potential applications in gas adsorption and catalysis.

However, due to the limitation of the cost and time to synthesize this linker (more discussion about attempting to synthesize this linker will be presented at the beginning of **chapter 4**) another target organic linker: 1,1'-binaphthyl-4,4'-dicarboxylic acid (**BNCD**) linker (**Figure 3.5**) which also has not been studied in the Zr-MOF research was chosen. Also, this molecule is not commercial available. Compare with the **BPDC** linker for UiO-67, this organic linker has similar length but with bigger size. It can be as a preliminary study to know whether the binaphthyl system could be well incorporated to the Zr-MOF structure formation. In addition, the UiO-66 analogue with dimethyl-functionalized linker has better adsorptions towards CO_2 and methane than that of the parent MOF UiO-66[62] and this suggests that using **BNDC** linker (which is much more hydrophobic than **BPDC** linker) to synthesize the UiO-67 analogue MOF may have better adsorptions towards CO_2 and methane than as UiO-67 did.

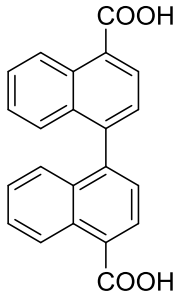

Figure 3.5 Organic linker 1,1'-binaphthyl-4,4'-dicarboxylic acid (**BNDC**) for the new Zr-MOF synthesis.

To synthesis the **BNDC** linker there are three main synthetic strategies have been investigated and the synthesis of some intermediated compounds have been tested in various synthetic pathways. Here gives two synthetic strategies, others will be discussed in **chapter 4** in details. The first retrosynthetic route of the **BNDC** linker is shown in **Figure 3.6** (Strategy I, the numbering of each compound will not be shown in this chapter, since the short retro synthesis route can be easily followed without numbering and only compounds related to the experiments in this work will be numbered in the further chapters).

The **BNDC** linker can be obtained by functional group interconversion (FIG) process from di-esters precursor which was disassembled by a retro homocoupling. The retro esterification of the mono ester precursor gives the mono carboxylic acid intermediate. The retro oxidation leads to a mono aldehyde intermediate which can be obtained from the primary bromide precursor by oxidation. Finally, the disconnection of C-Br bond leads to a commercially available cheap building block.

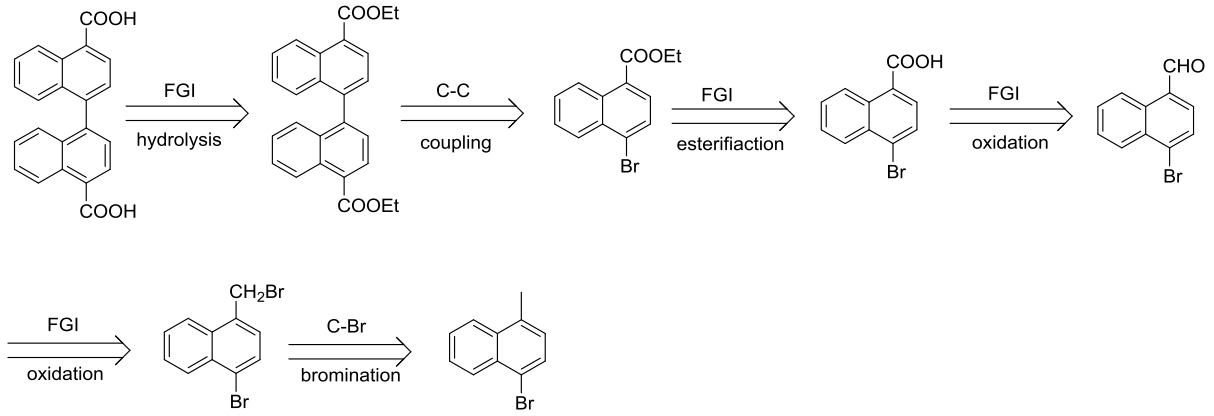

Figure 3.6 Retrosynthetic route of **BNDC** linker. Strategy I.

Alternatively, the second retrosynthetic route as shown in **Figure 3.7** (Strategy II) is a four steps synthesis. The **BNDC** linker can be obtained by a FIG process from the di-carbonitrile building block which can be converted from dibromo intermediate through cyanation. The disconnection of C-Br bonds affords 1,1'-binaphthalene intermediate which was disassembled by a retro coupling from a commercially available cheap starting material.

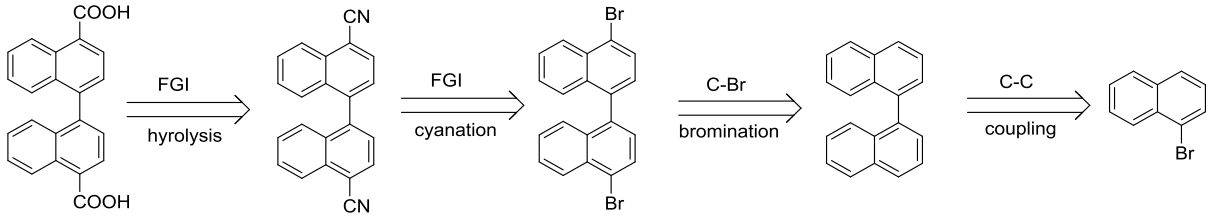

Figure 3.7 Retrosynthetic analysis of **BNDC** linker. Strategy II.

The most important step is to build the binaphthyl skeleton of the target compound. However, the coupling reaction which severs to give the carbon skeleton of the **BNDC** linker is the most expensive step which involves using expensive catalysis. Thus, the coupling reaction was studied under various reaction conditions. The relationship between catalyst loading and the yield of the product was studied in order to get reasonable yield with less catalyst loading. More details about the synthesis will be discussed in chapter four.

3.4 Limitations and safety aspects

There are several challenges for synthesis organic molecule on multi gram scale (more than 5 gram). Not only the choice of reagents for the reactions is challenging but also purification of intermediate is difficult when chromatographic separation is needed to achieve product with acceptable purity.

The potentially hazardous reagents such as CuCN and Br_2 used in this work should be carefully handled. The cyanide is poison because it can inhibit numerous enzyme systems can cause the oxygen consumption decrease in the body which finally leads to death.[65] The Br_2 is a strong oxidizer and also is highly corrosive and toxic. Thus, the information of proper handling of these hazardous reagents is important when perform such reactions involves these hazardous reagents.

There is another safety aspect need to be considered is control the gas pressure when using equipment involve using gas such as chromatography and building up pressure such as autoclave. For example, when perform the purification of the organic compounds by large chromatographic separation the pressure input should be proper, and the most important aspect is the connector should be not very tight, otherwise may cause explosion. When use the autoclave the pressure inside of the reactor should be calculated beforehand and it should be under safety level mentioned in the lab standard operation procedures.

3.5 Summary

This chapter gives a briefly overview of organic linkers used in our group and the motivation of organic linker synthesis in this project. The requirements and strategies of linker synthesis were discussed and the limitations and safety aspects of preparation of organic linker were specially mentioned in the end.

Chapter 4

Synthesis of organic linker

In this chapter, the synthetic routes of organic linker will be discussed in details. As mentioned in the chapter 3, the 2,2' -dihydroxy-1,1'-binaphthalene-4,4'-dicarboxylic acid linker (1) was considered at the initial stage of this project. This chapter will begin with a short discussion about attempting to the synthesis of the 2,2' -dihydroxy-1,1'-binaphthalene-4,4'-dicarboxylic acid linker (1). Next, synthesis of 1,1'-binaphthyl-4,4'-dicarboxylic acid (**BNDC**) linker will be discussed. In this part, some proposed reaction mechanisms and three main synthetic strategies of **BNDC** will be discussed. This chapter ends with a summary on the established synthetic routes of **BNDC**.

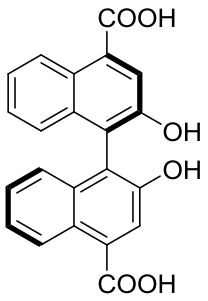

1

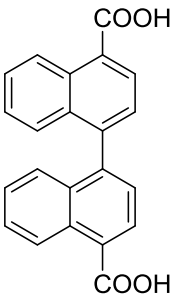

2

4.1 Synthesis routes of the 2,2' -dihydroxy-1,1'-binaphthalene-4,4'-dicarboxylic acid

Based on the reported synthetic methods, the first possible synthetic route (**Figure 4.1**) to synthesis the BINOL linker starts from the 4-bromo-2-napththol compound. The oxidative coupling catalyzed by CuCl(OH)-TMEDA affords the di-bromo intermediate[66] which can be converted to the dicyano intermediate and racemic form of the BINOL linker can be obtained by one more step hydrolysis. The optical pure of the BINOL linker can be separated by using the resolution agent such as cinchonidine. [67]

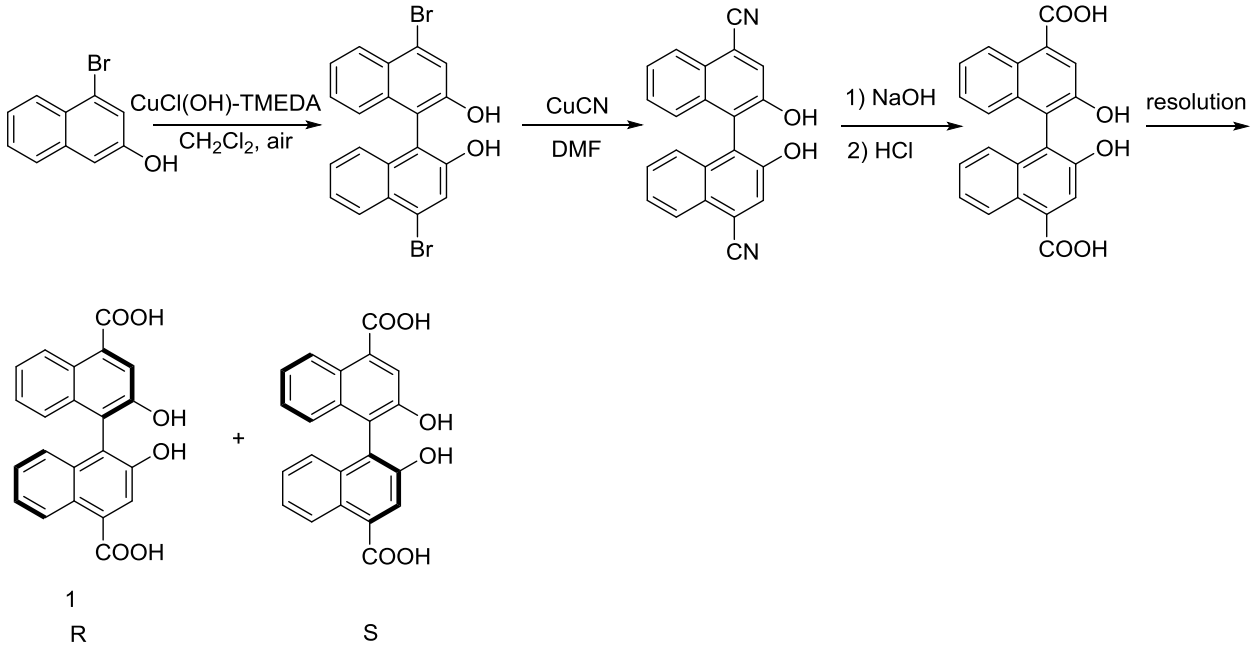

Figure 4.1 The first proposed synthesis route of BINOL linker.

However, the price of the starting material 4-bromo-2-napththol compound is very expensive and the possible building block for synthesis of 4-bromo-2-napththol in a short pathway is also expensive (**Table 4.1**). Hence, based on the cost, this synthetic route was not preferred for the BINOL linker preparation.

Table 4.1 Price of 4-bromo-2-napththol and possible building block for synthesis of 4-bromo-2-napththol (updated 19/04/2015)

Reagents	Price from commercial source
4-bromo-2-napththol compound	1800 kr/g, (calculated from 10 g) FCH Group Reagents for Synthesis
4-bromo-2-naphthalenamine	1800 kr/g, (calculated from 10 g) FCH Group Reagents for Synthesis
1-bromo-3-nitronaphthalene	1100 kr/g (calculated from 5 g), SynInnova Laboratories Product List

In order to reduce the cost for the synthesis of BINOL linker, another synthetic route was proposed.[67-70] It starts from the oxidation with the 1-bromo-2-methylnapthalene followed by other seven steps (homocoupling, esterification, bromination, cyanation, reduction, Baeyer-Villiger oxidation[70] followed by saponification, hydrolysis and resolution) shown in the **Figure 4.2**.

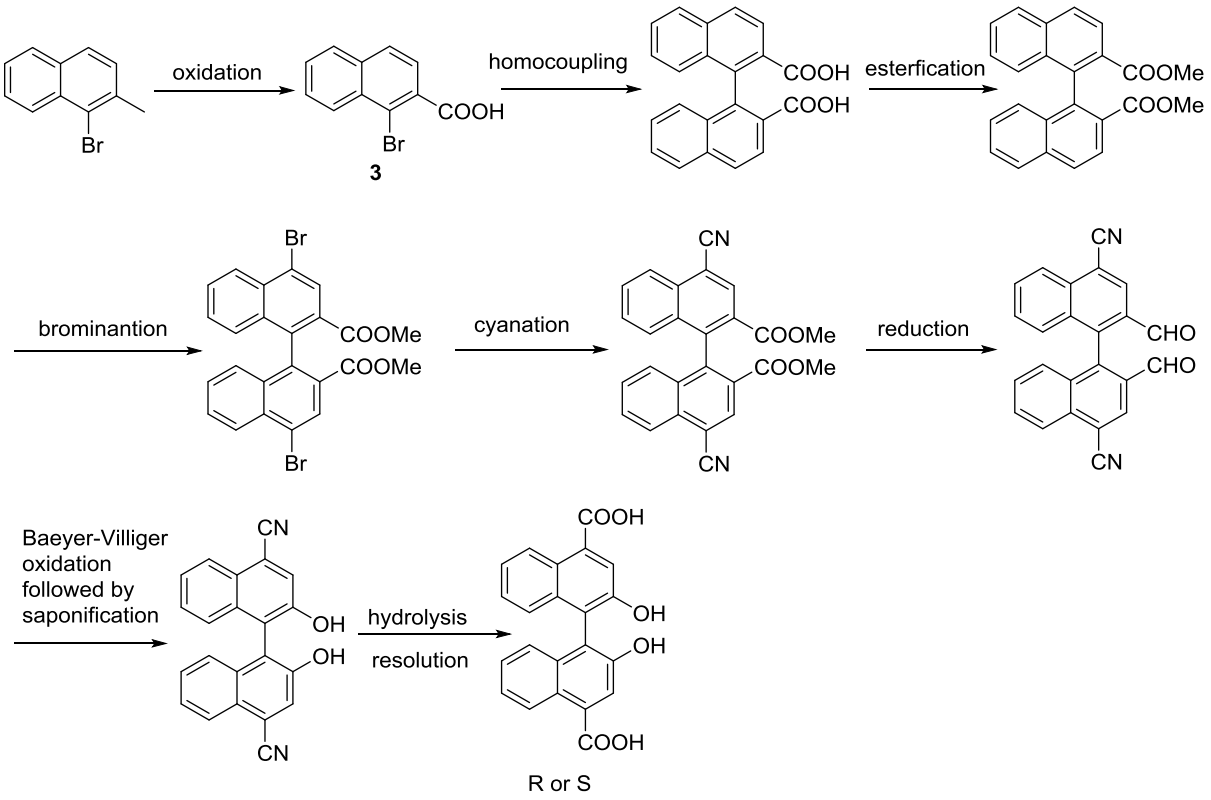

Figure 4.2 The second proposed synthesis route of BINOL linker.

In this work, only synthesis of compound **3** was tried (more discussion see next section 4.1.1 to 4.14) and the results were not very promising. Due to the limitation of time and budget for the project, the synthetic route was not further investigated.

4.1.1 Synthesis of 1-bromo-2-napthoic acid (3)

1-bromo-2-naphthoic acid (**3**) is commercial available but expensive (1 g/1380 kr, Acros Organics, 19-04/2015). There are some published methods[71,72] for the synthesis of compound **3** from the 1-Bromo-2-methylnaphthalene and the cheapest and shortest procedure is using $KMnO_4$ as the oxidative reagent. The published method[68] of oxidation was tested (**Figure 4.3**).

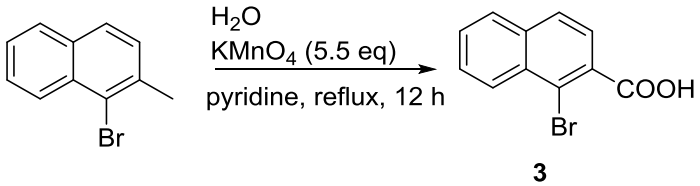

Figure 4.3 One step synthesis of **3** from 1-bromo-2-methylnapthalene.

According to the published method, the starting material was not completely converted and only 14 % isolated compound **3** was obtained (**Table 4.2 entry 3**). A further attempted was made to test whether increase the ratio of $KMnO_4$ and reaction time will improve the yield (**Table 4.2**).

Table 4.2 The oxidative conditions for the synthesis of compound **3**.

Entry	Scale mmol	Reaction condition	Results
1	2.7	12 eq $KMnO_4$, pyridine, H_2O, reflux 92 h	decomposition of the product
2	5.4	7.3 eq $KMnO_4$, pyridine, H_2O, reflux 47 h	decomposition of the product
3	2.7	5.5 eq $KMnO_4$, pyridine, H_2O, reflux 12 h	14 % [a] yield

[a] isolated yield.

However, the more amounts of $KMnO_4$ and longer reaction time (**entry 1** and **entry 2** in **Table 4.2**) leads to decomposition of the product and no desire compound was isolated. To improve the yield of compound **3**, another three steps synthetic route was explored (**Figure 4.4**).

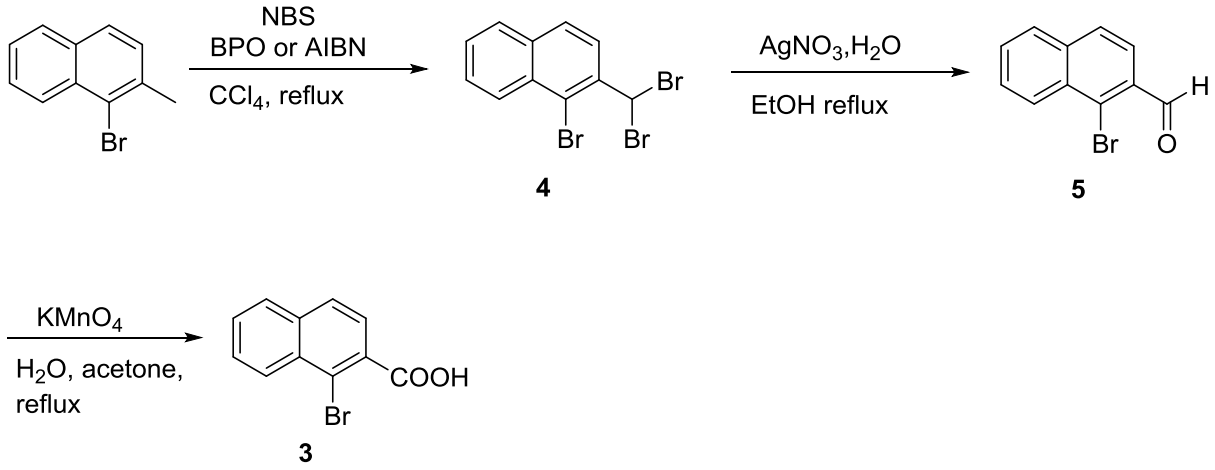

Figure 4.4 Three steps synthesis of **3** from 1-bromo-2-methylnapthalene.

In the first step, bromination of 1-bromo-2-methylnapthalene with *N*-bromosuccinimide (NBS) catalyzed by either benzoyl peroxide (BPO) or azobisisobutyronitrile (AIBN) under reflux condition to give intermediated **4**. After double radical bromination of the methyl group, the second step is the hydrolysis of the intermediate **4** in EtOH and H_2O in presence of silver nitrate to furnish an aldehyde **5**. The third step is the oxidation of the aldehyde via $KMnO_4$ in H_2O and acetone under reflux condition to give compound **3**.

4.1.2 Synthesis of 1-bromo-2-(dibromomethyl)naphthalene (4)

The synthesis of compound **4** was tested by using a mild bromination agent *N*-bromosuccinimide (NBS) catalyzed by BPO[73] or AIBN. The NBS was recrystallized from water and dried under vacuum overnight. The different conditions for bromination were compared in **Table 4.3**.

Table 4.3 Bromination conditions for synthesis compound **4**.

Entry	Scale mmol	Reaction condition	Results
1	2.7	2.3 eq NBS, 17 mol% BPO, CCl_4 reflux for 24 h	34 % yield
2	2.7	3.5 eq NBS, 18 mol% BPO, CCl_4 reflux for 46 h	contains mono brominated (at benzylic position) compound
3	2.7	4.0 eq NBS, 1.8 mol% AIBN, CCl_4, reflux for 32 h	contains mono brominated at benzylic position) compound (use for next reaction)
4	10.8	4.0 eq, NBS , 2.6 mol% AIBN, CCl_4,reflux 29 h	77 % yield

The reaction using benzoyl peroxide (BPO) as the radical initiating reagent gives only 34 % yield. This low yield is due to no full conversion of mono brominated (at benzylic position) intermediate to intermediate **4** and the difficulty of completely separate this mono brominated compound from the product **4** by silica gel chromatography using CH_2Cl_2: hexane =1:200 as eluent. In order to reduce the amount of the mono brominated intermediate, more equivalent NBS was added and the reaction time was prolonged. However, the mono brominated compound was still present in the reaction **entry 2**.

Another radical initiating reagent was also tested. As shown in the **Table 4.3**, the reaction catalysed by AIBN (**entry 3**) also gives mono brominated (at benzylic position) intermediate together with the compound **4**. Crude from **entry 3** was used directly for next step reaction to check if the purification step could be skipped and the compound **5** could be achieved in a good yield (more discussion see **4.1.3**). However, the mono brominated intermediate was completely converted to compound **4** in the **entry 4** after 29 h (**Figure 4.5**). The mono brominated intermediate was formed between 3 and 9 h as the peak (around 4.85 ppm) which belongs to mono brominated intermediate was detected.

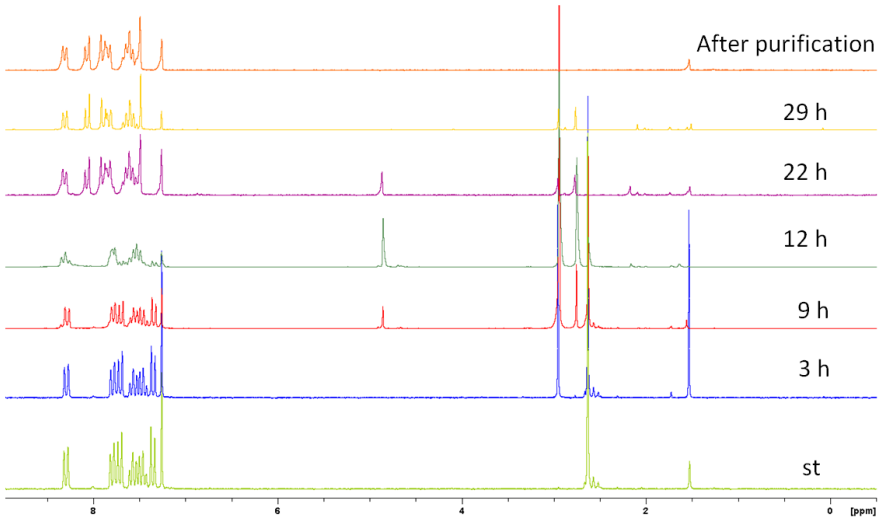

Figure 4.5 Monitoring of bromination reaction (**entry 4** in **table 4.3**) by Stacked ^{1}H NMR ($CDCl_3$, 200 MHz). The bottom spectra is the starting material, the top one is the compound **4**. The mixture taken from different reaction time were shown in the between.

The peak (around 2.65 ppm) which belongs to the starting material disappeared after 22 h. The **entry 4** was purified by silica gel chromatography using CH_2Cl_2: hexane =1:200 as eluent afford the compound **4** with good yield (77 %).

4.1.3 Synthesis of 1-bromo-2-naphthaldehyde (5)

The synthesis of compound **5** according to the published procedure[74] and good yield was obtained (**Figure 4.6**). The crude of starting material from **entry 3** in **Table 4.3** was tried and the mixture was purified by silica gel chromatography using CH_2Cl_2: hexane =1:3 as eluent to give 74 % yield. For comparison, the reaction using pure compound **4** as starting material (8.2 mmol) was tested and it gave 78 % yield.

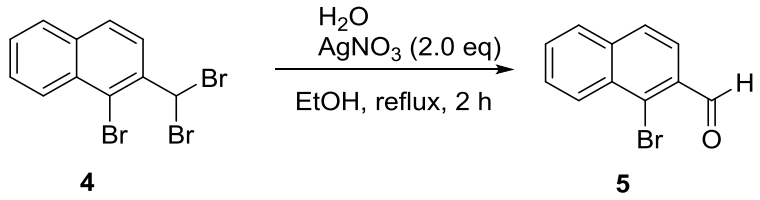

Figure 4.6 Synthesis of compound **5**.

This solvolysis reaction may follow the S_{N1} pathway. The reaction presumably starts with the ionization of the dibromo and followed by the nucleophilic attacked by water. Subsequent loss of a proton from the intermediate **b** and then the loss of bromide and another proton leads to the aldehyde **5** (**Figure 4.7**).[75]

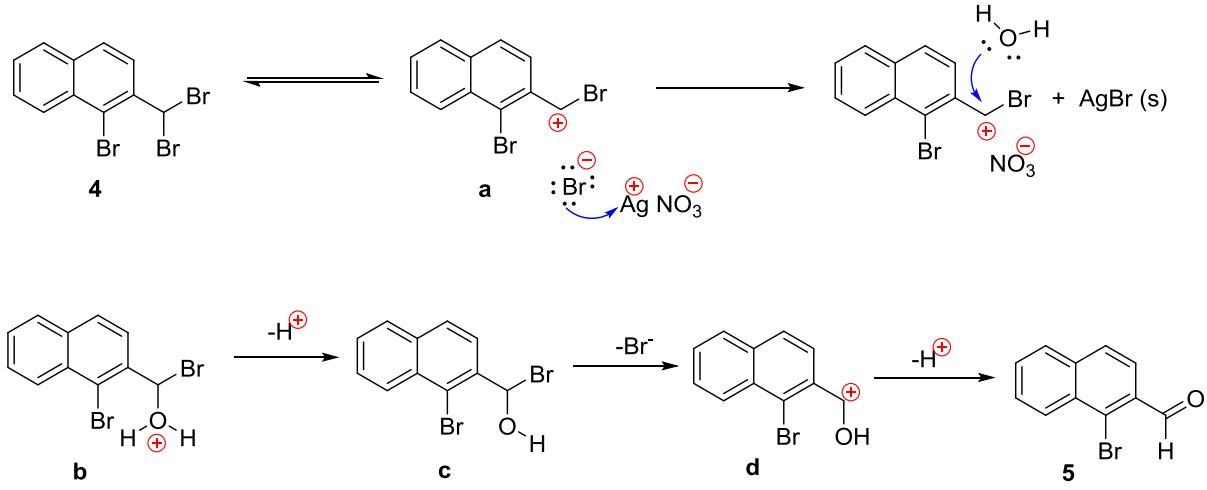

Figure 4.7 Possible reaction mechanism of solvolysis of compound **4**.

The ethanol combines water makes the solvent system polar and also capable dissolving the compound **4**. This solvent system favors the S_{N1} reaction because water is polar and protic solvent which can stabilize the ionic intermediates. The $AgNO_3$ was added to provide the Ag^+ which can form a precipitate with the bromide ion.[76] The precipitation indicates the balance of the initial ionization moves forward.

4.1.4 Synthesis of 1-bromo-2-naphthalenecarboxylic acid (3) from compound 5

In the literature[69] the synthesis of compound **3** from aldehyde compound **5** via oxidation using $KMnO_4$ as the oxidant (**Figure 4.8**). The compound **5** reacted with 1.7 eq $KMnO_4$ in the present of acetone and water under reflux condition. After the acetone solution of compound **5** starts to reflux, the $KMnO_4$ water solution was added slowly. Because this reaction is exothermic and the temperature rises quickly when added $KMnO_4$. Properly stirring and slowly adding can reduce the side reactions and avoid potential risk of violently boiling of the reaction mixture. The reaction was done in a short time but the yield of this reaction was poor. Only 38 % compound **3** was obtained.

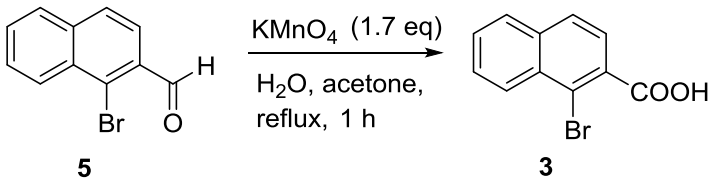

Figure 4.8 Synthesis of compound **3** by oxidation of compound **5** with $KMnO_4$.

In summary, the compound **3** synthesized by directly oxidization of 1-Bromo-2-methylnaphthalene with $KMnO_4$ gives poor yield and the three steps synthesis does not give promising results.

4.2 Synthetic route 1 of 1,1'-binaphthyl-4,4'-dicarboxylic acid (2)

As mentioned in chapter 3, three main synthetic routes for 1,1'-binaphthyl-4,4'-dicarboxylic acid (**BNDC**) were investigated in this work. The synthetic route 1 was studied at the initial stage of this project. And the synthetic route 2 was modified based on some similar reactions in synthetic route1. The synthetic route 3 was based on the strategies II which were mentioned in the **chapter 3** (**3.3**). In this part, the synthetic route 1 will be discussed.

The synthetic route 1 is a four steps synthesis, which starts from the 1-bromo-4-methylnaphathelen (**Figure 4.9**). The first two steps reaction for synthesis the aldehyde intermediate **7** use similar reaction conditions as that for the three steps synthesis of 1-bromo-2-naphthoic acid which was mentioned in the previous section. The third step is the coupling reaction of the aldehyde intermediate **7** catalyzed by $PdCl_2$(dppf) to afford compound **8**. The compound **8** was then oxidized with silver (I) in the fourth step.

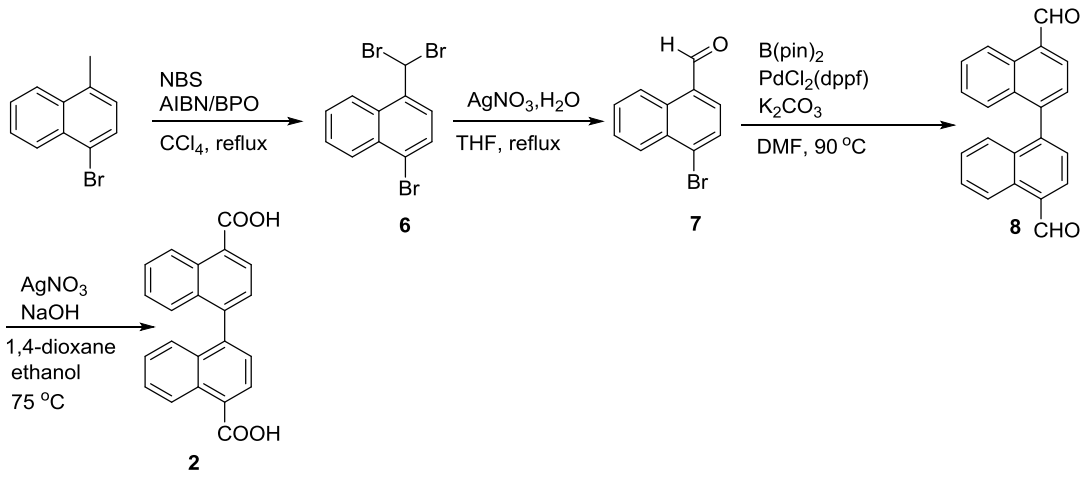

Figure 4.9 Synthetic route1 of **BNDC**.

4.2.1 Synthesis of 1-bromo-4-(bromomethyl)naphthalene (6)

According to the previous reaction condition for synthesis compound **4** (**Table 4.3, entry 4**), 2.5 mol % AIBN and 4.0 eq NBS were used in the first attempt synthesis (**Table 4.4 entry 1**). However, this condition only gives 28 % yield. The reaction was followed by TLC (CH_2Cl_2: hexane= 1:3) and ^1H NMR ($CDCl_3$, 200 MHz). After 31 h small amount of tri-brominated by product (brominated at benzylic position) and trace amount of mono brominated intermediate (brominated at benzylic position) were observed in the reaction mixture (see **appendix 1**).

In order to improve the yield of this reaction, another reported method[77] was attempted. Instead of using AIBN, the BPO was used as the radical initiating reagent (**Table 4.4**).

Table 4.4 Synthesis conditions for compound **6**.

entry	Scale mmol	Reaction condition	result
1	2.7	4.0 eq NBS, 2.5 mol% AIBN, CCl_4 reflux for 31 h	28 % yield
2	2.7	2.5 eq NBS, 4.9 mol% BPO, CCl_4 reflux for 13.5 h	50 % yield
3	13.5	2.5 eq NBS, 4.9 mol% BPO, CCl_4 reflux for 14.5h	49 % yield
4	27.0	2.5 eq NBS, 4.9 mol% BPO, CCl_4 reflux for 20 h	47 % yield
5	27.0	2.5 eq NBS, 4.9 mol% BPO, CCl_4 reflux for 20 h	crude used for next step
6	27.0	2.1 eq NBS, 4.9 mol% BPO, CCl_4 reflux for 20 h	48 % yield

As shown in the **Table 4.4** for the reaction entry using BPO as radical initial reagent, as the scale of the reaction increases from 2.7 mmol to 27 mmol the yield of the reaction are close.

However, there is a challenge to purify this compound when the reaction scale increases. For **entry 4** and **entry 6**, only by recrystallization of the crude from hexane could not give pure compound. Meanwhile, purified by the silica gel chromatography using hexane as eluent were also difficult to be performed. Not only because the separation of mono brominated compound from the product was difficult but also the product **6** can be hydrolyzed to

aldehyde which was developed together with the product and other a small amount of by product from the chromatography.

The crude of **entry 4** in the **Table 4.4** was purified by silica gel chromatography using hexane as eluent and tri-brominated by-product (0.57 mmol, 2 % yield) was isolated. The compound **6** was obtained after the column and then recrystallized from hexane to give 4.8 g (yield 47 %) compound **7**.

To prove the hydrolysis of compound **6** during the purification by the silica gel chromatography, a small testing experiment was performed. The pure compound **6** was loaded on the silica gel chromatography and developed by hexane several times. While washed the column with CH_2Cl_2. This resulting mixture was checked by comparing the NMR spectra with the pure compound **7** which was prepared later (**Figure 4.10**). The NMR study indicates there is a small amount of dibromide product **6** was hydrolyzed when it ran through the chromatography.

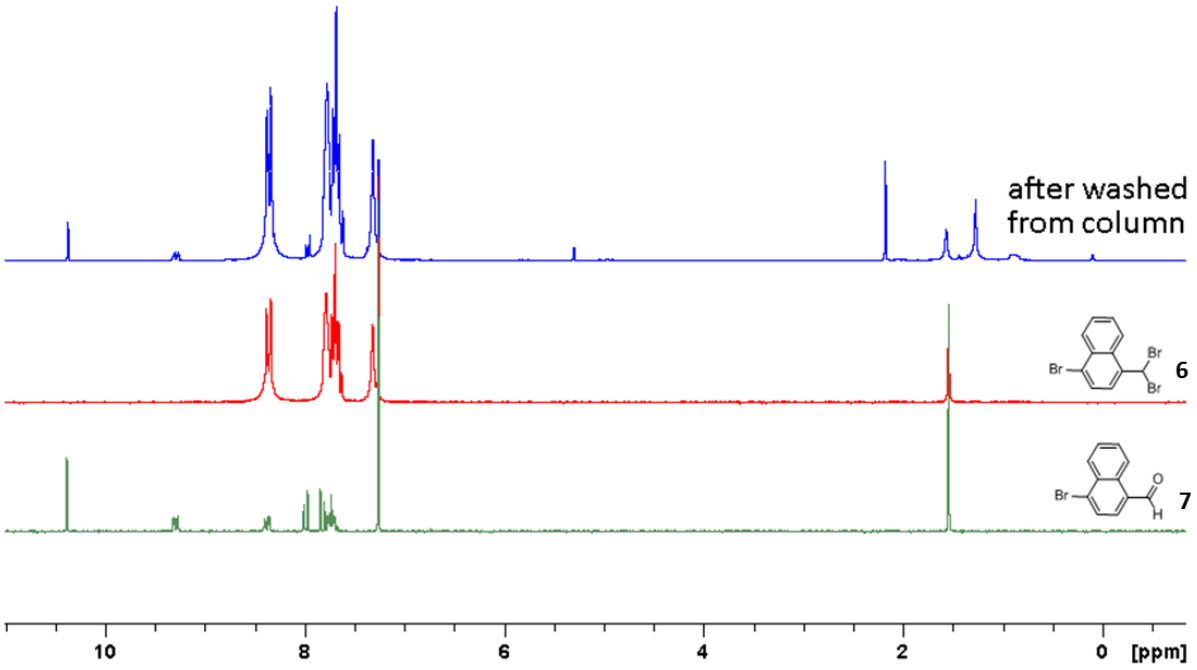

Figure 4.10 Stacked ^1H NMR ($CDCl_3$, 200 MHz) of hydrolysis of compound **6** on the silica gel chromatography.

Stirring the silica gel and pure compound **6** in CH_2Cl_2 and H_2O at room temperature for 1 h was also tested. But only small amount of compound **6** was hydrolyzed to the aldehyde.

In order to check if the purification step could be skipped and the compound **7** could be achieved in a good yield, the **entry 5** was prepared and used directly for next step reaction (more discussion see **4.2.2**).

4.2.2 Synthesis of 4-bromo-1-naphthaldyhe (7) from compound 6

The first attempt to synthesis of compound **7** by using the published method[77] was successfully. The pure compound **6** reacted with $AgNO_3$ and H_2O in THF and EtOH mixed

solvents (**Figure 4.11**). This reaction was performed in 2 h under reflux condition and the crude was purified by silica gel chromatography (5% ethyl acetate in hexane). The compound **7** as a pale yellow solid was obtained with 72% yield.

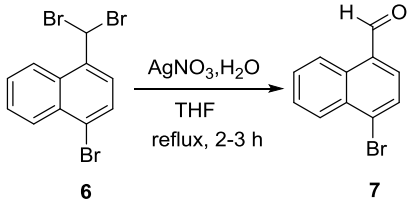

Figure 4.11 Synthesis of compound **7** from compound **6** by solvolysis.

The reaction was scaled up to (2.2 g, 5.9 mmol) using the same method as the first attempted experiment. After purification the pure compound was obtained with 77 % yield. However, the ethanol use in the solvent can react with the product to form the acetal which was detected by ^{1}H NMR ($CDCl_3$, 200 MHz) (see **appendix 2**). Hence, the reaction without using EtOH was tried. The pure compound **6** (8.8 mmol) reacted with $AgNO_3$ and H_2O in THF under reflux condition for 2 h. After purification, the compound **7** was obtained with 82 % yield. The purification by the chromatography did not give pure compound **7** and a further recrystallization from 1% ethyl acetate in hexane was needed. Due to the difficulty of the purification this reaction was not able to be scaled up under the same reaction condition as 8.8 mmol scale.

The crude 6 from the **Table 4.4** (**entry 5**) was tested in this reaction, without using EtOH as the part of solvent system. The crude compound **7** was obtained after 3 h stirring the crude compound **6** with the $AgNO_3$ (2.99 eq) solution in THF. However, compound **7** was not easily purified and only obtained in 25 % yield.

4.2.3 Synthesis of (1,1'-binaphthalene)-4,4'-dicarbaldehyde (8) from compound 7

The reaction for synthesized compound **8** from the compound **7** is a one-pot coupling reaction (**Figure 4.12**). The proposed mechanism of this type reaction was suggested by Nising etal. [78] The bis(pinacolato)diboron (B $(pin)_2$) servers as a reagent for transformation of the aryl halide to arylboronic ester and then the reaction continues with a Suzuki coupling step to yield the biaryl.

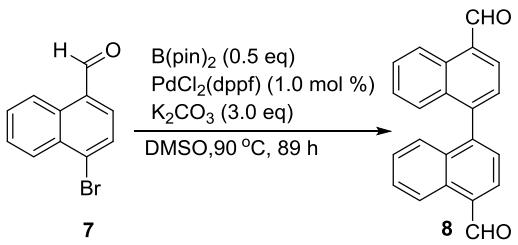

Figure 4.12 One-pot coupling reaction of compound **7**.

As mentioned in the chapter 3, the most important reaction step is to build the binaphthyl core of the target compound. Traditionally, the Ullmann reaction is used for synthesis of biaryls.

But it usually needs harsh condition (high temperature is required)[79] The Palladium catalyst generally allows the reaction at lower temperature and more efficient for large scale reaction.[80] Thus, the Palladium catalyst was chosen as the catalyst for the coupling reaction which severs to give the binaphthyl skeleton. Due to the high price of the Palladium catalyst, the coupling reaction was studied under various reaction conditions. The relationship between catalyst loading and the yield of the product was studied in order to get reasonable yield with less catalyst loading.

The first experiment (**Table 4.5, entry1**) was performed according to the published protocol[78] for synthesis of symmetrical biaryls. By loading 4.0 mol% catalyst the reaction time is the shortest and the yield is excellent. There is no starting material left in this entry.

Table 4.5 Synthesis conditions for compound **8**.

Entry	$PdCl_2$(dppf) mol%	Solvent	Reaction time h	Temperature ^oC	Yield %
1	4	DMSO	14	80	92
2	1	DMSO	41	80	51
3	1	DMSO	89	80	70
4	1	DMF	62	80-90	54
5	0.5[a]	DMF	108	90	45

[a] The ratio is refer to the starting material. **Entry 5** also added 0.5 % mol Pd $(OAc)_2$.
[b] All the Entries use 1.0 mmol starting material and the amount of solvent is 6 mL. The K_2CO_3 is 3.0 eq and the B $(pin)_2$ is 0.5 eq for all these entries.

However, when reduced the amount of the catalyst the yields decreased and the starting material was not completely converted in these cases. In addition, the reaction time is much longer than **entry 1**. Compare with the **entry 4**, the **entry 5** using 0.5 % mol $PdCl_2$(dppf) and 0.9% mol Pd $(OAc)_2$ as catalyst did not improve the yield. The crude of all these entry were purified by chromatography using CH_2Cl_2: hexane = 1:1 as eluent. The compound **8** was obtained as pale yellow solid. This compound was found to have bad solubility in DMSO.

4.2.4 Attempted synthesis of 1,1'-binaphthyl-4,4'-dicarboxylic acid (2) from compound 8

The synthesis of the compound **2** from compound **8** was test once time according to the published method (**Figure 4.13**).[81] In this reaction the Ag_2O as the oxidant which was formed by mixing the $AgNO_3$ solution and NaOH solution. However, there was no product detected by the NMR. The reason could be the bad solubility of compound **8** and the silver oxide is not strong enough to oxidize the compound **8** to compound **2**.

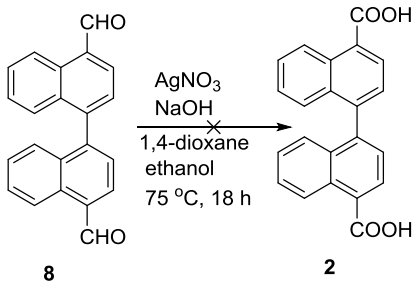

Figure 4.13 Synthesis of compound **2** from compound **8**.

In summary, the synthetic route 1 has difficulty with the purification in the first two steps. The condition for the one-coupling reaction was investigated and the optimal condition is 1 mol% catalyst loading in DMSO with 3.0 eq K_2CO_3 and 0.5 eq B $(pin)_2$. This synthesis route ends up with a bad solubility of intermediated **8**.Hence, alternative need be investigated.

4.3 Synthesis route 2 of BNDC (2)

The synthetic route 2 is based on the modification of the synthetic route 1. (**Figure 4.14**)

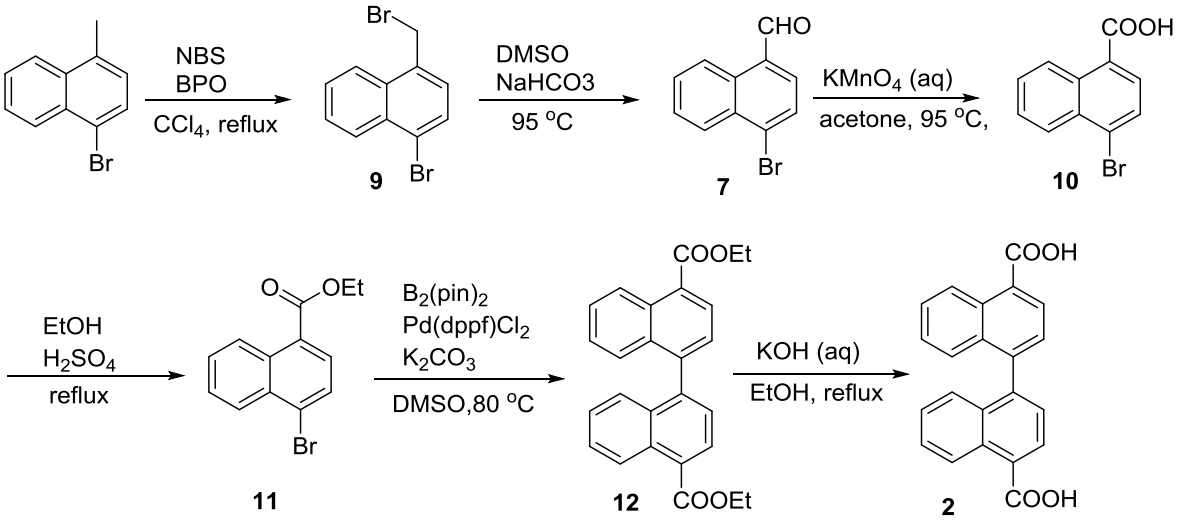

Figure 4.14 Synthetic route 2 of **BNDC**.

This route starts with the same starting material as the synthetic route 1. Starting from the mono bromination of the starting material gives intermediate **9** followed by Kornblum oxidation.[82] The aldehyde intermediated **7** then is oxidized by $KMnO_4$ in acetone under reflux condition to the carboxylic acid intermediate **10**. Ester group is introduced by Fischer esterification to give compound **11**.The one-pot coupling reaction used in the synthetic route 1 is also applied to achieve the di-ester precursor **12** which then can be hydrolyzed to the target compound **2** under alkaline condition.

4.3.1 Synthesis of 1-bromo-4-(bromomethyl)-naphthalene (9)

The preliminary experiment of mono bromination reaction was performed according to the published method [83] by using 1.08 eq NBS and 3.5 mol% BPO in CCl_4 under reflux condition

for 18 h. However, there still have starting material left. After tuning the amount of NBS to 1.2 eq and the BPO to 6.6 mol%, the reaction can be finished in 3 h and relative pure crude was obtained (**Table 4.6 entry 1**). Furthermore, the work up is much simpler than the reported method.[83] Simple recrystallization of the crude from hexane affords pure product.

Based on this condition, different scales of this reaction were performed. As shown in the **Table 4.6**, the scale of this reaction ranges from 2.7 mmol to 90.0 mmol. After recrystallization from hexane, the pure compound **9** was isolated. Among these entries only the 27 mmol scale gives excellent yield. As the scale increases the by-product of the reaction also increases which was detected by the TLC (CH_2Cl_2: hexane =1:3).

Table 4.6 Different scales of compound **9** synthesis.

Entry	Scale mmol	Reaction condition	Yield %
1	2.7	1.2 eq NBS, 6.6 mol% BPO,9 mL CCl_4 reflux for 3 h	63
2	27.0	1.2 eq NBS, 6.6 mol% BPO, 90 mL CCl_4 reflux for 3 h	92
3	54.0	1.2 eq NBS, 6.6 mol% BPO, 180 mL CCl_4 reflux for 3h	60
4	90.0	1.1 eq NBS, 6.6 mol% BPO, 300 mL CCl_4 reflux for 3 h	68

The crude of each entry was also checked by ^{1}HNMR ($CDCl_3$, 200 MHz) as shown in the **Figure 4.15**.

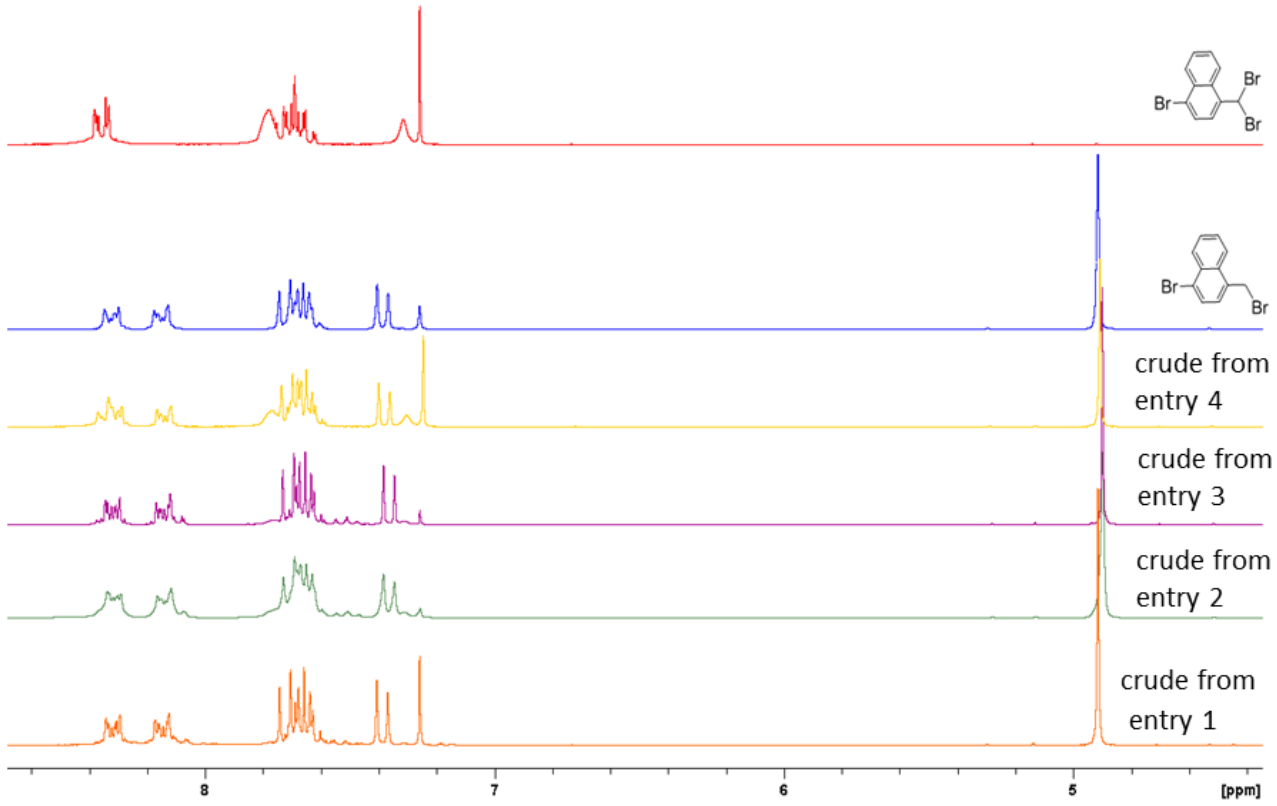

Figure 4.15 Stacked ^{1}H NMR ($CDCl_3$, 200 MHz) of the crude samples from different entries in **Table 4.6**. The spectrum of the top one is the pure di-brominated compound, the second one on the top is the pure compound **9**.

The **entry 1** has no di-brominated by product formed while for **entry 2** and **entry 3** they are quite similar. Both of them contain little amount of di-brominated compound. For the **entry 4**, a significant amount of di-brominated by product formed though the NBS of this entry is less than other entries. These results above show that the optimal scale under the chose reaction condition for this reaction is 27 mmol.

Because the solvent CCl_4 used in this reaction is toxic[84], alternative less toxic solvent such as hexane was chosen in a test experiment. The reason for chose the hexane as alternative solvent is both of these solvent is no polar solvent and the boiling point of hexane is 68.5 ^oC which is close to that of CCl_4 (76.7 ^oC). The reaction using hexane as solvent was performed on 7.2 mmol scale. As expected, the reaction time is much longer than using CCl_4. Even the amount of NBS (1.5 eq) and BPO (8.0 mol %) increase, there was still have small amount of starting material left after 25 h refluxing. However, there was no di-brominated by product (brominated at benzylic position) formed. After purification by recrystallization from hexane, the pure compound was obtained with 31 % yield which is much lower than using CCl_4 as solvent. Due to the time constrain, no further investigations on this reaction condition were performed.

4.3.2 Synthesis of 4-bromonaphthaldehyde (7) from compound 9

With compound **9** on hand, the compound **7** was synthesized by the Kornblum oxidation[82] (**Figure 4.16**). The Kornblum oxidation is a mild oxidation leading to a carbonyl compound using DMSO. The reaction can efficiently oxidize activated primary benzyl bromide and α-bromo aromatic ketones to corresponding aldehydes and phenylglyoxals just by simply dissolving the substrates in DMSO. The DMSO in this reaction works as the oxidant and either organic or in organic base such as triethyl amine and sodium bicarbonate are usually used to remove the proton of the reaction intermediate.[85]

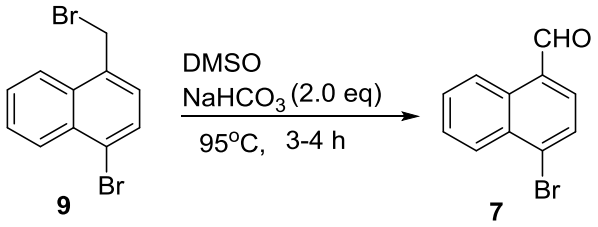

Figure 4.16 Synthesis of 4-Bromonaphthaldehyde **7** by Kornblum oxidation.

In the synthesis of compound **7**, the sodium bicarbonate was used the base and the reaction was performed at 95 ^oC according to the published method.[83]Generally, this reaction works well for active alkyl halide, because its proposed mechanism involves the nucleophilic substitution (S_{N2}) of a halide into alkyoxysulphonium ion which transforms into an aldehyde after deprotonation by the base (**Figure 4.17**).[85]

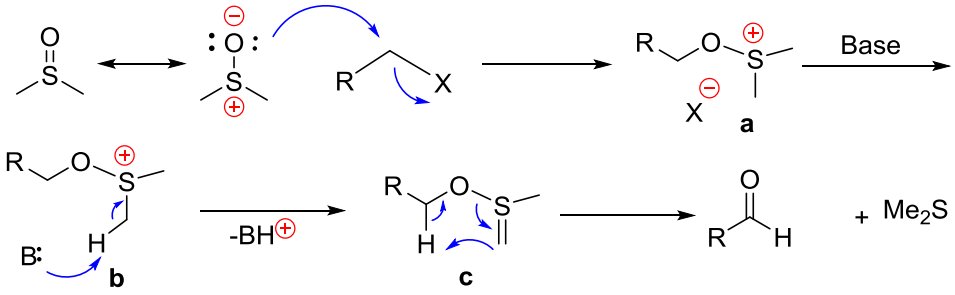

Figure 4.17 Proposed mechanism of Kornblum oxidation.[85]

However, for compound **7** in this study, this reaction did not proceed well as the reported method.[83] The yield is much lower than the reported 91% yield.

In this reaction, the base plays as a proton acceptor which has a dual role: it neutralizes the hydrogen bromide to avoid the oxidation of HBr by DMSO (Br_2 can cause side reactions), and it also works in the deprotonation of the alkyoxysulphonium intermediate.[85]

Different scales of this reaction were tested, from 1.4 mmol to 60.9 mmol (**Table 4.7**). The reaction conditions for all these entries are similar, ($NaHCO_3$ 1.99 eq and the mixture was heated at 95 ^oC) and the only different is the reaction time. For each of these bathes, the reaction was monitored by TLC (3% ethyl acetate in hexane) and ^{1}HNMR ($CDCl_3$, 200 MHz). The main by-product was detected which has a higher Rf value than that of the product and it shows a different UV activity (the main by-product was observed as a deep blue spot) from the product. The small scale (**entry 1** and **entry 2**) was purified by chromatography using 3% ethyl acetate in hexane as eluent. While the large scale (**entry 3** and **entry 4**) was filtered with silica gel (3% ethyl acetate in hexane) by suction filtration and most by-products were removed. The crude product of **entry 3** was used directly for next step and the crude product of **entry 4** was purified by chromatography using 3% ethyl acetate in hexane as eluent (more details see experimental part).

Table 4.7 Different scales of compound **7** synthesis.

Entry	Scale mmol	DMSO mL	NaHCO3 mmol	Reaction time h	Yield %
1	1.4	4.2	2.9	4	42
2	5.9	16.8	5.9	2	77
3	37.0	104.0	73.3	3	Use for next step reaction
4	60.1	170.0	120.7	3	52

The purification of the reaction is challenging because the by-products always run together with the product in the silica gel chromatography. Recrystallizations of this crude from different solvents (such as hexane, toluene) were tried but none were succeed. In order to reduce the heavy purification process of this step, one option is to use the crude after suction filtration through silica gel directly for next step reaction such as the **entry 3** in **Table 4.7** (more discussion see **4.3.3**).

Other methods for transformation of the compound **9** to compound **7** were also tried. Such as using H_2O_2 in EtOH under reflux for 12 h condition[86] only gives small amount of product and the starting material was not completely converted. The method reported by Raju et al.[87] using nitrate as an oxidant with 10% sodium hydroxide in water and 1,4-dioxane at 120 ^oC was also tried. After 6 h heating of the mixture, the starting material was converted to the desire product but at the same time it gives many by-products.

Hence, the Kornblum oxidation is the mainly studied method used for the synthesis of compound **7** from compound **9**.

4.3.3 Synthesis of 4-bromo-1-naphthoic acid (10)

The method[88] for the synthesis compound **10** directly from the 1-bromo-4-methylnapthelen by using $KMnO_4$ as oxidant have been reported in the literature but the yield is only 7 %.

To synthesis the compound **10**, our strategy is oxidization of the aldehyde intermediated **7** which is much easier to be oxidized than the methyl group (**Figure 4.18**). The first attempt experiment (**Table 4.8 entry1**) was performed based on the reported protocol.[69] When the scale of the reaction increase the addition time of the $KMnO_4$ also increase (except the **entry 3** in **Table 4.8**). The key for this reaction is the addition of the $KMnO_4$ solution to the mixture should be slowly. Because the reaction is exothermic, the side reactions may happen if the heat was generated quickly. Also, there is potential danger that the mixture can boil violently if the addition $KMnO_4$ was fast.

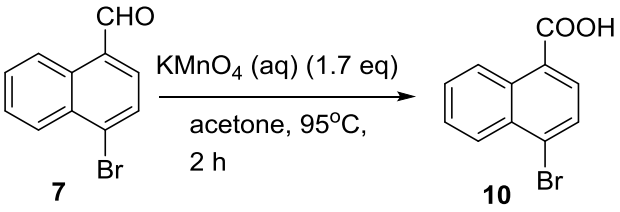

Figure 4.18 Synthesis of compound 10 by oxidation of the aldehyde intermediate **7**.

Thus, the scale (31.9 mmol) of this reaction was performed by adding the $KMnO_4$ for 1.5 h through the dropping funnel. Afterwards, continually stirring for another half an hour until the reaction was finished. The purification for the step is much easier than last step because no chromatography is needed.

Table 4.8 Different scales of compound **10** synthesis.

Entry	Scale mmol	$KMnO_4$ eq	Acetone mL	H_2O mL	Reaction time	Yield
1	1.0	1.4	2.1	1.2	15 min[b] + 10 min[c]	40 %
2	2.5	1.7	3.2	3.6	15 min[b] + 10 min[c]	57 %
3	10.1	1.7	21.8	42.7	1 h[b] + 50 min[c]	78 %
4	22.5[a]	1.7	48.5	95.1	1 h[b] + 50 min[c]	42 %
5	31.9	1.7	69	135	1.5 h[b] + 30 min[c]	76 %

[a] The crude from **table 4.7 entry 3** and the yield was calculated based on two steps.
[b] The time of adding $KMnO_4$ water solution to acetone solution under reflux condition.
[c] The time of continuing reflux after finish the addition of $KMnO_4$.

As shown in the **Table 4.8**, same yield was obtained for **entry 5** and **entry 3**. The **entry 4** using the crude starting material from last step reaction (**Table 4.7, entry 3**) gives 42 % based on the two steps. These shows the reaction can be done on 31 mmol scale from the pure starting material with good yield. And two steps reaction without using chromatography for purification is possible to get the pure compound **10** with acceptable yield.

Other method for preparing the compound **10** from the primary bromide intermediate **9** was also tried (**Figure 4.19**).[89] This reaction was performed on 4 mmol scale, and monitored by both TLC ($C_2H_2Cl_2$: hexane =4:1 with one drop acetic acid) and ^{1}H NMR (DMSO-d_6, 200 MHz).

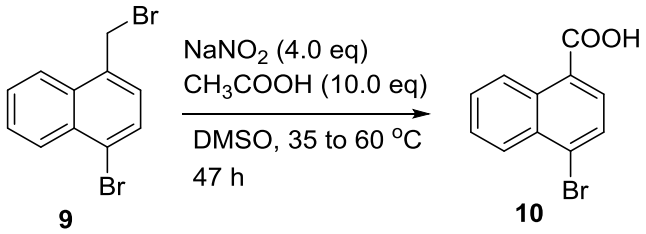

Figure 4.19 Synthesis of compound **10** from primary bromide **9**.

This reaction proceeded slowly, after 47 h there was no starting material left and the product was obtained with 26 % yield. In the crude sample a strong peak around 8.0 ppm (marked as * in the **Figure 4.20**) was observed in the ^{1}H NMR (DMSO-d_6, 200 MHz) after 2 h. But it has no significant change after 26 h. Meanwhile, no significant changes between the TLC of the 26 h and 47 h were observed. After work up (see experimental part), the pure compound **10** was obtained.

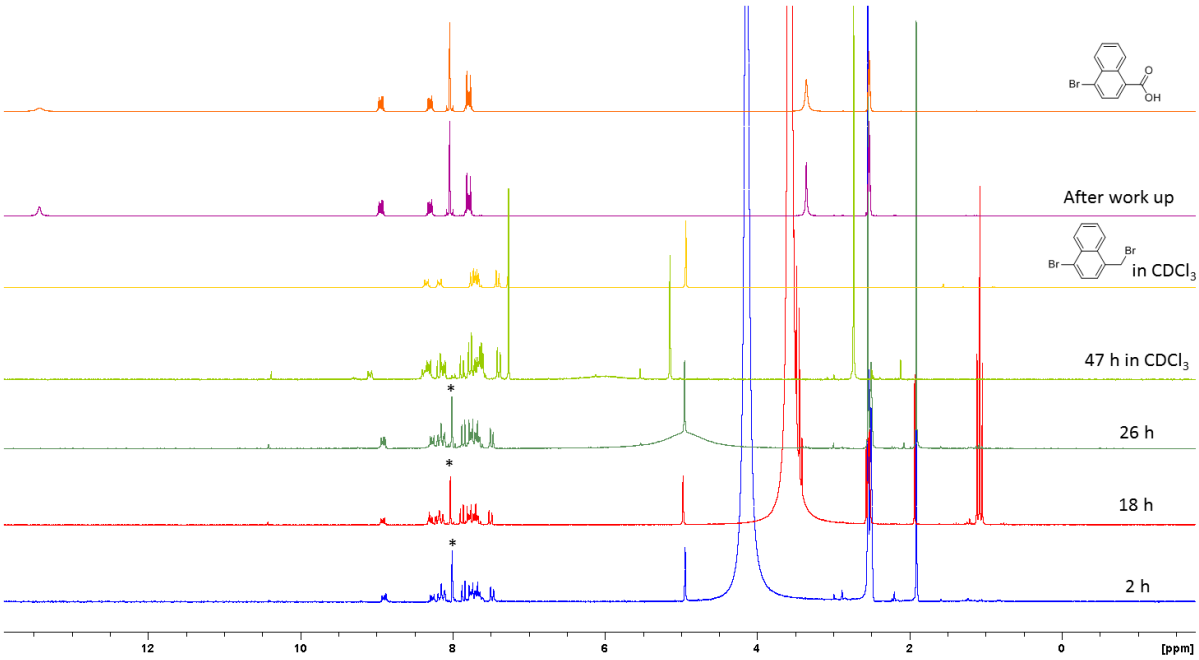

Figure 4.20 Stacked ^{1}H NMR (DMSO-d_6, 200 MHz) of transformation primary bromide **9** to compound **10** under the acidic condition with sodium nitrite in DMSO. Except the mixture of 47 h and starting material were run in $CDCl_3$ others were run in DMSO-d_6.

In summary, the synthesis of compound **10** was preformed mainly by the oxidization of the aldehyde intermediated **7**. The reaction scale can be scaled up to 31.9 mmol.

4.3.4 Synthesis of ethyl 4-bromo-1-naphthoate (11)

Compare with the reactions mentioned before this reaction is much easier to be performed. Three different scales (1.4 mmol, 27.3 mmol, 36.6 mmol) have been attempted (Figure 4.21).

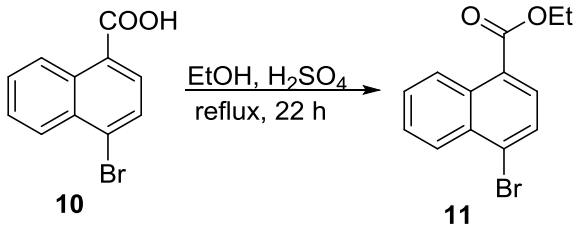

Figure 4.21 Synthesis of compound 11 by Fisher esterification.

Furthermore, a simple work up gives pure compound with excellent yields 92 % to 95 %. The concentrated H_2SO_4 used in this reaction has a dual role: as a catalyst, the more amount of the H_2SO_4 added, the less reaction time was needed; as a water scavenger, the concentrated H_2SO_4 can absorb the water which was generated during the reaction.

4.3.5 Synthesis of diethyl 1,1'-binaphthyl-4,4'-dicarboxylate (12)

The directly coupling from the mono carboxylate acid **10**, have been reported in a Japan patent[90] with 54 % yield. This reaction was performed by heating the mixture of 4-bromo-1-

naphthoic acid, KOH (aq), Pd-C and glycol at 160 ^{o}C under 5 kg/cm^{2} pressures. This method may have problem with the separation of unreacted starting material from product.

Thus, the synthetic route 2 was considered. Though it has two more extract steps, esterification and hydrolysis of the ester, they are easy to be performed and the yields of these two steps are good. These two steps were designed with two purposes: one is increase the solubility of the intermediate by esterification, the other is to improve the purification of compound **12** in an efficient way. Because the hydrolysis can give very pure target compound to get the pure compound **12** is a one important step in this synthetic route.

With compound **7** on hand, the one- pot coupling reaction was first attempted with $PdCl_2$(dppf), K_2CO_3 and B(pin)$_2$ in DMSO under anhydrous inert condition at 80 ^{o}C. However, the starting material was not completely converted. Only 62 % product was obtained (**Table 4.9 entry 1**).

Table 4.9 Different scales of compound **12** synthesis.

Entry	Scale mmol	$PdCl_2$(dppf) mol%	B_2(pin) mmol	K_2CO_3 mmol	Solvent mL	Temperature ^{o}C	Reaction time h	Yield %
1	1.0	1	0.5 (0.5eq)	3.0	6.0	80	48	62
2	2.0	1.5	1.0 (0.5eq)	6.0	12.0	80	28	78
3	8.0	1.5	4.1 (0.51eq)	24.0	48.0	80	28	87
4	39.3	1.5	21.6 (0.54eq)	117.9	235.0	80	24	90

Based on this condition **entry 2** was tested by increasing the catalyst loading to 1.5 mol%. This changes not only increase the yield of this reaction but also almost half the reaction time. Compared with **entry 2**, **entry 3** and **entry 4** were tested by changing the amount of the B_2(pin) while still kept the catalyst loading as **entry 2**. It shows the amount of the B_2(pin) over 0.5 eq of the starting material helps the improvements of the yield and reduced the reaction time even if the scale (**entry 4**) is almost 20 times than **entry 2**.

As mentioned before (**4.2.3**) the bis(pinacolato)diboron (B (pin)$_2$) servers as a reagent for transformation of the aryl halide to arylboronic ester which then reacts with the aryl halide (in this case is the ethyl 4-bromo-1-naphthoate) through a Suzuki coupling step to yield the biaryl. The reason for this reaction works well at large scale is much amount of catalyst still active compare with the small scale. As the starting material was converted to the product the ratio between the catalyst and starting material may increase and this improves the reaction.

The crude of sample of each entry at the end of each reaction was collected and compared by the ^{1}H NMR. The **entry 2**, **entry 3** and **entry 4** give similar crudes while **entry 1** still have small amount of starting material left (**Figure 4.22**).

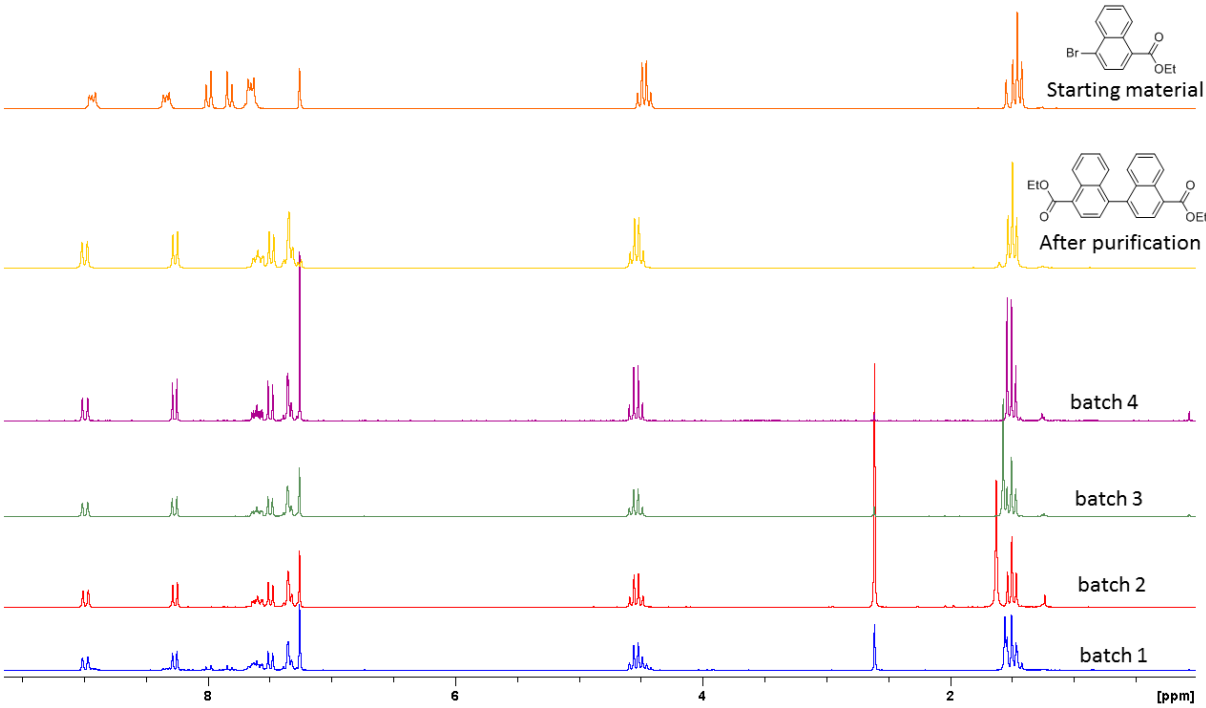

Figure 4.22 Stacked ^{1}H NMR (DMSO-d_6, 200 MHz) of the crude samples from different entries in **Table 4.9**. The spectrum of the top one is the starting material, the second one on the top is the pure compound **12**.

The purification for the small scale (1.0 mmol, 2.0 mmol) of this reaction was done by diluting the mixture in large amount of water (almost 8 times as solvent) and then washed with NaOH (20%) followed by extraction with CH_2Cl_2 in order to separate the product from the DMSO. Afterwards, the residue was purified by silica gel chromatography (CH_2Cl_2: hexane =1:1) gives pale yellow solid.

However, using the same procedure to remove the solvent for the large scale (8.0 mmol, 39.3 mmol), will be difficult. The best option is to pour the reaction mixture over ice and then filter the product by suction filtration to remove the solvent. The crude then filtered with silica gel, crude product was obtained almost pure. After a short chromatography (CH_2Cl_2: hexane =1:1), the pure compound was obtained.

In summary, the synthesis of compound **12** was preformed mainly by using 1.5 % mmol catalyst. The reaction scale can be scaled up to 39.3 mmol.

4.3.6 Synthesis of BNDC (2) from compound 12

The compound **2** can be obtained through the hydrolysis of compound **12** under alkaline condition (**Figure 4.23**). This classical reaction was easy to be performed. Several scales were performed and the largest scale is 17.5 mmol which ends with 88 % yield.

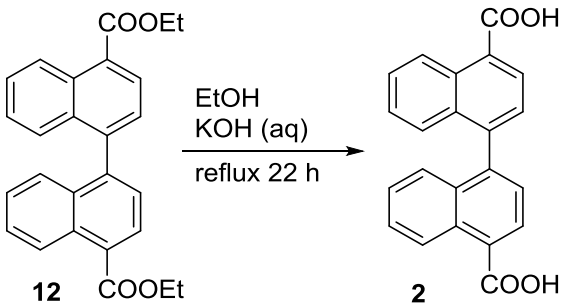

Figure 4.23 Synthesis of compound **2** from compound **12**.

The only problem of this reaction is the filtration of the pure product from the work up solution. Because the precipitate is a very fine solid, the suction filtration therefore is very slowly.

To dry this compound, the resulted solid from suction filtration was dried in the 110 ^{o}C oven for 24 h. During the drying process the solid was took out of the oven once time and crashed into powder. In order to check whether the water was still present in the compound, three NMR experiments were performed (**Figure 4.24**).3.0 mg teterphthalic acid dissolved in 0.5 mL DMSO-d_6 as a standard reference, and 3.0 mg terterphthalic acid and 8.0 mg compound **2** (before dried in oven and after dried in oven separately) dissolved in 0.5 mL DMSO-d_6 were used as test samples. By comparing the NMR signal of these three samples, whether the sample is dry can be detected.

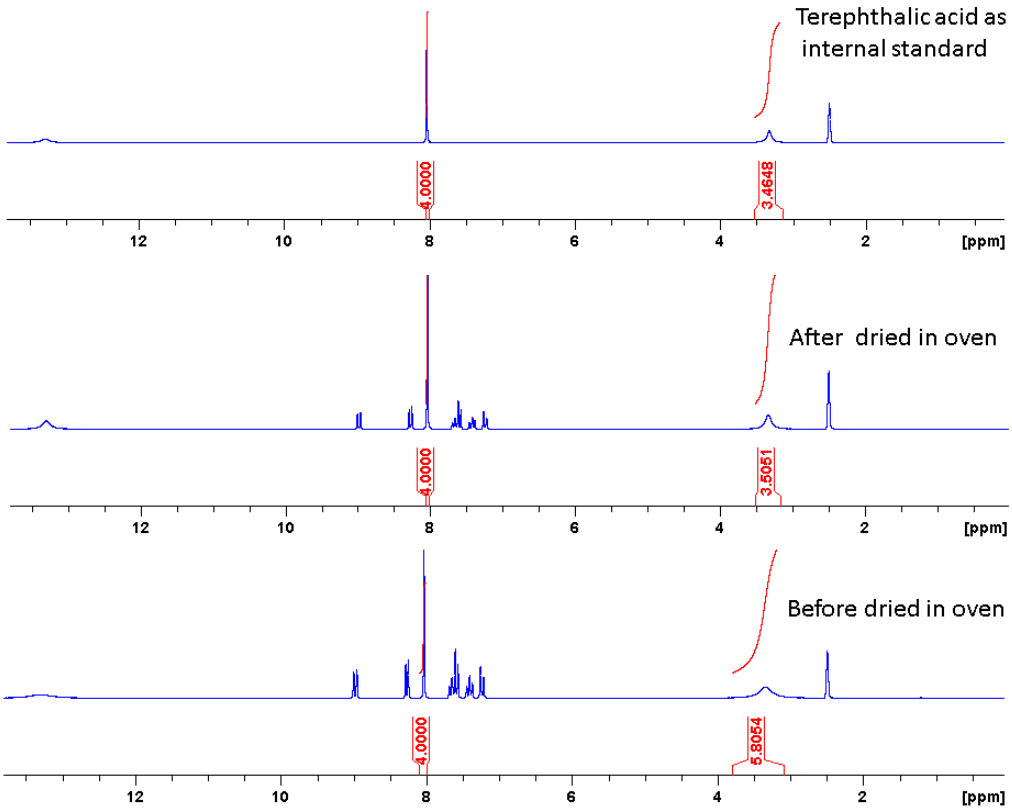

Figure 4.24 Stacked ^{1}H NMR (DMSO-d_6, 200 MHz) of compound **2** before drying (bottom) in the oven and after drying oven (middle) in the terephthalic acid as internal standard (top).

As shown in the **Figure 4.24**, the integration between terephthalic proton and water in the sample after dried in the oven is very close to the standard. This indicates 24 h drying in the 110 ^{o}C oven is enough to get the compound dry and the compound is not decomposed under this temperature.

4.4 Synthesis route 3 of BNDC (2)

With the goal of making the synthesis of **BNDC** in a shorter route, the third synthetic route was developed (**Figure 4.25**).

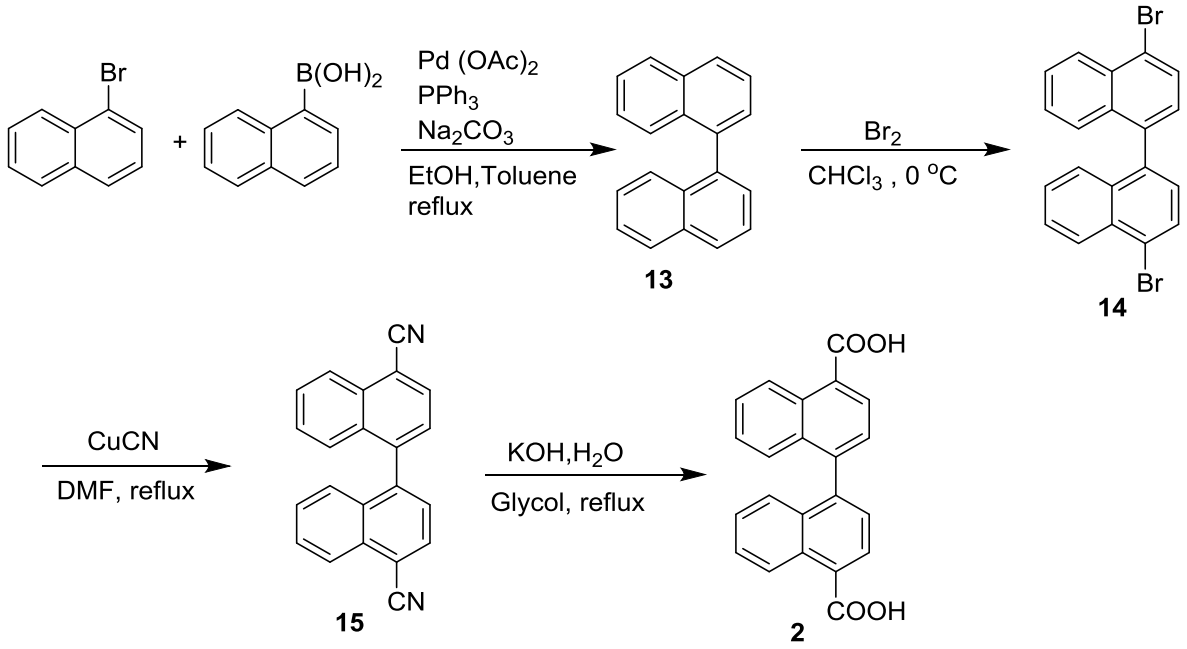

Figure 4.25 Synthetic route 3 of **BNDC**.

The coupling reaction gives the binaphthyl core **13**, followed by bromination under dark and cold condition to afford compound **14**. The treatment of compound **14** with CuCN in DMF under reflux condition gives dicyano moiety **15**, which then was hydrolyzed under alkaline condition to yield the target compound **2**.

4.4.1Synthesis of 1,1'-binaphthalene (13)

To synthesize compound **13**, both the previous one-pot coupling method and the Suzuki cross-coupling method were tested (**Figure 4.26**).

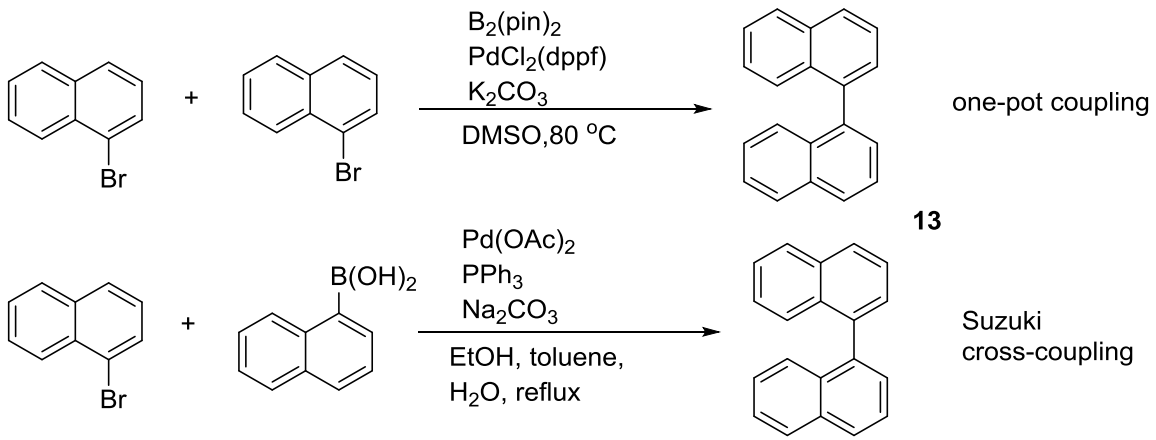

Figure 4.26 Synthesis of compound **13** by one-pot coupling and Suzuki cross coupling.

In order to find out the best condition for the one-pot coupling reaction with low catalyst loading and give acceptable yield. Different reaction conditions for the one-pot coupling reaction have been tested (**Table 4.10**). Based on the condition used for synthesis of compound **12** (**4.4.5**), the first experiment was performed using the 1.5 mol % $PdCl_2$(dppf) catalyst (**Table 4.10**, **entry 1**). However, under this condition the starting material cannot completely be converted and these results a poor yield. Thus, with 4 mol % catalyst was tried (**Table 4.10**, **entry 3**) and the yield turned out to be excellent. Another strategy is to use combine catalysts, such as $PdCl_2$(dppf) and $Pd(OAc)_2$, in the reaction (**entry 2**). Because the $Pd(OAc)_2$ is much cheaper than $PdCl_2$(dppf). Though the amount of Palladium catalyst in **entry 2** and **entry 3** is the same, but the yield in **entry 2** is lower than that of **entry 3**. This suggests the $PdCl_2$ (dppf) is much better than Pd $(OAC)_2$ under the similar reaction condition.

Table 4.10 One-pot coupling reaction conditions for the synthesis of compound **13**.

Entry	Scale mmol	$B_2(pin)_2$ mmol	$PdCl_2$(dppf) mol%	$Pd(OAc)_2$ mol%	Reaction time h	Result
1	2.0	1.0	1.5	/	50	15 %
2	2.0	1.3	2.0	2.0	41.5	63 %
3	2.0	1.3	4.0	/	66	90 %

[a] All these entries are 2.0 mmol scale and run in 12 mL DMSO with 3.0 mmol K_2CO_3 at 80 °C

Furthermore, all these entries contained starting material when each reaction was stopped. These was evidenced by checking each reaction mixture with1H NMR ($CDCl_3$, 200 MHz) (**Figure 4.27**). By comparing the integration of the protons (marked proton peak were selected for analysis) from the product and starting material in each mixture, the approximate ratio of the starting material in crude was obtained (around 40 % for **entry 1**, 10 % for **entry 2** and trace amount for **entry 3**). The crude of all these entries were purified by silica gel chromatography (hexane as eluent) and the pure compound was obtained as a white solid which has a bad solubility in THF.

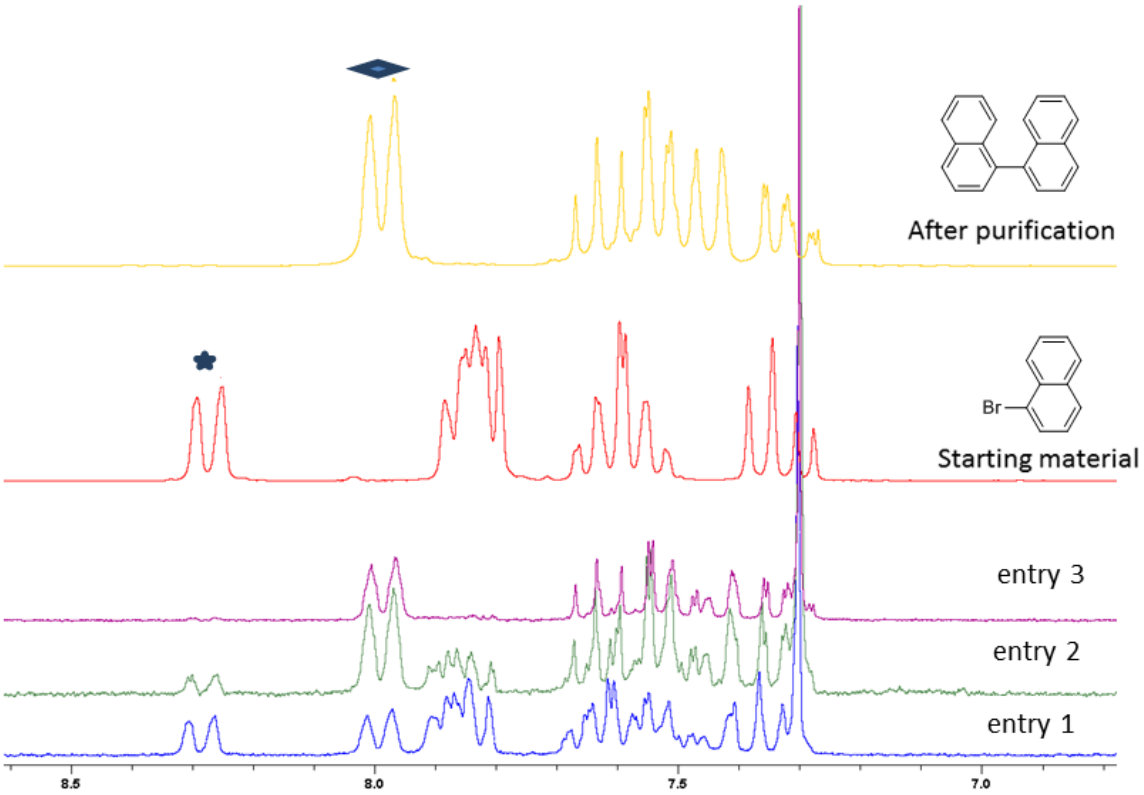

Figure4.27 Stacked ^{1}H NMR ($CDCl_3$, 200 MHz) of the crude of compound **13** from the three entries in the **Table 4.10**. The selected proton in the starting material and product was used for estimating the ratio of starting material in the mixture.

Another method [91](2 mmol scale) using $Pd(OAc)_2$ (5 % mmol), PPh_3 (10 % mmol) and Cs_2CO_3 (1.1 eq) in MeCN under reflux condition also was tried. After 50 h refluxing of the mixture, there was still a large amount of starting material present in the mixture.

To obtain the compound **13** in good yield with low catalyst loading, the Suzuki cross coupling were in investigated in this study (**Figure 4.28**). Suzuki cross-coupling is the palladium-catalyzed cross-coupling between organic halide or triflates and organoboron compounds. It is a useful method for the formation of biaryls.[82] There are several advantages for using this method: the reagent 1-naphthaleneboronic acid is commercial available and the reaction is tolerant in water.

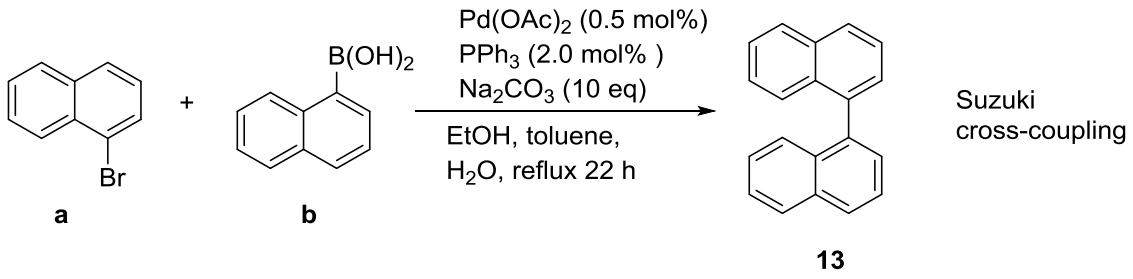

Figure 4.28 Suzuki reaction for the synthesis of compound**13**.

In this study, three different scales were tested (**Table 4.11**). The first experiment of this reaction is according to the published protocol.[92] The Suzuki reaction was complete after heating the mixture to reflux for 26 h. Though the reaction time is longer than reported method, the yield is higher than that of the reported (90% yield).

Table 4.11 Cross coupling reaction conditions for the synthesis of compound **13**.

Entry	a mmol	b mmol	Pd $(OAc)_2$ mol%	PPh_3 mol%	Na_2CO_3 2 M (mL)	Solvents ml	Reaction Time h	Yield %
1	2.0	5.0	0.5	2.0	10	20	26	100
2	10.0	11.0	0.5	2.0	12	100	22	82
3	41.2	45.4	0.5	2.0	50	200	24	78

[a]The reaction was performed in EtOH and toluene = 1:1 mixed solvents.

In the literature, the homo coupling of synthesis of 1-naphthaleneboronic acid by $Pd(OAc)_2$ were also reported.[93] Hence, in the next experiments the amount of 1-naphthaleneboronic acid was reduced (1.1 eq). As shown in the **Table 4.11**, **entry 2** and **3** with less amount of base and 1-naphthaleneboronic acid still give good yields.

The purification of this compound on a large scale (41.2 mmol) was done by chromatography (hexane as eluent). Before that a filtration with celite was applied to remove the most part of impurity from the mixture. After the purification, the compound was obtained as a while solid.

Compare with the one-pot coupling, the cross coupling reaction gives a good yield when the catalyst loading is 0.5% mol.

In summary, for this step synthesis, the cross coupling reaction method is much better than the one-pot coupling method and the reaction can be scaled up to 41.2 mmol.

4.4.2 Synthesis of 4,4′-dibromo-1,1'-binaphthalene (14)

The synthesis of compound **14** was according to the report method (**Figure 4.29**).[94] The different scales (3.9 mmol, 7.9 mmol) of this reaction have been tested and the yields of the both are good (74 % for 3.9 mmol scale, and 91 % for 7.9 mmol scale).

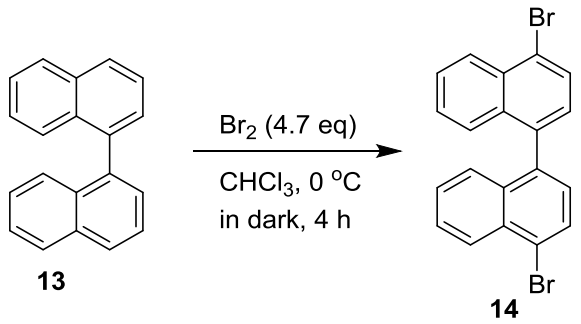

Figure 4.29 Synthesis of compound **14** by bromination.

This reaction was done by slowly adding the bromine to the cold chloroform (0 ^{o}C) in dark condition. Afterwards, the resulting mixture was stirring in the dark and cold (0 ^{o}C) condition for another 3-4 h. The potential danger for this large scale is the used of bromine. Because the bromine is a toxic and corrosive liquid, proper work up for this reaction is important. After the reaction is finished, aqueous $NaHSO_3$ was added to quench the excess of bromine and the NaOH (2M) was added to neutralize the mixture and the sodium bromide was formed.

The purification for the crude is easy to be performed. After the proper work up to remove the bromine and Hydrogen bromide, the organic residue was then recrystallized from the chloroform. A nice needle white crystal was obtained.

4.4.3 Synthesis of 4,4′-dicyano-1,1′-binaphthyl (15)

Compound **15** was synthesized via the Rosenmund-von braun reaction (**Figure 4.30**). This reaction usually is used for synthesis of aryl nitriles from aryl halide and CuCN in a high boiling solvent such as nitrobenzene and DMF. [85]

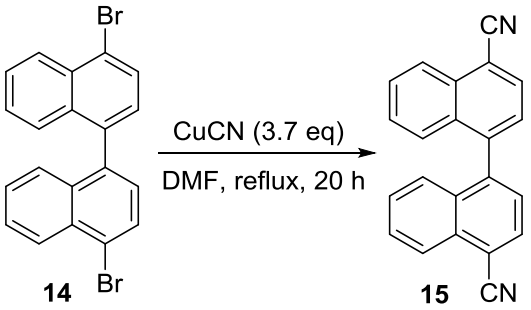

Figure 4.30 Synthesis of compound **15** via Rosenmund-von braun reaction.

The experiment was done according to the published method using 3.7 equivalent CuCN in dry DMF under reflux condition.[95] The first experiment (2.4 mmol scale) reaction time (47 h) is longer than the reported (overnight). Furthermore, work up process is different from the paper reported. To get rid of the CuCN the reported method involves boiling the mixture in 10 % hydrochloric acid. This may have risk to form the HCN. Hence, another mild work process[96] was followed to get rid of the CuCN. The mixture firstly was poured in the mixture of water and ammonium hydroxide and extracted by $CHCl_3$ and then washed with water until there is no blue colour can be observed in the water phase. After the solvent was evaporated, the organic residue was purified by silica gel chromatography (CH_2Cl_2: hexane = 1:1). In this way the obtained yield (69 %) is lower than reported (81 %).[95]

Using the same procedure as the first test experiment, the reaction was scaled up to the 9.6 mmol. However, there were trace by-products (Lower Rf value than that of product) were observed by the TLC (25 % ethyl acetate in hexane). The crude was purified by chromatography. After the column, the compound was obtained as a yellow solid with 78 % yield.

The drawback for this reaction is more than stoichiometric amount of CuCN is required. As mentioned before the cyanide is poison (3.4).[65] The scale up of this reaction should be done carefully when preparation the reaction and work up the reaction mixture. The cooper

bromide waste formed during the reaction which may cause problem (difficult to be moved) for further scale up.[97]

This reaction can also be done by replacing the CuCN with other cyanide source such as NaCN in the present of palladium or nickel catalyst. The stoichiometric amounts of environmentally harmful CuBr can be avoided.[98] Due to the time constrain, this reaction was just tested twice, modification the on large scale has not been done yet.

In summary, this reaction can be scaled up to 9.6 mmol under the above condition. The purification was done by chromatograph.

4.4.4 Synthesis of BNDC (2) from compound 15

In theory, hydrolysis of nitriles to carboxylic acid can be done under either acid or base condition. Both of these conditions give the same hydroxy-imine and amide intermediate [99] In this study, the hydrolysis of compound **15** was investigated under base condition.

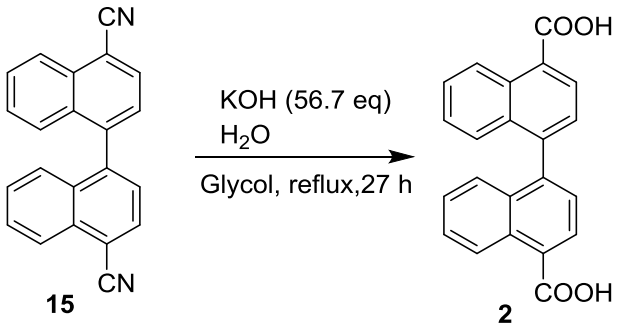

Figure 4.31 Hydrolysis of compound **15** to compound **2**.

According to the literature[67] the first hydrolysis experiment was tired. 1.55 mmol starting material refluxed with 10 mL NaOH (6 M) in 5 mL EtOH under reflux condition for one week but no desire product was obtained. The reason for this could be the temperature for the reaction is not high enough to form the carboxylate. Hence, another experiment (1.0 mmol) was tested by using high boiling point solvent (glycol, as the condition shown in the **Figure 4.31**)[100] and the compound **2** was obtained with 75%.

4.5 Other synthetic strategies

Besides the three synthetic routes mentioned above, the other short synthetic path way was also tested during this study (**Figure 4.32**). The **BNDC** linker can be obtained by a retro hydrolysis[101] from the building block **17** which can be converted from intermediate **16** through bromination.[101] The intermediate **16** can be disassembled by a retro coupling from a commercially available cheap starting material 1-methylnaphthalene.

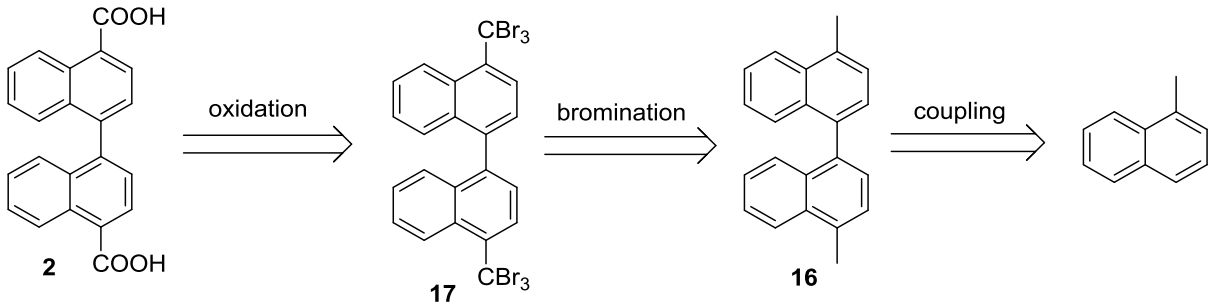

Figure 4.32 Other synthetic strategies of BNDC synthesis.

For this synthetic strategy, the bromination will be challenging due to the selectivity problem. The synthesis of compound **16** according reported method was successful for the first testing experiment. But the synthesis compound **17** from **16** by using 7.0 eq NBS were not success. There were three main compounds formed after refluxing 53 h, but they were not able to be separated by chromatography, so identification of those compounds became difficult. Hence, this synthesis route was not tried later.

In the literature, the synthesis the compound **2** from **16** by oxidation by $Na_2Cr_2O_7$ in autocalve with pressurized CO_2 at room temperature has been reported. [102] The directly oxidation from compound **16** was not tried due to the time constrains.

4.6 Summary of the synthetic routes

In summary, three main synthetic routes have been explored and two of them (synthetic route 2 and synthetic route 3) work.

There are some advantages of the synthetic route 2. The scale can be up to 17.5 mmol, and the purification is easy to be performed for some steps. The only shortcoming is the low yield of the Kolbe oxidation in the second step. Due to the time constrain, the modification of Kolbe oxidation reaction (such as choose different bases as mentioned above) was not tried during this study. It may change the outcome of this reaction to be much better.

The synthetic route 3 can be performed on small scale (1.0 mmol), the scale up condition need to be further investigated.

Chapter 5

Synthesis of UiO-67 BNDC

In this chapter the synthesis and characterization of UiO-67-**BNDC** MOF will be discussed. It starts with details of synthesis methods and continues with discussions around the details of different characterization methods. The characterization methods include PXRD, TGA, Nitrogen Sorption Measurements and its simulations result, NMR analysis, SEM. Some properties of this new Zr-MOF such as thermal stability, pH stability, BET surface etc. will be revealed. This chapter ends up with a summary of the general properties of UiO-67-**BNDC** synthesized under different synthetic conditions.

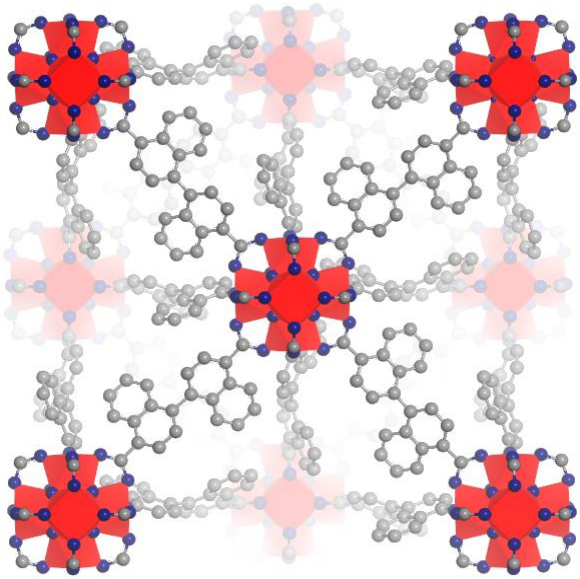

UiO-67-BNDC

5.1 Synthesis of UiO-67-BNDC

General method for synthesis of UiO-67-**BNDC** was according to the similar method[13] for synthesis of UiO-67 MOF. There are three main processes for synthesis the MOF: 1) reaction solution preparation, 2) static heating in an oven for MOF growing, and 3) Isolated the MOF from the solvent and washing MOF with low boiling point solvent and dried the MOF in the oven to get MOF with free pore site.

For synthesis UiO MOF material, the general way for preparing the reaction solution is firstly, dissolve the $ZrCl_4$, water, and modulator (usually is monocarboxylic acid 5-30 eq. with respect to the $ZrCl_4$) in hot DMF with vigorous stirring. Once all the substance is dissolved in the DMF (the solution becomes clear), the organic linker can be added. In order to dissolve the organic linker, the heat may need to be increased. The volume of the DMF used in the preparation is related to the solubility of the organic linker. For the **BNDC** linker used in this study is soluble in a molar ratio of about 1:150 in hot DMF.

Once the reaction solution was ready, the magnet bar can be removed and solution will be transfer to a close container (usually it is a flask with a small cap, in case too much solvent evaporated during the MOF grow stage) and stay in the oven with static heating (typically is 80-130 ^{o}C) for several days. In this course, as mentioned in the previous section (1.2.5), the exchange of chlorides with carboxylate groups from the linker /modulator and hydroxides from water to form intermediate complexes happens.

Finally, the MOF material will precipitate out from the solvent. The precipitate can be collected by decant the most of the solvent. Then the MOF will be washed with other low boiling point solvent (such as methanol, THF) to remove the modulator and the DMF solvent which was trapped in the pores of the MOF.[12] During the washing process, the centrifugation is needed in order to reduce the sample lose. In this study, different washing procedures have been tested and evaluated (more details will be discussed in the next characterization section).

After the washing is done, sample will then be dried in the oven (60 ^{o}C) overnight. The final weight of the sample then can be obtained. The yield of the synthesis then can be calculated. But this yield is not very accurate because there may still have solvent or modulator was trapped in the pores. However, this can give an idea of how efficient the MOF grows if the synthesis condition changed.

The MOF sample can also be synthesized by using two different organic linkers. In this study, the MOFs have been synthesized including powder sample and single crystal of the new MOF with pure **BNDC** linker and a powder sample which using 80% 4, 4'-biphenyldicarboxylate (**BPDC**) linker 20 % **BNDC** linker in the MOF synthesis (more details see section 7.3).

With the dried MOF sample on hand, different properties of the MOF can be measured by the different characterization methods such as PXRD, TGA and N_2 adsorption.

5.2 Characterization

5.2.1PXRD

In the MOF research, the PXRD is a useful tool to check the sample's crystallinity. As mentioned before (2.1.2), each crystalline phase has unique powder diffraction which can be used as fingerprint for the phase. Sample with same structure will have the similar powder diffraction pattern. In this study the sample used for the PXRD is dried sample after washing. Two different sample preparations were used in this study: one is the sample was mounted on the sample holder and covered with a plastic wrap to keep the powder on the plate. The other is the sample was dispersed on the sample holder with 2-propanol, this is the most frequently used method in this study.

In the **Figure 5.1**, the synthesized MOF-67-BNDC-5 sample (use 12 eq. benzoic acid see experimental part, in the next section this after washing and dried sample will mainly be used for the characterization) was compared with the UiO-67 XRD pattern which was obtained from the library of this group.

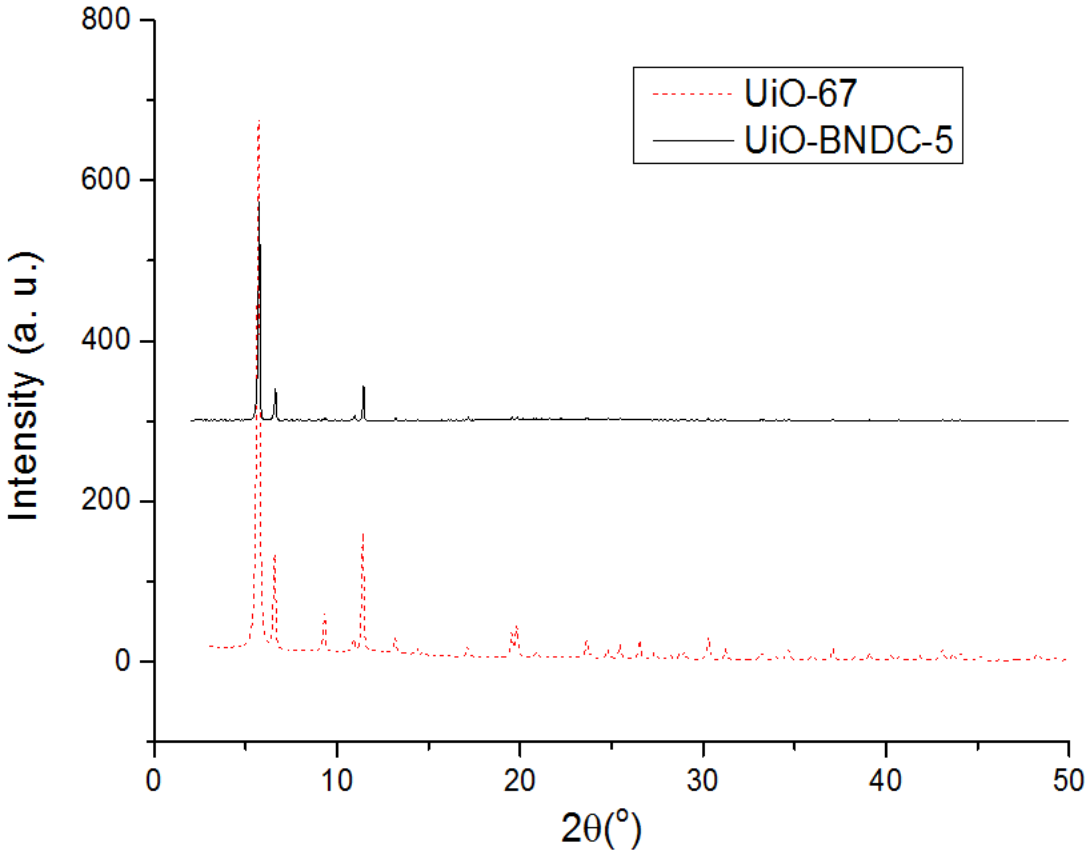

Figure 5.1 PXRD pattern of UiO-67 (bottom) and UiO-67-BNDC-5 (top).

As shown in the **Figure 5.1** this two have quite similar XRD pattern at low angle. According the Bragg' law, it suggests this new MOF have similar long distance connection in the

structure. With this information in hand, the structure of this MOF was built in the material studio by modified the CIF date of the UiO-67. By replacing the organic linker of the UiO-67 to the BNDC linker, the perfect structure was built. This was used to simulate the XRD pattern programme in the materials studio. The perfect XRD pattern was than obtained.

As show in the **Figure 5.2**, the XRD pattern of this UiO-67-BNDC-5 sample fits with the simulated pattern from the material studio very well.

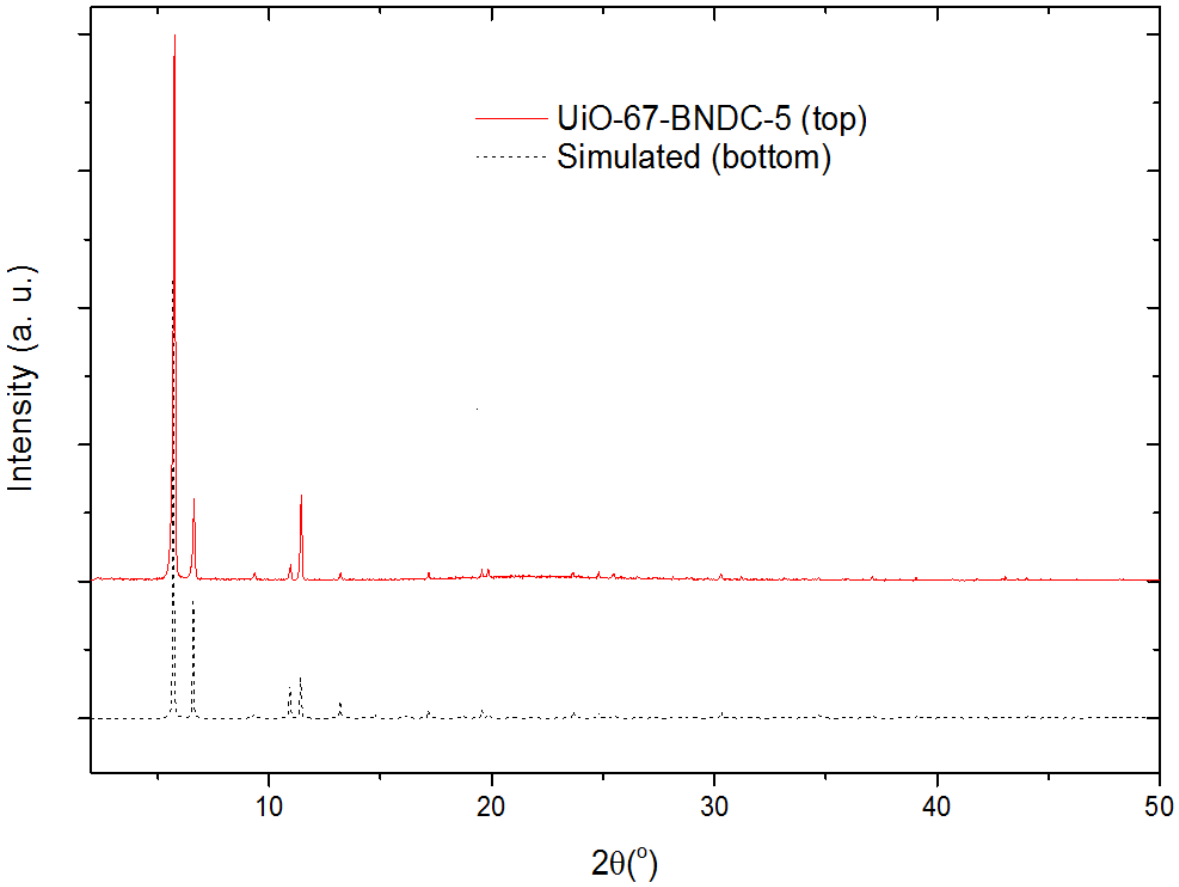

Figure 5.2 PXRD pattern of UiO-67-BNDC-5 with simulated pattern from material studio.

Thus, the XRD pattern of this material shows this new Zr-MOF was obtained with good crystallinity.

5.2.2 NMR

In this study, the NMR can be used for checked the substances (such as solvents, modulator) have trapped in the MOF material. This experiment was done by sink the 15 mg MOF in the 600 µl D_2O (1 M NaOH) overnight in the NMR tube (this was called NMR digest

experiment). By doing this experiment the possible chemicals present in the MOF will be determined.

In the **Figure 5.4** gives the possible chemicals will be presented in the MOF. The reference chemical has the same treatment with MOF sample before getting the NMR spectrum.

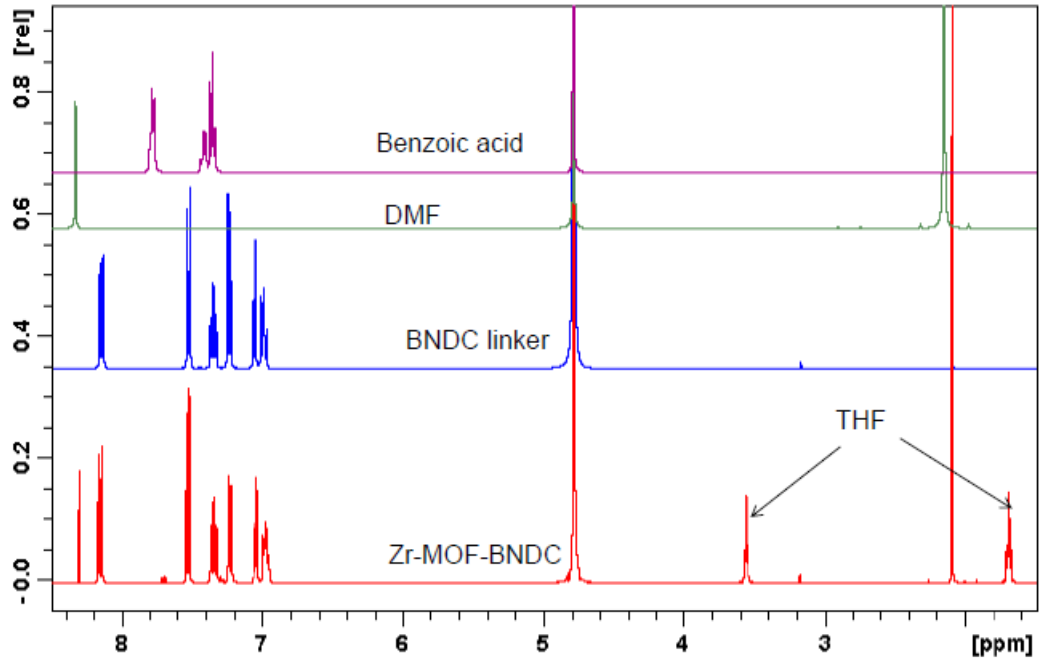

Figure 5.4 NMR spectra of the benzoic acid, DMF, BNCD linker and the MOF in the digested solution (1M NaOH in D_2O).

This spectrum shows this sample after washing treatment still has the modulator (Benzoic acid presents in the sample). The DMF and THF in this sample were detected by NMR shows the solvents were still trapped in the pore.

As this information in hand the integration of each proton in this MOF digest sample can be performed. **Figure 5.5** gives the integration of each proton in the digest sample. By comparing the integration of the protons, the estimated ratio between each chemical and the BNDC can be calculated.

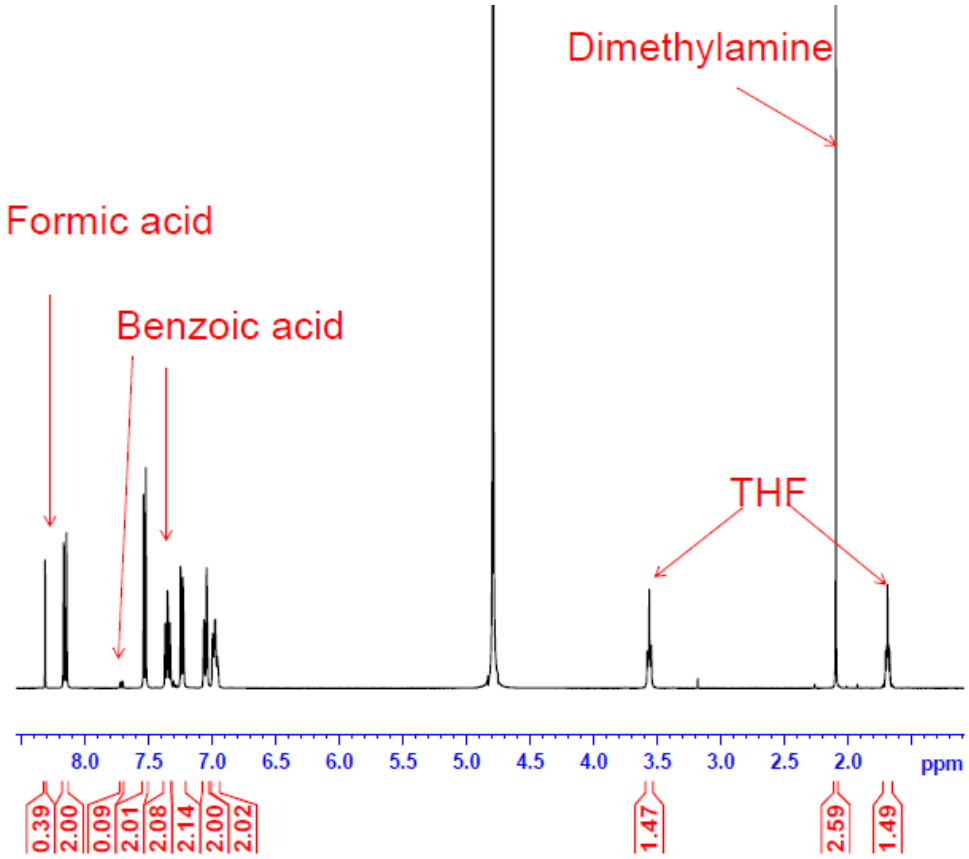

Figure 5.5 The integration of the Zr-MOF-BNDC after the MOF was digested in 1M NaOH in D_2O. BNDC:Benzoic acid:DMF:THF = 1:0.04:0.19:0.78.

The ratio between BNDC and benzoic acid combines the TGA date can be used for calculate ratio of the linker missing in the structure.

5.2.3 TGA

The thermal stability of UiO-67-BNDC was obtained by measure the sample on the Netzsch STA 449 DSC+TG. The sample was measured under 80% N2 and 20% O2. The temperature rises from 25 to 700 with 5^{o}C/min. As the **Figure 5.6** shows that this new MOF has a good thermal stability (up to 440 ℃) and suggests that there is a linker missing in the MOF structure. TGA curves fit the type C curve as mention in chapter 2 (2.2.2). The procedural decomposition temperature of this material is 440 ^{o}C, and the final temperature is close to 500 ^{o}C. The plateau is the region of the TG where the weight is constant, which means the sample is stable under this condition. The drop of the curve at the beginning is due to the solvent was removed. When the temperature increase the dehydration of the cluster happens around at 300 ^{o}C (see 1.1.3).

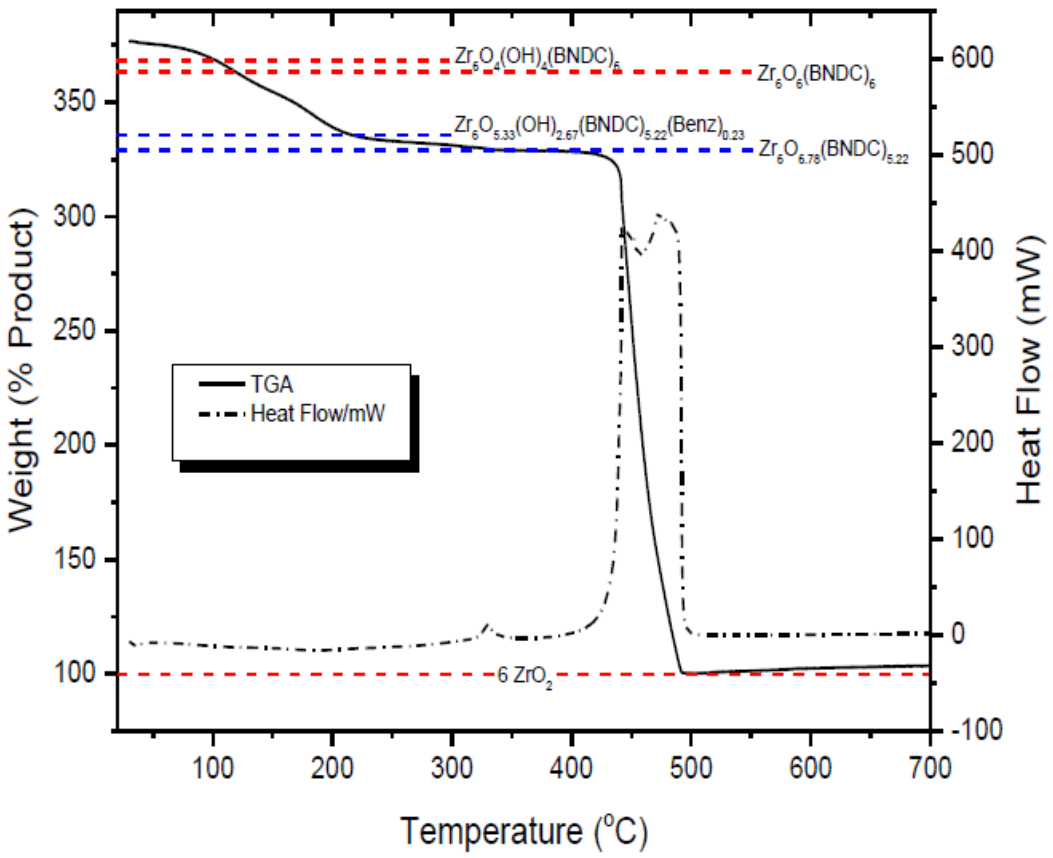

Figure 5.6 TGA curve of the MOF material, measured in 80% N_2 and 20% O_2.

5.2.4 N_2 adsorption

The N_2 adsorption was measured by treated the 12 mg sample under 80°C for 1 h and 2h at 300 °C to empty the pore of the MOF. After that the sample was treated with liquid Nitrogen. Then the adsorption and desorption of N_2 can be measured. This gives the information of the pore volume and BET surface of the MOF material (UiO-67-BNDC-5). (**Figure 5.7**)

This adsorption date fit the Type I b curve in the classification of physisorption isotherms (see section 2.3.1) It suggests that this material has wider micropores. In the **Figure 5.7**, the adsorption and desorption fits very well. The BET surface of this material is 1519 m^2/g (**appendix 3**).

Due to the time constrain the simulated adsorption was not presented in this part.

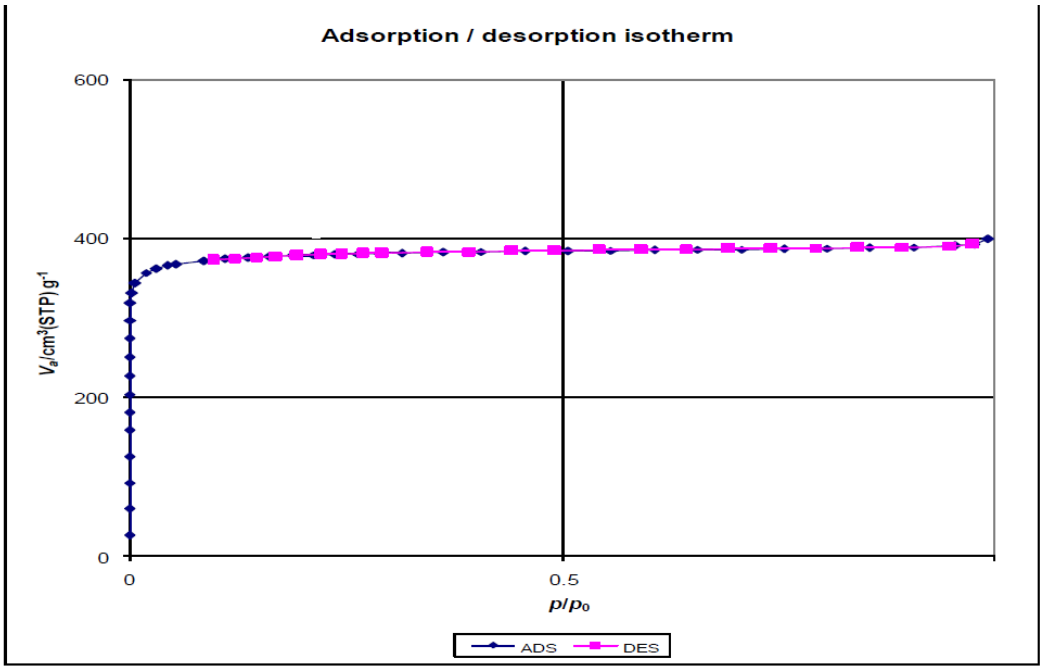

Figure 5.7 Adsorption / desorption isotherm of UiO-67-BNDC-5.

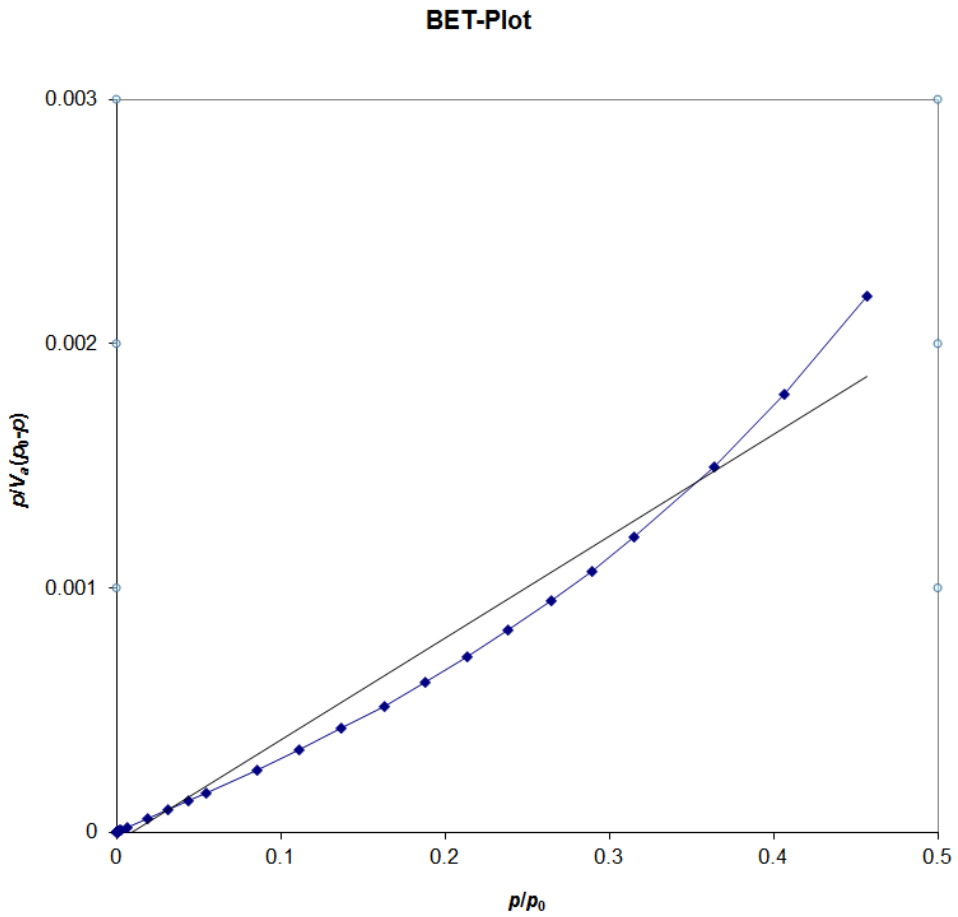

Figure 5.8 BET plot of UiO-67-BNDC-5.

5.2.5 SEM and EDS

The sample Zr-MOF was prepared on the carbon tape and was analyzed by the High resolution SEM (HITACHI SU8200). The sample UiO-67-BNDC-4 was the sample after general washing then treated with water in auto calve at 150 ^{o}C. The morphology of the material can be clearly see from this measure (as show in the **Figure 5.9**,octagedral)

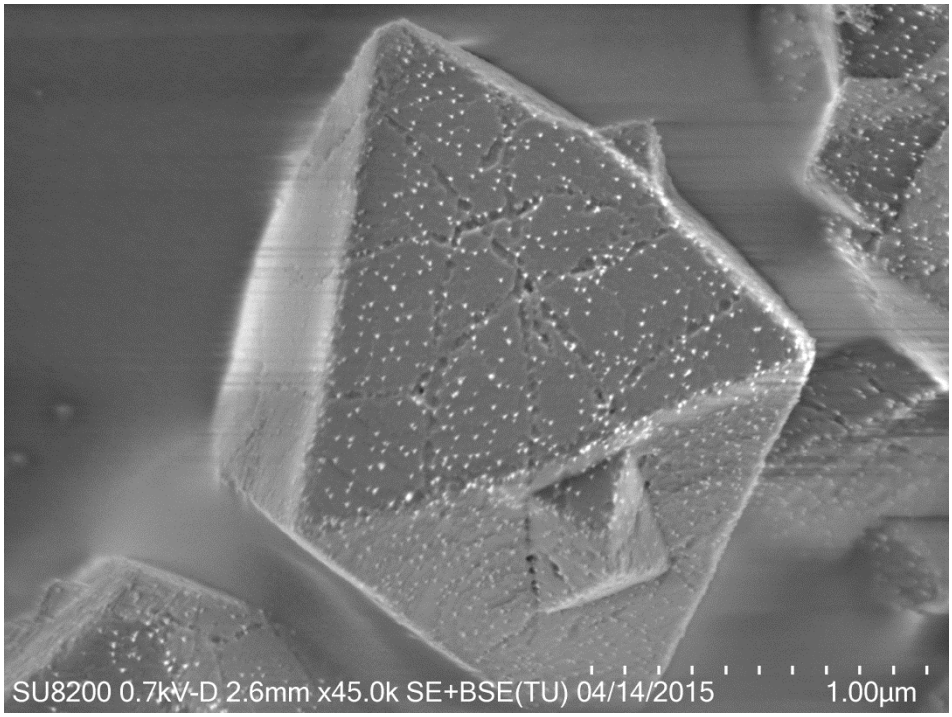

Figure 5.9 SEM image of the UiO-67-BNDC-4 at 1.00 µm.

There is some small bright dots on the surface could be belong to the Zr $(OH)_4$ formed during this process (water treatment with auto clave).

The EDS study of the sample was done to check if other metals were in the material (like Pd from the organic linker synthesis). The sample was mounted on the Cu tape (to reduce the back ground from the sample holder) when did this test. The EDS shows only the Zr is the metal in the sample. Hence is bright is most likely belong to the Zr $(OH)_4$.

5.2.6 Single crystal synthesis

In order to get the single crystal of the MOF many modulator (such as benzoic acid , phenyl acetic acid , 4-nitrobenozic acid) were tried. Only the sample UiO-67-BNDC-7 which was treated with 4-nitrobenozic acid (38 eq.) in Zr: DMF1:150 reaction mixture **Figure 5.11**. The single crystal which was abstained is around 20 µm.

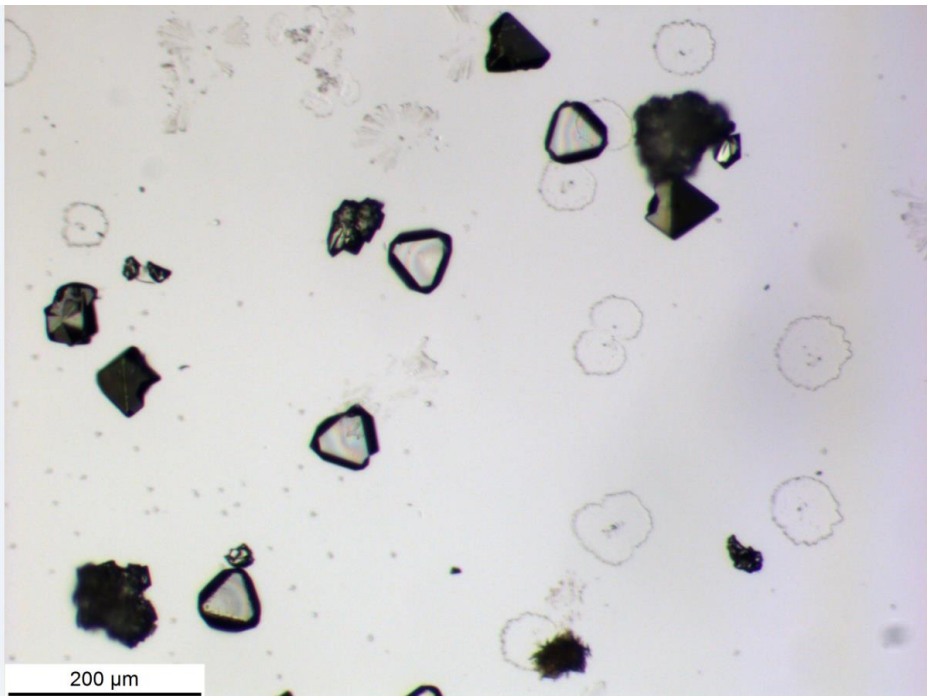

Figure 5.11 Microscope image of the UiO-67-BNDC-7 MOF.

5.2.7 Water stability and pH stability test

The sample UiO-67-BNDC-4 was use for this test. 150 mg at 25 mL water 150 degree in autoclave overnight and XRD pattern was compared with the sample before treatment. **Figure 5.12**

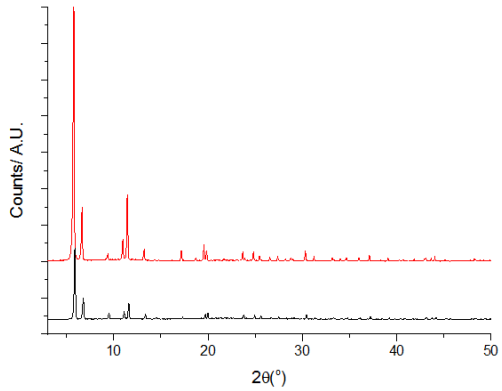

Figure 5.12 XRD of sample water stability test. Top is after water treatment, bottom is raw sample. (Sample UiO-67-BNDC-4)

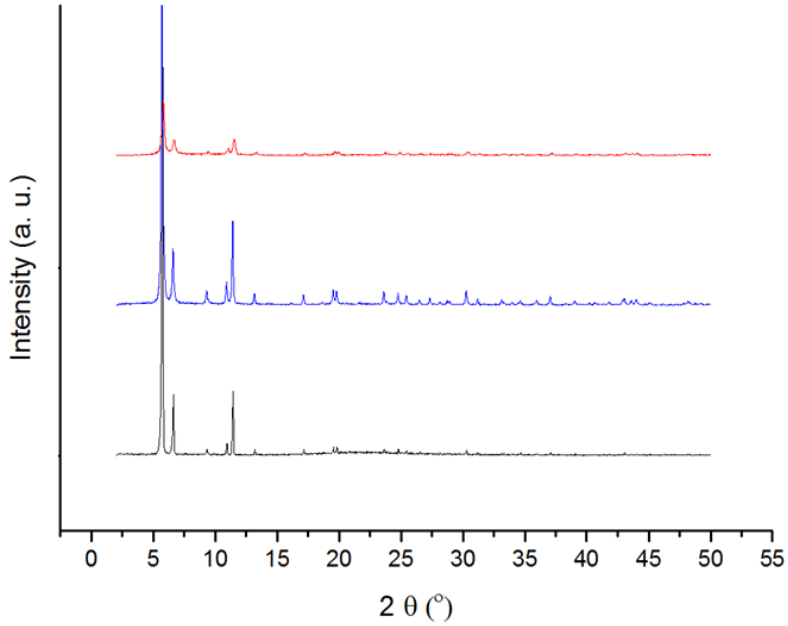

Figure 5.13 XRD of sample pH stability test. Top is after water treatment, bottom is raw sample. (Sample UiO-67-BNDC-4)

Both the pH stability test is done by the follow method: the original samples 100 mgx2 each was stirring in pH=4 and pH=10 buffer solution each for 0.5h and then washed with 15 mLx3 water. Water was removed by centrifugation. The sample was put on the XRD sample hold; let it dry in the air.

The results show that this MOF is stable in water and acid condition little unstable in base.

Chapter 6

Conclusion and future work

6.1 Conclusion

Six step synthesis of **BNDC** have been developed for more than 5 gram scale.

The four step synthesis of the **BNCD** linker is successfully performed in small scale. Further scale up test can be done in the future.

The UiO-67-**BNDC** MOF is water stable MOF and it has BET surface 1519 m^2/g, and it is stable in the acid condition less stable in base. Its thermal stability is around 440 ^oC

6.2 Future work

Further modification for **BNDC** linker synthesis based on the four steps synthetic route can be tested

This new linker can be used in the mix linker synthesis with the organic linker in our group library to see if new mixed linker MOF can be obtained with the interesting property.

Other naphthalene based linkers can be tested in the Zr MOF with different function group in the linker (such as amino group).

Mechanical stability of this material can be tested. The single crystal can be used for the synchrotron experiment in the coming future to get more structure information of this MOF.

Chapter 7

Experimental part

In this chapter both the organic linker synthesis and MOF material synthesis will be presented.

7.1 General

Unless otherwise stated all the reactions were carried out in oven-dried glassware which were cooled under a flow of argon or nitrogen gas. Commercial reagents were purchased from standard Chemical Suppliers and used without further purification. Solvents DMF, THF, CH_2Cl_2 and CH_3CN used in the reactions were dried through MBSPS-800 solvent cleaning system of MBraun. DMSO was dried over 3 Å molecular sieves. Hexane was distilled before use. Ethanol used was absolute ethanol. Tap water was distilled in a GFL 2002 distillatory (Type II water). Other solvents for recrystallization and Flash column chromatography were used as it from commercial source.

The concentrated H_2SO_4 is 98% H_2SO_4 and the concentrated HCl is 37% HCl.

TLC was carried out on Merck silica gel 60 F-254 analytical plates. Flash column chromatography was performed on silica from Merck (60, 0.040-0.063 mm). All chromatography was performed by manually.

NMR spectra were recorded on spectrometers Bruker Avance DPX200 operating at 200 MHz for ^1H. Bruker Avance DPX300 operating at 300 MHz for 1H, Bruker Avance AVII400 operating at 400 MHz for 1H and 100 MHz for ^{13}C NMR. Chemical shifts are given in parts per million (ppm, δ scale), coupling constants (J) and in Hertz (Hz). All the spectra were recorded at 293K. The spectra were calibrated using the residual peak of solvent as internal standard [$CDCl_3$ ($CHCl_3$ δ_H 7.26 ppm, $CDCl_3$ δ_C 77.1 ppm), DMSO-d_6 (DMSO-d_5 δ_H 2.49 ppm, DMSO-d_6 δ_C 40.0 ppm). For some compounds DEPT135, HMQC, HMBC were used for assigning ^1H and ^{13}C.

Mass spectra were recorded on a Micromass QTOFII spectrometer (ESI) and on a Fision VG Prospec sector instrument at 70eV (EI) operated by Osamu Sekiguchi.

N_2 adsoprtion experiments were performed on the Belsorp mini II adsorption instrument.

XRD were recorded on a Bruker D8 Discovery diffractionmeter with a bruker LYNXEYE detector

TGA were measure on Netzsch STA 449 DSC+TG

SEM measurement was performed on High resolution SEM (HITACHI SU8200)

7.2 1- bromo-2-napthoic acid (3)

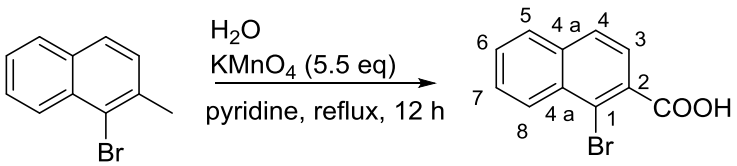

3

Procedure A [68] :

1-bromo-2-methylnapthalene (0.42 mL, 2.71 mmol, 1.0 eq.) and pyridine (6.7 mL) were mixed, and $KMnO_4$ (1038 mg, 6.57 mmol) and H_2O (0.8 mL) was added in 10 min. After finishing addition, H_2O (1.6 mL) were added. The mixture were stirring at reflux for 2 h, and then $KMnO_4$ (333 mg, 2.11mmol, 0.78 eq.) in H_2O (1.0 mL) was added four times every 30 min. After the fourth time addition, distilled water (6.7 mL) was added and the mixture was refluxed for 12 h. The mixture was filtered while and washed with distilled water (3x30 mL) the filtrate was concentrated and then the solution was acidified to pH=0 by adding 3 M HCl (aq) in the ice bath. The precipitate was isolated by suction filtration was washed by water and dried in 110 ^oC overnight. A light brown solid (99 mg, 0.39 mmol) was obtained. Yield: 14 %.

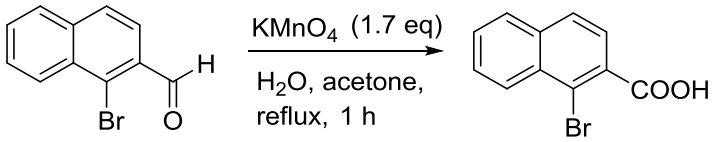

5 **3**

Procedure B [69] :

Compound **5** (589 mg, 2.51 mmol, 1.0 eq.) was dissolved in acetone (5.4 mL) and heated at reflux. $KMnO_4$ (674 mg, 4.0 mmol, 1.7 eq.) was dissolved in H_2O (10.5 mL) and the solution was added to the reaction mixture by dropping funnel for 15 min. The resulting mixture was refluxed for 1 h. The mixture was filtered while hot and washed with acetone (2x10 mL), the filtrate was concentrated then diluted by H_2O (15 mL). The mixture was cooled to 0 ^oC in ice/water bath and acidified by slowly added HCl (37 %). The precipitate was isolated by suction filtration was washed by water and dried in 110 ^oC overnight. A light brown solid (240 mg, 0.95 mmol) was obtained. Yield: 38 %.

^{1}H-NMR (400 MHz, DMSO-d_6) δ: 13.63 (br s, 1H, -COO<u>H</u>), 8.32 (d, *J* = 8.3 Hz, 1H, C_8-H), 8.04-8.06 (m, 2H, C_5-H, C_3-H), 7.76 (td, *J* = 8.3, 1.4 Hz, 1H, C_7-H), 7.68-7.72 (m, 2H, C_6-H, C_4-H).

^{13}C-NMR (100 MHz, DMSO-d_6) δ: 168.9 (-<u>C</u>OOH), 134.8 (C-4a), 133.9 (C-8a), 131.7 (C-1), 129.1 (C-7), 129.0 (C-8), 128.7 (C-3), 128.5 (C-5), 127.8 (C-6), 125.8 (C-4), 120.2 (C-2).

MS (EI, DMSO) m/z (rel%): 252/250 (M^+,99/100), 235/233 (M^+-OH, 36/37), 207/205 (M^+-COOH, 13/13), 126 (M^+-HCO_2Br, 50), 115 (14), 74(6), 63 (12).

The spectroscopic data were in accordance with the literature.[73]

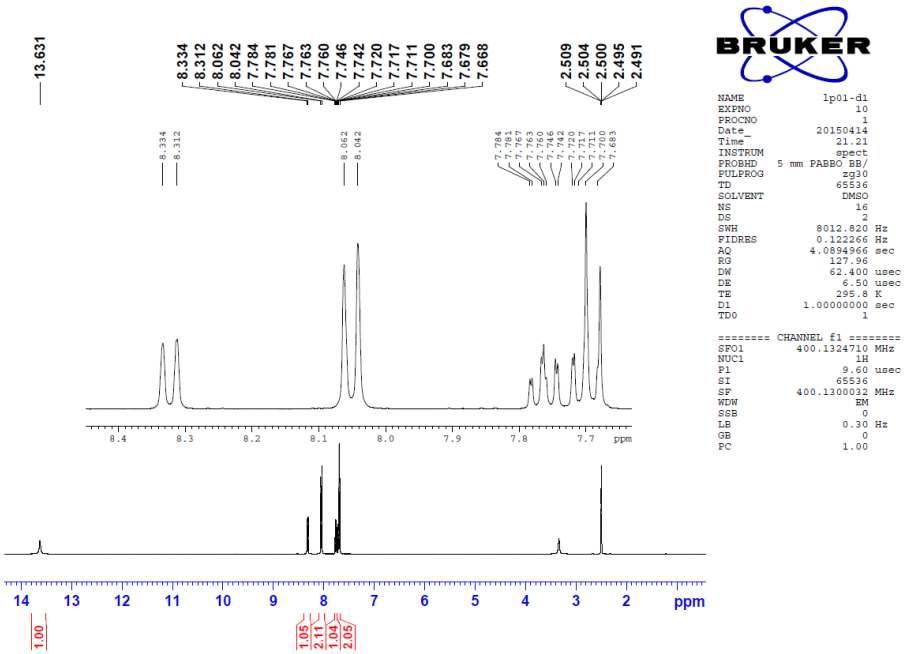

Figure 7.1 ^{1}H-NMR spectrum of compound **3**.

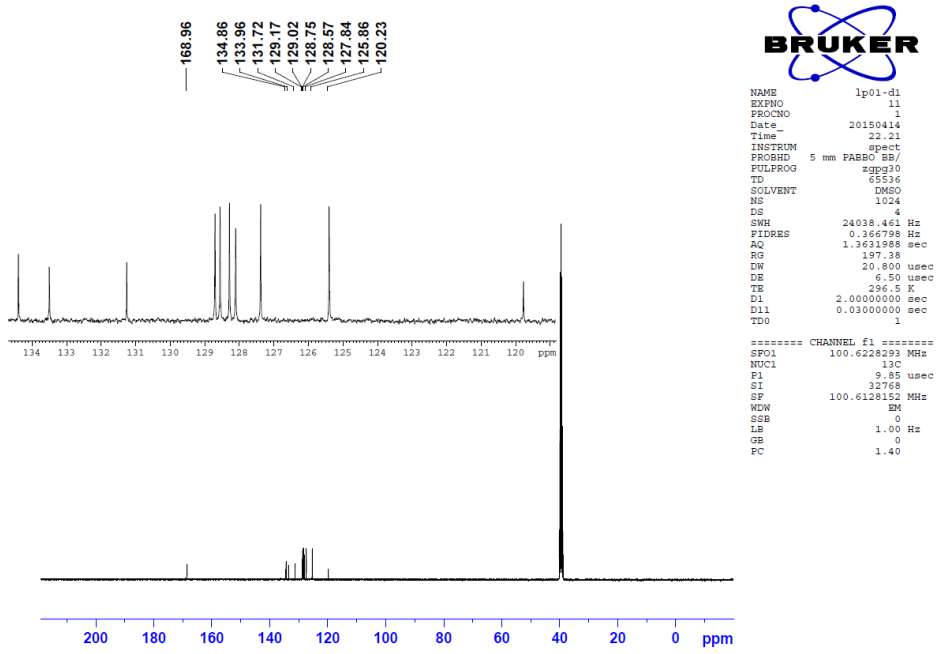

Figure 7.2 ^{13}C-NMR spectrum of compound **3**.

7.3 1- bromo-2-(dibromomethyl) naphthalene (4)

Table 4.3 from **Chapter 4** is reproduced below as **Table 7.1**.

Table7.1 Bromination conditions for synthesis compound **4**.

Entry	Scale mmol	Reaction condition	Results
1	2.7	2.3 eq NBS, 17 mol % BPO, CCl_4 reflux for 24 h	34 % yield
2	2.7	3.5 eq NBS, 18 mol % BPO, CCl_4 reflux for 46 h	contains mono brominated compound
3	2.7	4.0 eq NBS, 1.8 mol % AIBN, CCl_4, reflux for 43 h	contains mono brominated compound (use for next reaction)
4	10.8	4.0 eq, NBS , 2.6 mol % AIBN, CCl_4, reflux 29 h	77 % yield

Procedure[73]A (for **entry 1** and **entry 2**, here use **entry 1** as an example):

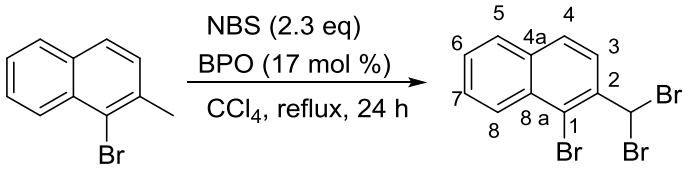

4

A suspension of 1-bromo-2-methylnaphthalene (600 mg, 2.7 mmol, 1.0 eq.), *N*-bromosuccinimide (1108 mg, 6.2 mmol, 2.3 eq.) and benzoyl peroxide (111 mg, 0.46 mmol, 0.17 eq.) in anhydrous CCl_4 (13 mL) was refluxed under N_2 atmosphere for 24 h. The TLC shows two main spots (hexane as eluent). After cooling to room temperature, the suspension was filtered off and washed with CCl_4 (3x10 mL). The mixture was washed with saturated Na_2SO_3 (13 mL) and the yellow organic layer was dried over Na_2SO_4. The organic solvent was evaporated and the resulting yellow solid was purified by silica gel chromatography (DCM: Hexane=1:200) to give a white solid (350 mg, 0.92 mmol). Yield: 34 %.

Procedure B (for **entry 3** and **entry 4**, here use **entry 4** as an example):

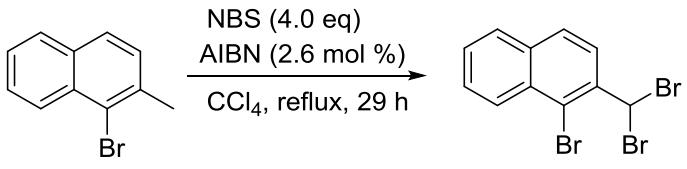

4

A suspension of 1-bromo-2-methylnaphthalene (2400 mg, 10.8 mmol, 1.0 eq.), *N*-bromosuccinimide (1929 mg, 10.8 mmol) and AIBN (6.8 mg, 0.04 mmol, 0.003 eq.) in anhydrous CCl_4 (13 mL) was refluxed under N_2 atmosphere. The mixture was stirring at reflux for 5 h, and then *N*-bromosuccinimide (1929 mg, 10.8 mmol) and AIBN (6.8 mg, 0.04

mmol, 0.003 eq.) were added four times every 3 h. After 22 h, the AIBN (6.8 mg, 0.46 mmol, 0.003 eq.) were added 2 times every 5 h. The resulting mixture continued refluxing for 7 h. After cooling to the room temperature, the suspension was filtered off and washed with CCl_4 (3x50 mL). The mixture was washed with saturated $NaHSO_3$ (60 mL) and the yellow organic layer was dried over Na_2SO_4. The organic solvent was evaporated and the resulting yellow solid was purified by silica gel chromatography (DCM: Hexane=1:200) to give a white solid (3.15 g, 8.3 mmol). Yield: 77 %.

^{1}H-NMR (600 MHz, $CDCl_3$) δ: 8.31 (d, *J* = 8.4 Hz, 1H, C_8-H), 8.07 (d, *J* = 8.7 Hz, 1H, C_3-H), 7.90 (d, *J* = 8.7 Hz, 1H, C_4-H), 7.84 (d, *J* = 8.4 Hz, 1H, C_5-H), 7.65 (td, *J* = 7.6, 0.8 Hz, 1H, C_7-H), 7.58 (td, *J* = 7.6, 0.8 Hz, 1H, C_6-H), 7.50 (s,1H, -C<u>H</u>Br_2).

^{13}C-NMR (150 MHz, $CDCl_3$) δ: 138.1 (C-4a) 134.8 (C-8a), 131.4 (C-1), 129.1 (C-7), 128.6 (C-8), 128.5 (C-3), 128.4 (C-5), 128.1 (C-6), 126.9 (C-4), 119.7 (C-2), 41.3 (-<u>C</u>HBr_2).

MS (EI, CH_2Cl_2) m/z (rel%): 382/380/378/376 (M^+, 2/6/6/2), 301/299/297 (M^+-Br, 48/100/50), 139 (M^+-3Br, 66), 70 (20), 63 (6).

The spectroscopic data were in accordance with the literature.[73]

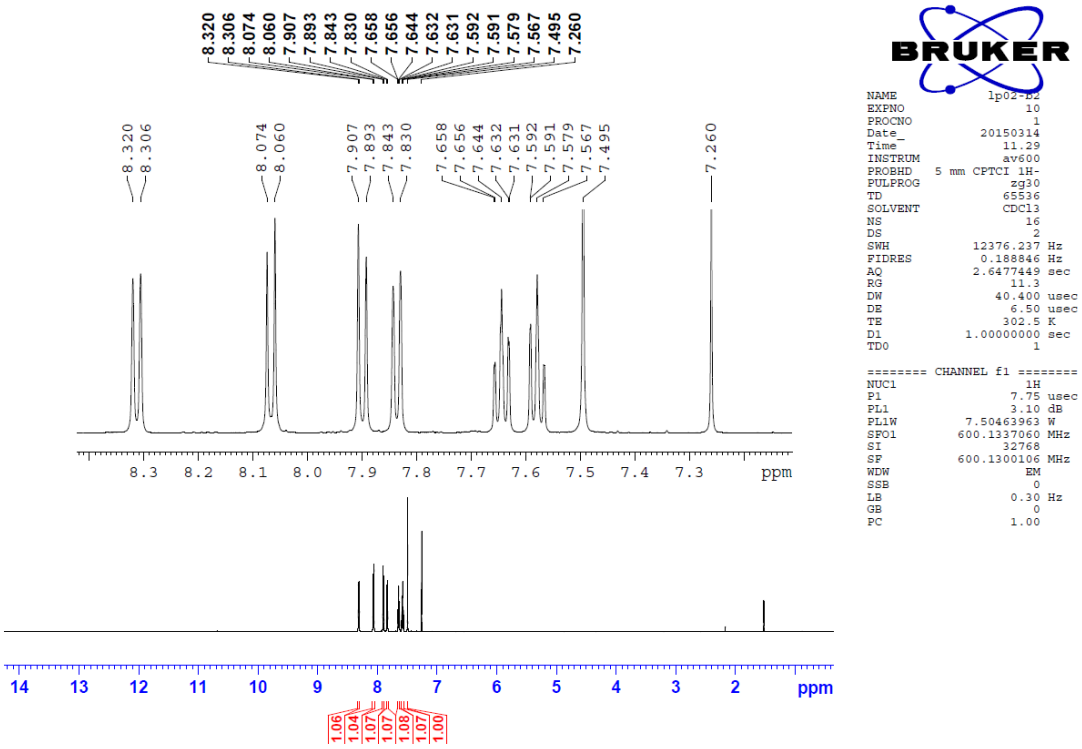

Figure 7.3 ^{1}H-NMR spectrum of compound **4**.

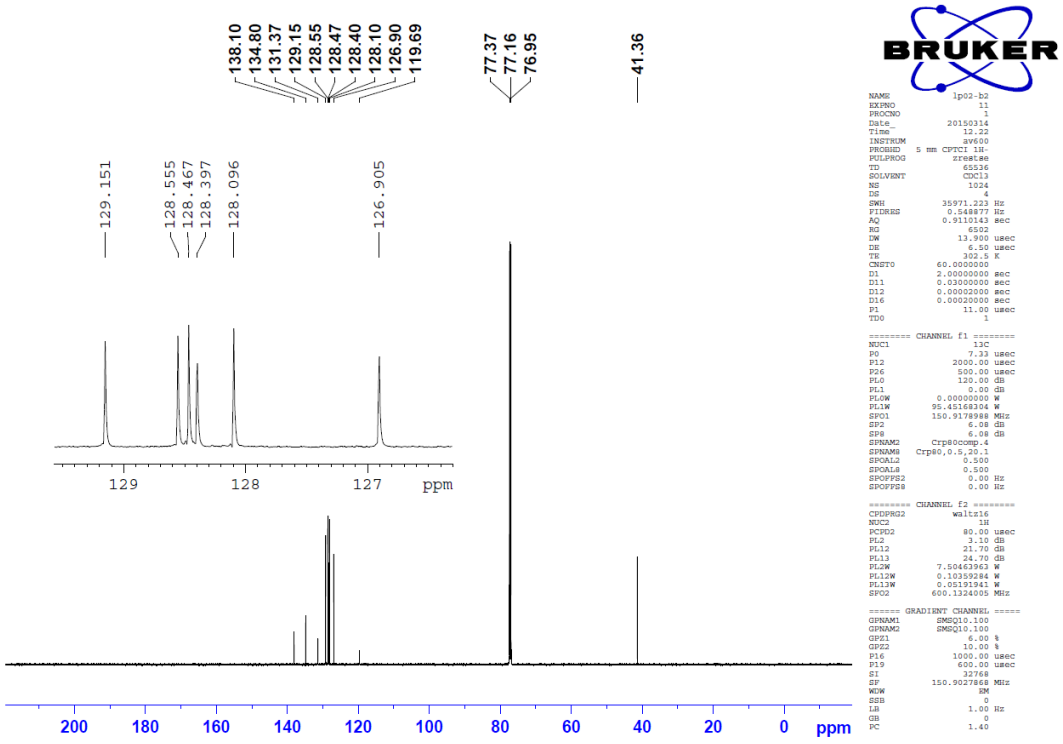

Figure 7.4 ^{13}C-NMR spectrum of compound **4**.

7.4 1-bromo-2-naphthalenecarbaldehyde (5)

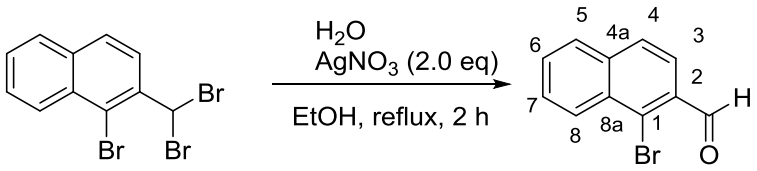

4 **5**

1-bromo-2-(dibromomethyl) naphthalene (3.14 g, 8.29 mmol, 1.0 eq.) and ethanol (300 mL) were placed in an oven dried 500 mL round bottom flask. A solution of $AgNO_3$ (2.81 g, 16.58 mmol, 2.0 eq.) in H_2O (75 mL) was added thereto and the mixture was heated at reflux for 2 h. The white yellow mixture gave a green precipitate in the solution. The green precipitate was filtered off under reduced pressure while the mixture was still hot. The solid washed with hot THF. The organic phases were combined and evaporated under vacuum. The resulting crude was washed with H_2O (60 mL) and CH_2Cl_2 (3x60 mL). The organic phase was separated and dried over Na_2SO_4. The solvent was removed and the crude solid was recrystallized from ethyl acetate and hexane (5:95, 40 mL). A yellow solid (1.52 g, 6.46 mmol) was obtained. Yield: 78 %.

^{1}H-NMR (600 MHz, $CDCl_3$) δ: 10.67 (s, 1H, -C<u>H</u>O), 8.49-8.51(m, 1H, C_8-H), 7.93 (d, *J* = 8.5 Hz, 1H, C_5-H), 7.84-7.88 (m, 2H, C_3-H, C_7-H), 7.66-7.70 (m, 2H, C_4-H, C_6-H).

^{13}C-NMR(150 MHz, $CDCl_3$) δ: 192.9 (d, *J* = 7.8 Hz, -<u>C</u>HO), 137.4 (s, C-4a), 132.3 (s,C-8a), 131.5 (s, C-1), 131.3 (d, C-7), 129.9 (d, C-8), 128.6 (d, C-3), 128.4 (d, C-5), 128.3 (d, C-6), 128.2 (d, C-4), 124.2 (s, C-2).

MS (EI, CH_2Cl_2) m/z (rel%): 236/234 (M^+, 97/100), 235/233 (M^+-H, 86/76), 207/205 (M^+-HCO, 21/21), 126 (M^+-HCOBr, 97), 99 (7), 87 (5), 76 (10), 63 (16), 50 (7).

The spectroscopic data were in accordance with the literature.[73]

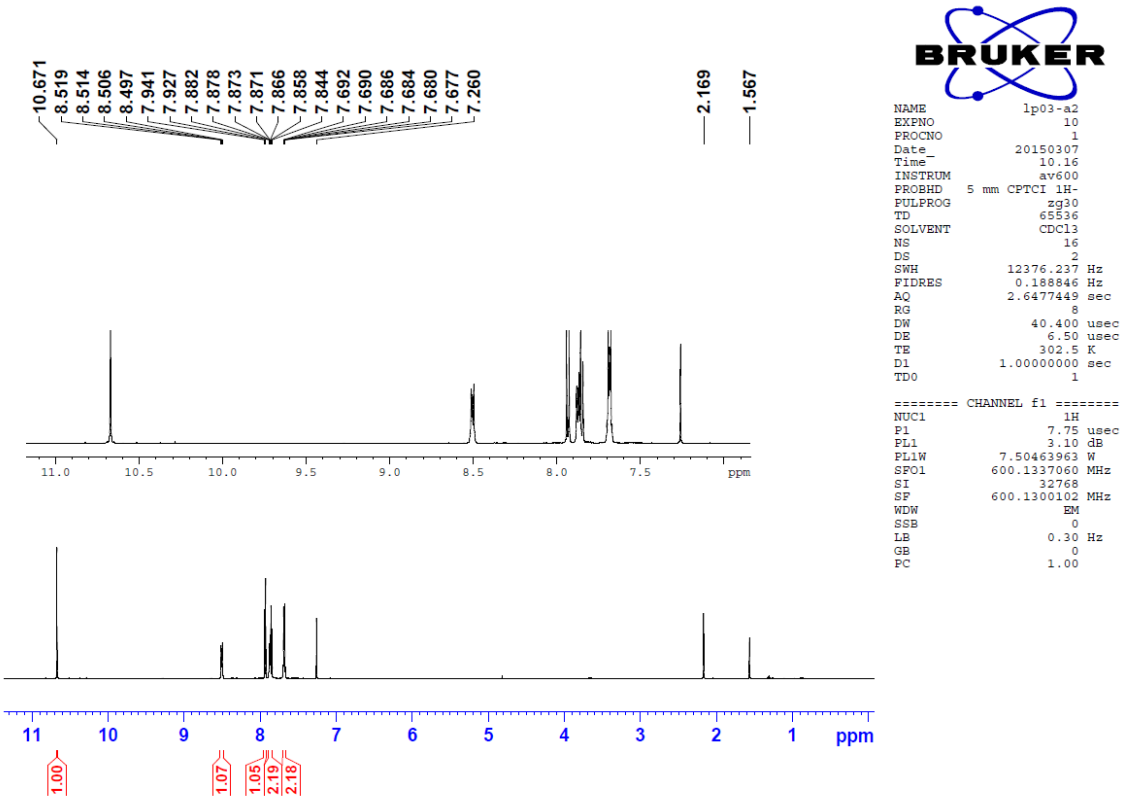

Figure 7.5 ^{1}H-NMR spectrum of compound **5**.

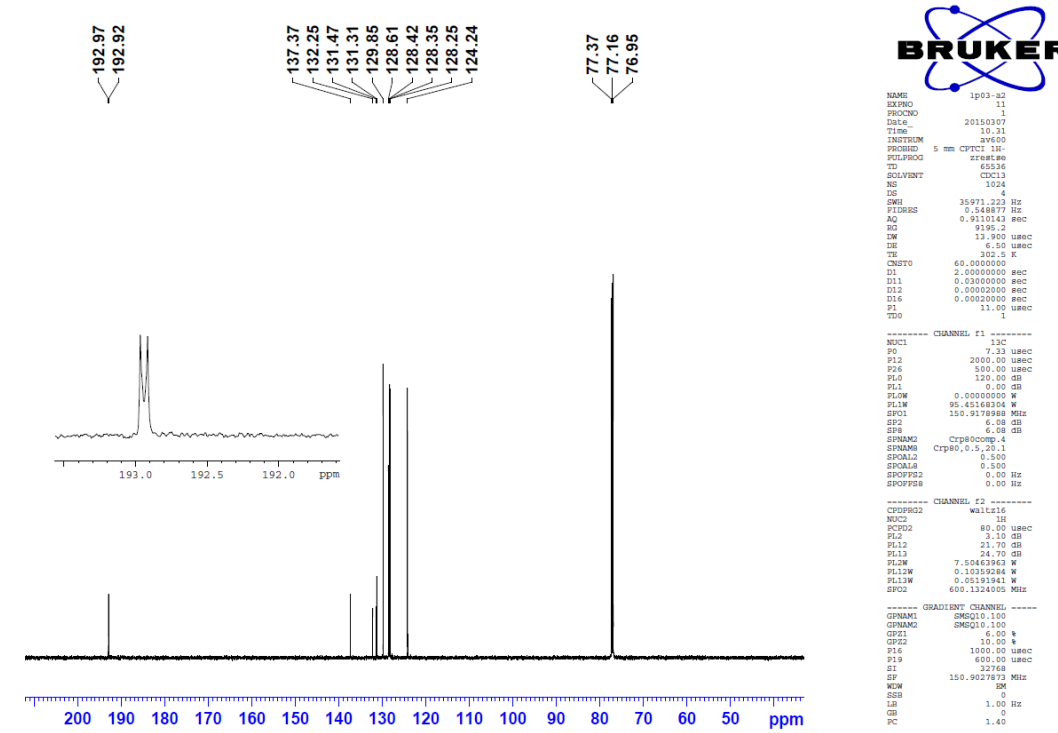

Figure 7.6 ^{13}C-NMR spectrum of compound **5**.

7.5 1-bromo-4-(dibromomethyl) naphthalene (6)

Table 4.4 from **Chapter 4** is reproduced below as **Table 7.2**.

Table 7.2 Synthesis conditions for compound **6**.

entry	Scale mmol	Reaction condition	result
1	2.7	4.0 eq NBS, 2.5 mol% AIBN, CCl_4 reflux for 31 h	28 % yield
2	2.7	2.5 eq NBS, 4.9 mol% BPO, CCl_4 reflux for 13.5 h	50 % yield
3	13.5	2.5 eq NBS, 4.9 mol% BPO, CCl_4 reflux for 14.5h	49 % yield
4	27.0	2.5 eq NBS, 4.9 mol% BPO, CCl_4 reflux for 20 h	47 % yield
5	27.0	2.5 eq NBS, 4.9 mol% BPO, CCl_4 reflux for 20 h	crude used for next step
6	27.0	2.1 eq NBS, 4.9 mol% BPO, CCl_4 reflux for 20 h	48 % yield

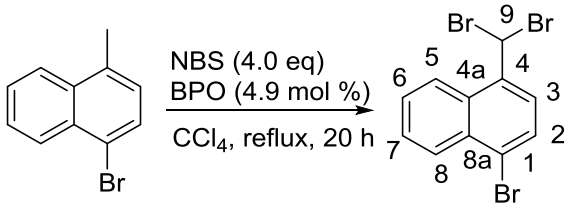

6

(Procedure is similar as prepare compound **4**, here use **entry 6** as an example)

A suspension of 1-bromo-4-methylnaphthalene (6.0 g, 27.1 mmol, 1.0 eq.), *N*-bromosuccinimide (10.1 g, 56.9 mmol, 2.1 eq.) and benzoyl peroxide (344.8 mg, 1.3 mmol, 0.05 eq.) in CCl_4 (100 mL) was refluxed under N_2 atmosphere for 20 h. After cooling to room temperature, the suspension was filtered off, washed with chloroform. The mixture was washed with saturated Na_2SO_3. And the yellow organic layer was dried over Na_2SO_4. The organic solvent was evaporated and the resulting yellow solid was purified by silica gel chromatography (100 % hexane) to give a yellowish white solid which was recrystallized from hexane to give a white solid (5.0 g, 13.1 mmol). Yield: 48%.

^{1}H-NMR (400 MHz, $CDCl_3$) δ: 8.40-8.37 (m, 1H), 8.37-8.35 (m, 1H), 7.85-7.77 (m, 1H), 7.76-7.65 (m, 4H), 7.34 (br s, 1H, C_9-H).

^{13}C-NMR (100 MHz, $CDCl_3$) δ: 136.15 (s, C-4), 129.2 (s, C-8a), 128.3 (s, 3C, C-2, C-8), 127.9 (s, 2C, C-3, C-6), 127.6 (s, C-3) 126.1 (s, C-1) 37.9 (s, C-9).

EI-MS (CH_2Cl_2) 382/380/378/376 (M^+, 1/5/5/1), 301/299/297 (M^+-Br, 50/100/52), 139 (M^+-3Br, 55), 70 (18), 63 (6).

No reported NMR data

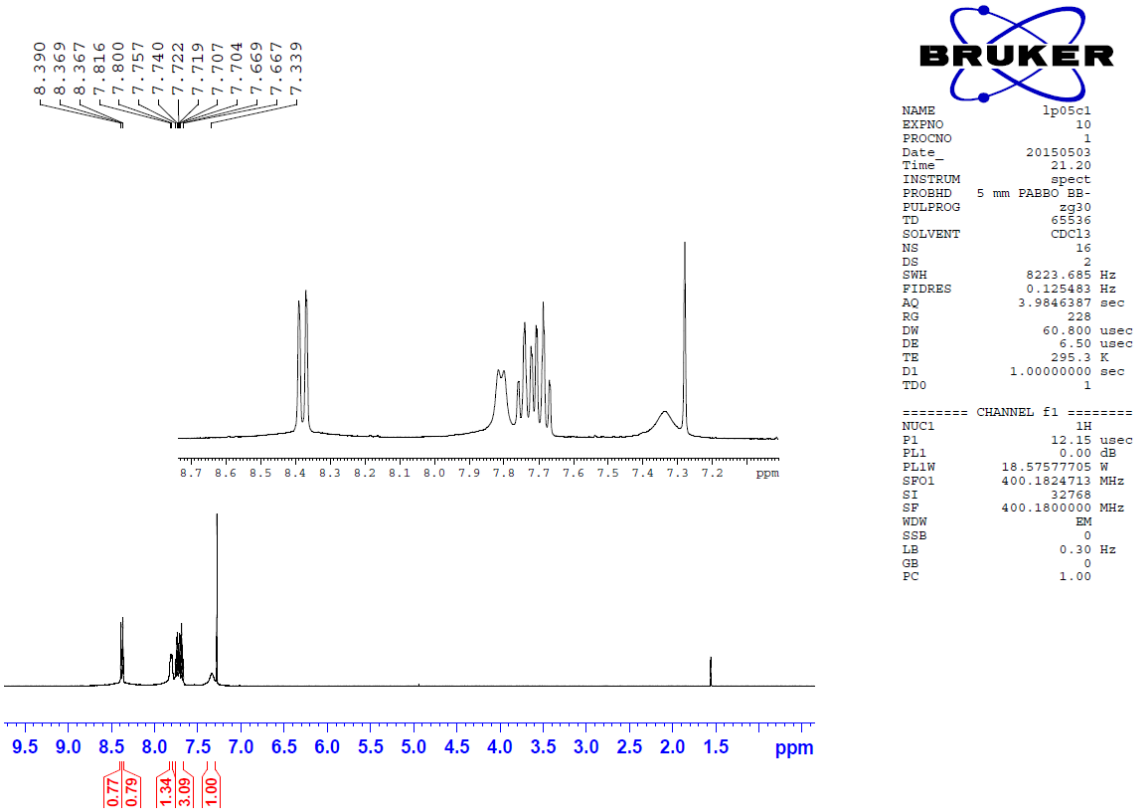

Figure 7.7 ^{1}H-NMR spectrum of compound **6**.

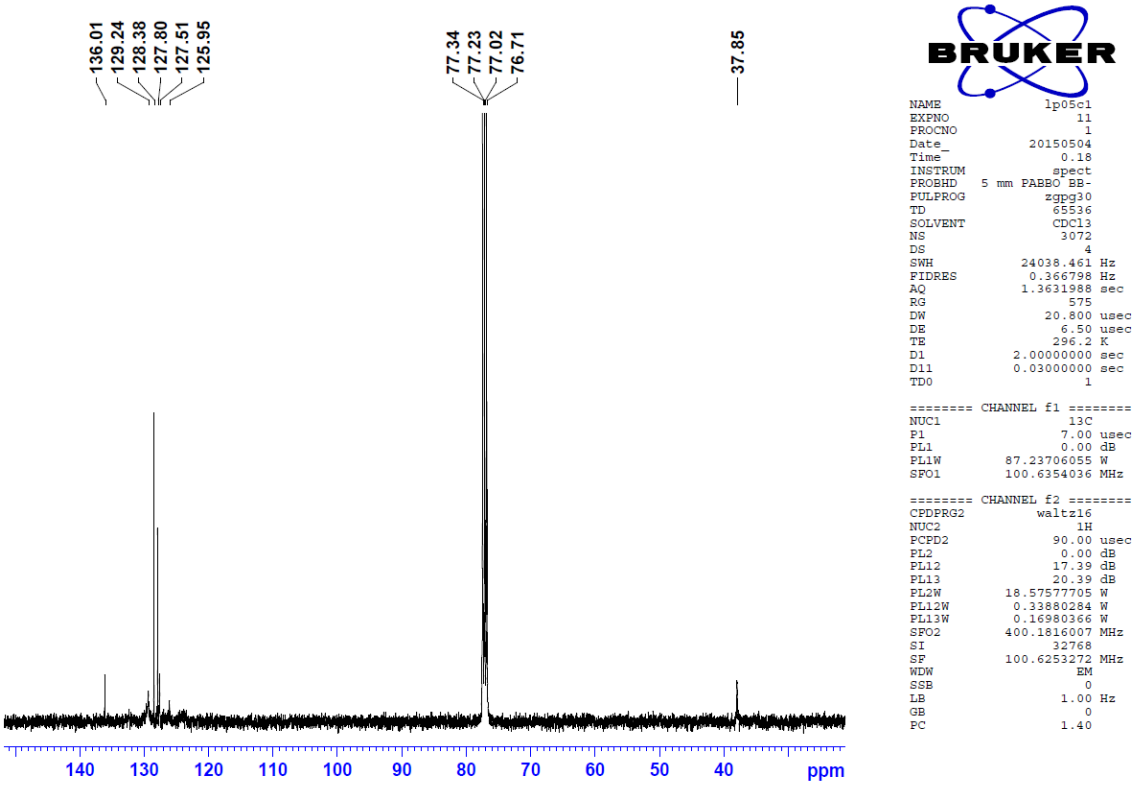

Figure 7.8 ^{13}C-NMR spectrum of compound **6**.

7.6 4-bromo-1-naphthaldehyde (7)

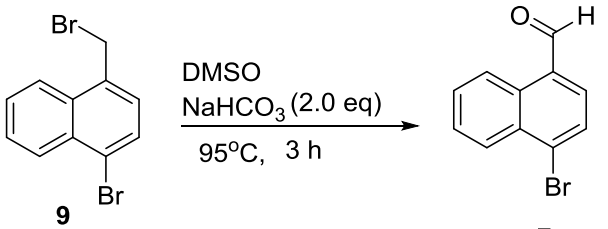

9 **7**

Procedure A[83]

To a dry round bottom flask (500 mL) added 1-bromo-4-(bromomethyl) naphthalene (18.3g, 60.1 mmol, 1.0 eq), DMSO (170 mL), $NaHCO_3$ (10.1 g, 120.7 mmol, 1.97 eq.). The pale yellow reaction mixture was heated at 95 ^oC for 3 h. Then the mixture was cooled to room temperature, diluted with water (400 mL), and extracted by ethyl acetate (3x400 mL). The organic layer was collected and dried over Na_2SO_4. The solvent was removed and the crude solid was purified by silica gel chromatography (3 % ethyl acetate in hexane) to give a pale yellow solid (7.5 g, 31.9 mmol). Yield: 52 %.

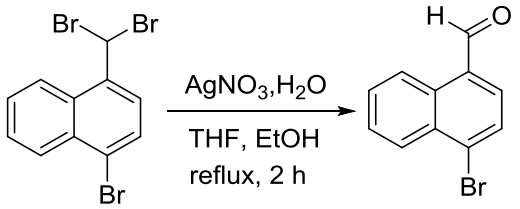

6 **7**

Procedure B [77]

1-bromo-4-(dibromomethyl) naphthalene (2.2 g, 5.9 mmol, 1.0 eq.) in THF (18 mL) and ethanol (27 mL) were heated at reflux, and a solution of silver nitrate (3.0 g, 17.14 mmol, 2.9 eq.) in H_2O (9.0 mL) was added drop wise. The mixture turned yellow and was kept at reflux for 2 h, and green solid precipitated in the mixture. The green precipitate was filtered off under reduced pressure while the mixture was still hot and then the green precipitate washed with hot THF. Organic mixtures were combined and the evaporated under vacuum. The resulting crude was washed with H_2O (60 mL) and CH2Cl2 (3x60 mL). The organic phase was separated and dried over Na_2SO_4. The solvent was removed and the crude solid was washed on the silica by using ethyl acetate and hexane (5: 95) under reduced pressure. The product was recrystallized from ethyl acetate and hexane (5: 95) to give pale yellow solid (1.08 g, 4.5 mmol).Yield: 77 %

^{1}H-NMR (600 MHz, $CDCl_3$) δ: 10.38 (s, 1H, -C<u>H</u>O), 9.28 (d, *J* = 8.6 Hz, 1H), 8.37 (dd, *J* = 8.5, 0.6 Hz, 1H), 7.98 (d, *J* = 8.0 Hz, 1H), 7.81 (d, *J* = 8.0 Hz, 1H), 7.76-7.69 (m, 2H).

^{13}C-NMR (150 MHz, $CDCl_3$) δ: 192.7, 136.2, 132.3, 131.6, 131.4, 131.1, 129.9, 129.5, 128.4, 127.9, 125.2.

MS (EI, CH_2Cl_2) m/z (rel%): 236/234 (M^+, 97/100), 235/233 (M^+-H, 68/57), 207/205 (M^+-HCO, 26/24), 126 (M^+-HCOBr, 91), 99 (8), 87 (6), 76 (10), 63 (24), 50 (9).

The spectroscopic data were in accordance with the literature.[83]

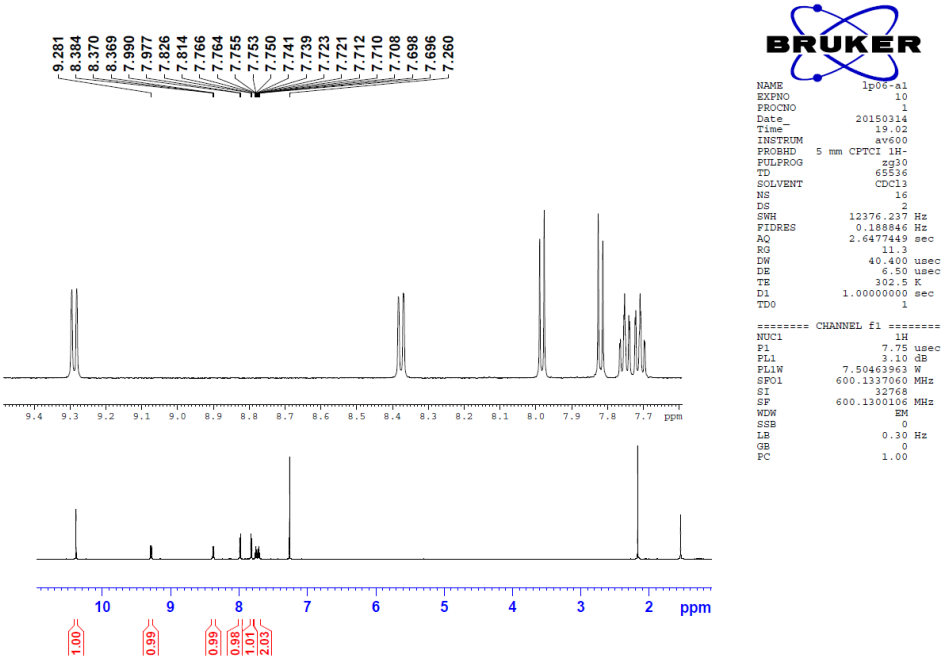

Figure 7.9 ^{1}H-NMR spectrum of compound **7**.

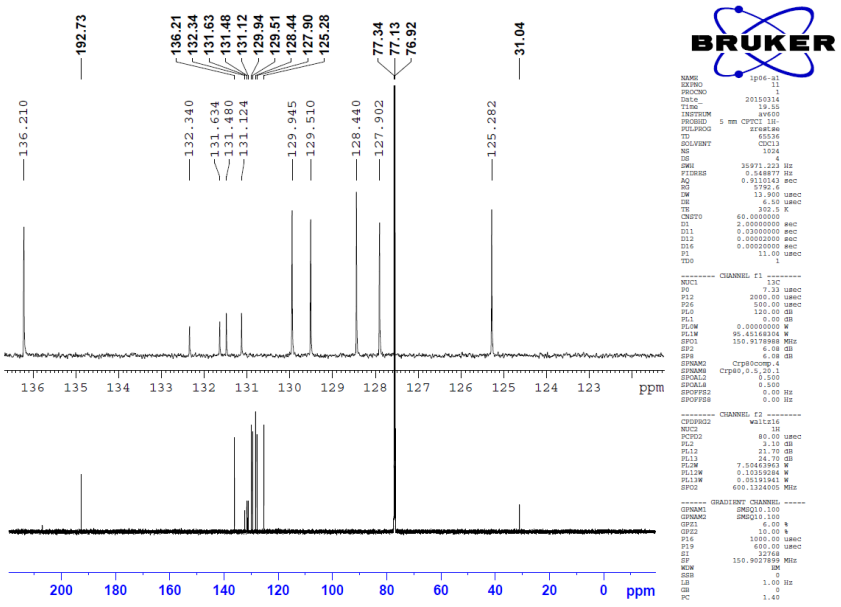

Figure 7.10 ^{13}C-NMR spectrum of compound **7**.

7.7 1,1'-binaphthyl-4,4'-dicarboxaldehyde (8)

Table 4.5 from **Chapter 4** is reproduced below as **Table 7.3**.

Entry	$PdCl_2$(dppf) mol%	Solvent	Reaction time h	Temperature ^oC	Yield %
1	4	DMSO	14	80	92
2	1	DMSO	41	80	51
3	1	DMSO	89	80	70
4	1	DMF	62	80-90	54
5	0.5[a]	DMF	108	90	45

Here use **entry 3** as an example, the procedure [78] is similar.

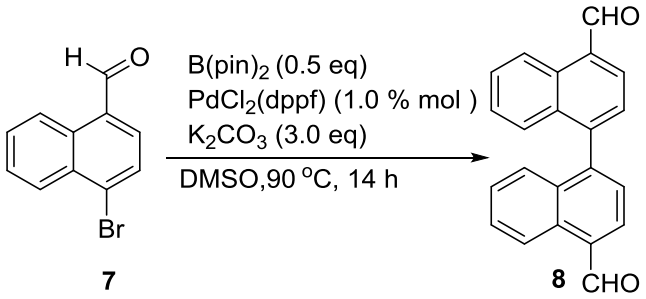

7 **8**

To a dry flask with argon atmosphere were added 4-bromo-1-naphthalenecarbaldehyde (235.1 mg, 1.0 mmol, 1.0 eq.), bis(pinacolato)diboron (128.4 mg, 0.5 mmol, 0.5 eq.), $PdCl_2$(dppf)**.** CH_2Cl_2 complex (8.2 mg, 0.01 mmol, 1% mol), and K_2CO_3 (419.7 mg, 3.0 mmol, 3.0 eq.). The light organge mixture was kept on stirring at 80^{o}C for 89 h. The mixture was cooled to room temperature, diluted by water (50 mL) and extracted with CH_2Cl_2 (30 mL). This was washing with NaOH (aq, 20%, 15 mL) and H_2O (3X50 mL), and the organic phase were dried over Na_2SO_4. The solvent was removed and the crude solid was purified by silica gel chromatography (CH_2Cl_2: hexane =1:1 as eluent) to afford a pale yellow solid (109.1 mg, 0.35 mmol). Yield: 70 %.

^{1}H-NMR (400 MHz, DMSO-d_6) δ: 10.53 (s, 2H), 9.31 (d, *J* = 8.5 Hz, 2H) 8.36 (d, *J* = 7.3 Hz, 2H), 7.80 (d, *J* = 7.3 Hz, 2H), 7.79-7.74 (m, 2H), 7.52-7.47 (m, 2H), 7.29 (d, *J* = 8.5 Hz, 2H).

^{13}C-NMR (100 MHz, DMSO-d_6) δ: 194.2, 143.9, 135.9, 132.0, 131.0, 129.9, 129.0, 127.4, 127.0, 126.3, 124.5,

MS (EI, DMSO) m/z (rel%): 310 (M^+, 100), 281 (M^+-HCO, 22), 252 (M^+-2HCO, 74), 126 (22), 113 (7).

No reported NMR data in the literature.

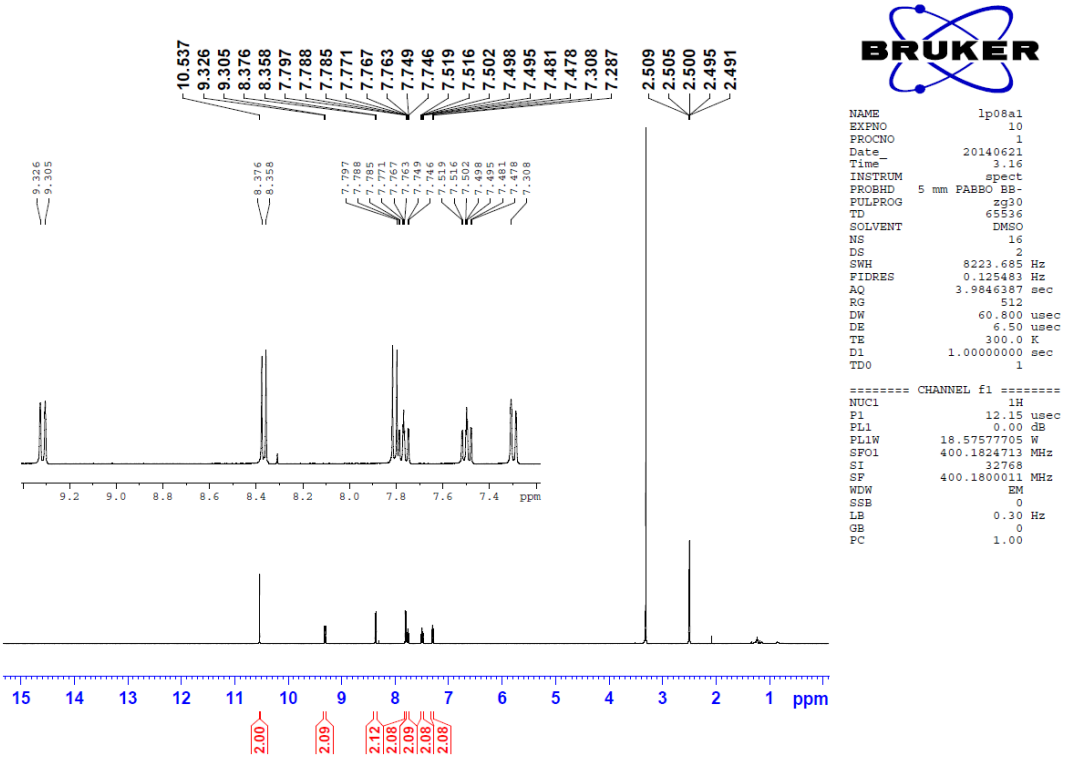

Figure 7.11 ^{1}H-NMR spectrum of compound **8**.

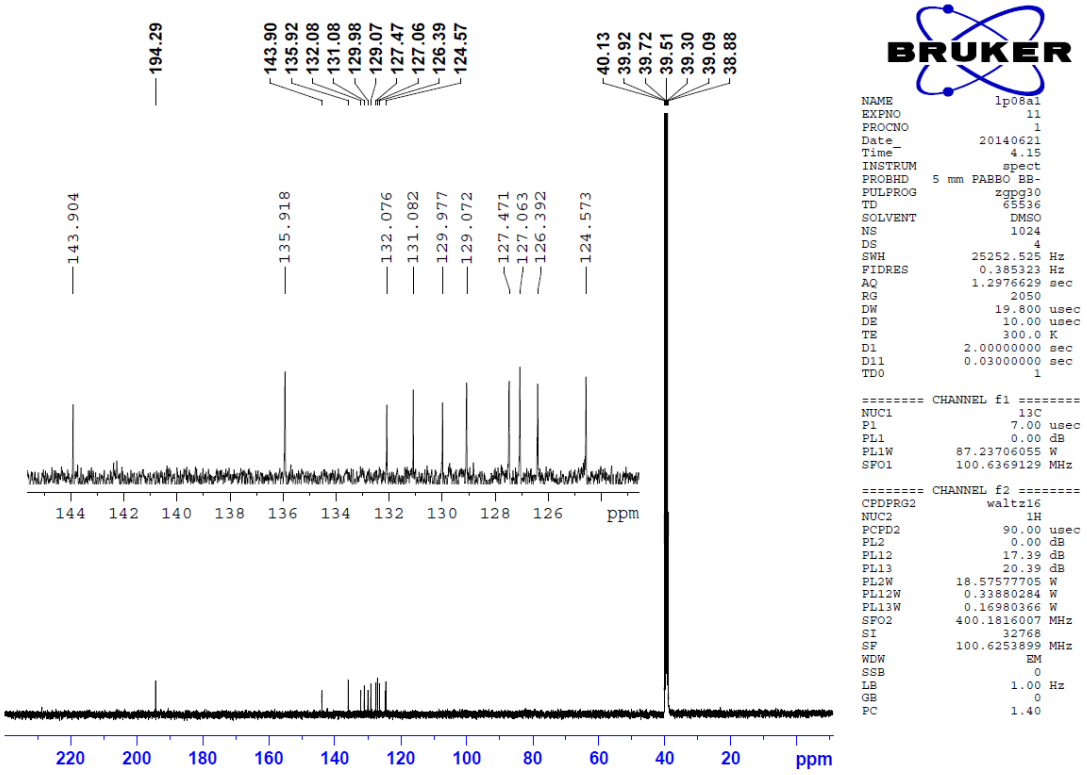

Figure 7.12 ^{13}C-NMR spectrum of compound **7**.

7.8 1-bromo-4-(bromomethyl)naphthalene (9)

Table 4.5 from **Chapter 4** is reproduced below as **Table 7.4**.

Entry	Scale mmol	Reaction condition	Yield %
1	2.7	1.2 eq NBS, 6.6 mol% BPO,9 mL CCl_4 reflux for 3 h	63
2	27.0	1.2 eq NBS, 6.6 mol% BPO, 90 mL CCl_4 reflux for 3 h	92
3	54.0	1.2 eq NBS, 6.6 mol% BPO, 180 mL CCl_4 reflux for 3h	60
4	90.0	1.1 eq NBS, 6.6 mol% BPO, 300 mL CCl_4 reflux for 3 h	68

Entry 4 used an example for the synthesis

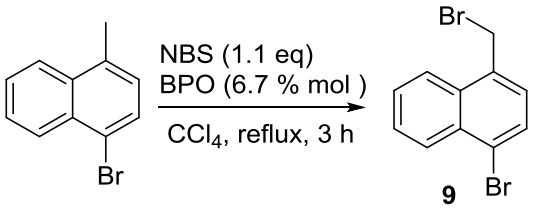

To a dry Schlenk flask (500 mL) were added N-bromosuccinimide (18.4 g, 103.4 mmol, 1.1 eq.), benzoyl peroxide (1.5 g, 6.0 mmol, 0.067 eq.) and 1-bromo-4-methylnapthalene (20.0 g, 90.4 mmol, 1.0 eq.) in CCl_4 (300 mL). The mixture was refluxed under N_2 atmosphere for 3 h. After cooling to room temperature, the suspension was filtered off, washed with CCl_4 (200 mL), and the mixture was washed with saturated Na_2SO_3 solution (100 mL). The organic layer was collected and dried over Na_2SO_4. The organic solvent was mixed with silica and was evaporated and the resulting yellow solid was filtered with silica gel using (100 % hexane) to give a yellowish white solid which was recrystallized twice from hexane to give a white solid (18.42 g, 61.4 mmol). Yield: 68 %

^{1}H-NMR (400 MHz, $CDCl_3$) δ: 8.34-8.30 (m, 1H), 8.17-8.13 (m, 1H), 7.72 (d, *J* = 7.6 Hz, 1H), 7.70-7.61 (m, 2H), 7.39 (d, *J* = 7.6 Hz, 1H), 4.91 (s, 2H, CH_2).

^{13}C-NMR (100 MHz, $CDCl_3$) δ: 133.3, 132.4, 132.1, 129.5, 128.1, 127.9, 127.6, 127.4, 124.5, 124.3, 30.9.

MS (EI, CH_2Cl_2) m/z (rel%): 302/300/298 (M^+, 6/13/6), 221/219 (M^+-Br, 98/100), 140/139 (M^+-2Br, 32/38), 110 (7), 70 (20).

The spectroscopic data were in accordance with the literature.[83]

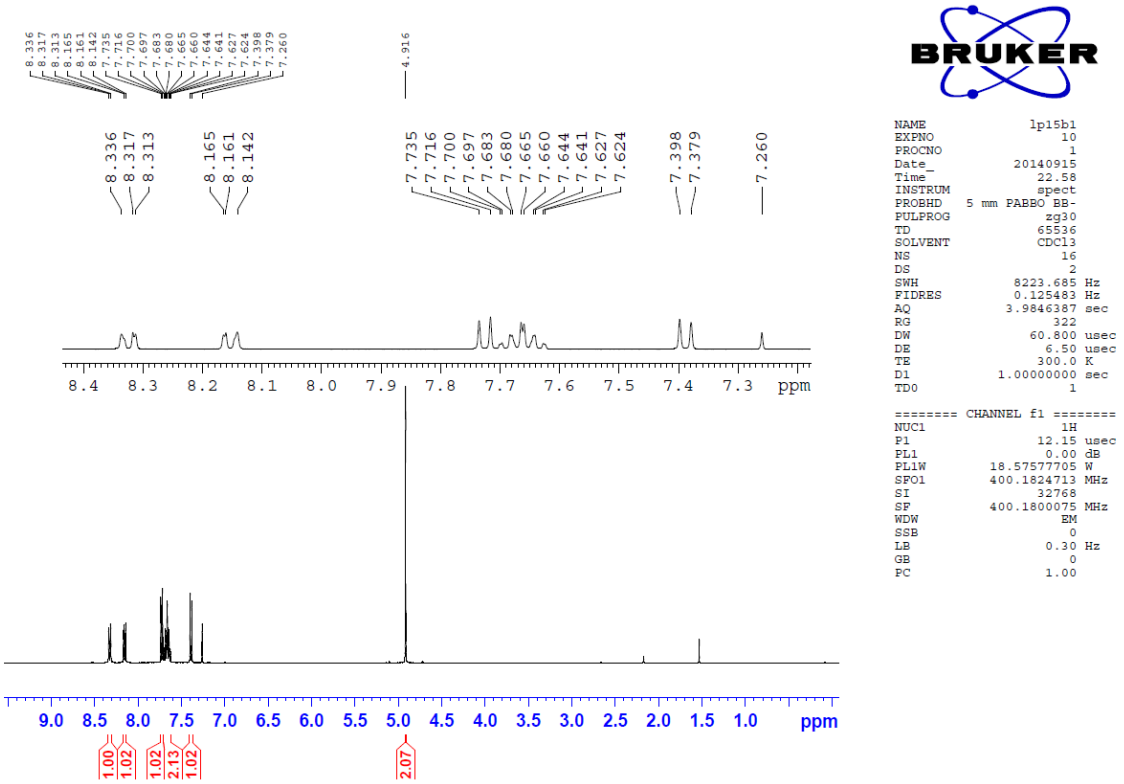

BRUKER

```
NAME                lp15b1
EXPNO                   10
PROCNO                   1
Date_             20140915
Time                 22.58
INSTRUM              spect
PROBHD    5 mm PABBO BB-
PULPROG               zg30
TD                   65536
SOLVENT              CDCl3
NS                      16
DS                       2
SWH               8223.685 Hz
FIDRES            0.125483 Hz
AQ                3.9846387 sec
RG                     322
DW                  60.800 usec
DE                   6.50 usec
TE                  300.0 K
D1                1.00000000 sec
TD0                      1

======== CHANNEL f1 ========
NUC1                    1H
P1                   12.15 usec
PL1                   0.00 dB
PL1W         18.57577705 W
SFO1         400.1824713 MHz
SI                   32768
SF           400.1800075 MHz
WDW                     EM
SSB                      0
LB                    0.30 Hz
GB                       0
PC                    1.00
```

Figure 7.13 ^{1}H-NMR spectrum of compound **9**.

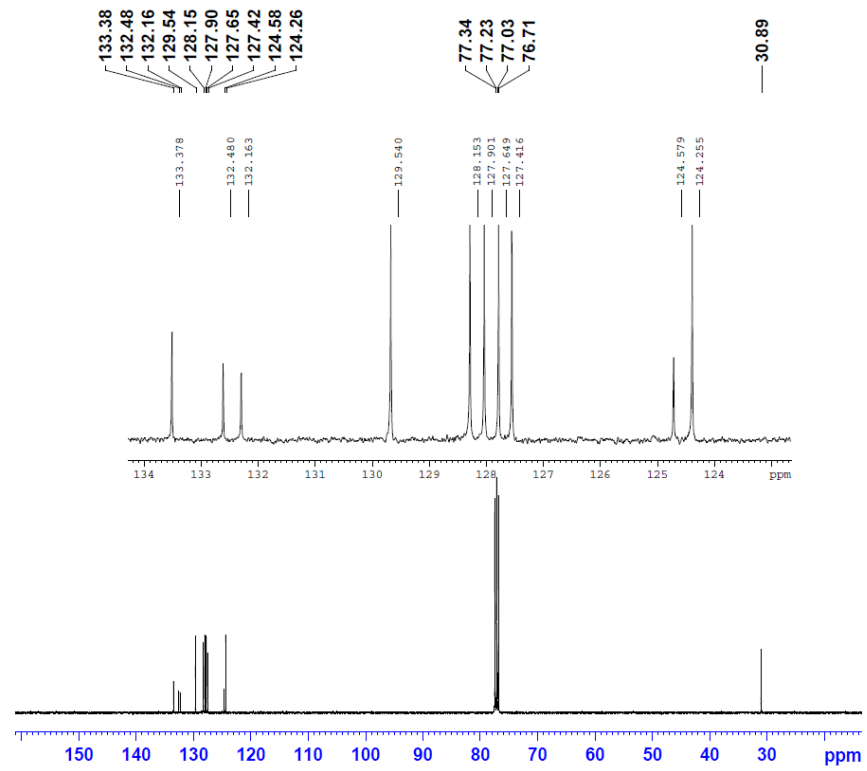

BRUKER

```
NAME                lp15b1
EXPNO                   11
PROCNO                   1
Date_             20140915
Time                 23.57
INSTRUM              spect
PROBHD    5 mm PABBO BB-
PULPROG             zgpg30
TD                   65536
SOLVENT              CDCl3
NS                    1024
DS                       4
SWH              25252.525 Hz
FIDRES            0.385323 Hz
AQ                1.2976629 sec
RG                    2050
DW                  19.800 usec
DE                  10.00 usec
TE                  300.0 K
D1                2.00000000 sec
D11               0.03000000 sec
TD0                      1

======== CHANNEL f1 ========
NUC1                   13C
P1                    7.00 usec
PL1                   0.00 dB
PL1W         87.23706055 W
SFO1         100.6369129 MHz

======== CHANNEL f2 ========
CPDPRG2            waltz16
NUC2                    1H
PCPD2                90.00 usec
PL2                   0.00 dB
PL12                 17.39 dB
PL13                 20.39 dB
PL2W         18.57577705 W
PL12W         0.33880284 W
PL13W         0.16980366 W
SFO2         400.1816007 MHz
SI                   32768
SF           100.6253274 MHz
WDW                     EM
SSB                      0
LB                    1.00 Hz
GB                       0
PC                    1.40
```

Figure 7.14 ^{13}C-NMR spectrum of compound **9**.

7.9 4-bromo-1-naphthalenecarboxylic acid (10)

Procedure A[69]

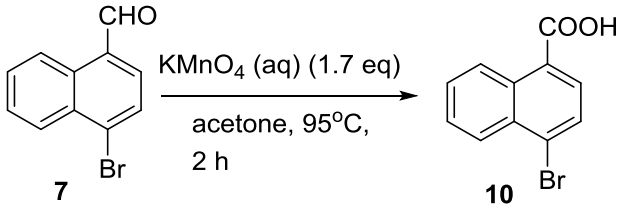

4-bromo-1-naphthalenecarbaldehyde (7.5 g, 31.9 mmol, 1.0 eq.) was dissolved in acetone (69 mL) and was heated to reflux. $KMnO_4$ (8.6 g, 54.2 mmol, 1.7 eq.) in H_2O (135 mL) was added through dropping funnel for 1.5 h. The reaction mixture was stirred for another half hour. The mixture was filtered under reduced pressure while still hot, and washed with acetone (3x60 mL). The water phase was collected after evaporated under vacuum. Washed with saturated Na_2SO_3 (90 mL) and diethyl ether (3x70 mL). The water layer was collected and cooled to 0 ^oC in ice bath and acidified with concentrated HCl (aq, 37%) The resulting precipitate was filtered under reduced pressure and washed with H_2O until the filtrate was neutral. The dried solid was collected and suspended in hot water (500 mL), and stirred for 1h. The water was filtered off and the solid was collected and dried in oven 110 ^oC for 24 h. The title compound was obtained as a beige solid (6.1 g, 24.2 mmol). Yield: 76 %

Procedure B[89]

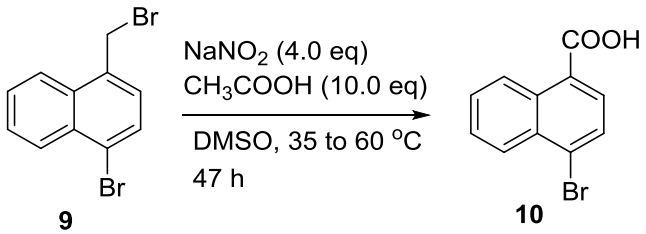

Compound **9** (942 mg, 4.0 mol, 1.0 eq.) and $NaNO_2$ (1120 mg, 16.0 mmol, 4.0 eq.) were mixed in DMSO (8 mL). Then, added the acetic acid (2.3 mL, 40.0 mmol, 10.0 eq.) to the mixture. The resulting yellow mixture was stirred at 35 ^oC for 2 h, then change to 45 ^oC for 40h and 60 ^oC for another 5 h. The resulting mixture was diluted with H_2O (20 mL) and washed with ether (3x15 mL). The water phase was diluted to 40 mL and acidified with 37 % HCl in the ice/water bath. The pale yellow precipitate was filtered and dried in an oven at 110 ^oC. The title compound was obtained as a beige solid (268 mg, 1.06 mmol). Yield: 26 %

^{1}H-NMR (400 MHz, DMSO-d_6) δ: 13.4 (br s, 1H), 8.93-8.88 (m, 1H), 8.28-8.22 (m, 1H), 8.03-7.96 (m, 2H), 7.79-7.71 (m, 2H).

^{13}C-NMR (100 MHz, DMSO-d_6) δ: 168.0, 131.7, 131.3, 130.0, 129.3, 128.4, 128.1, 128.0, 127.0, 126.9, 126.2

MS (EI, DMSO) m/z (rel%): 252/250 (M^+,97/100), 235/233 (M^+-OH, 36/36), 207/205 (M^+-COOH, 15/16), 126 (M^+-HCO_2Br, 42), 115 (15), 74(7), 63 (11).

The spectroscopic data were in accordance with the literature.[103]

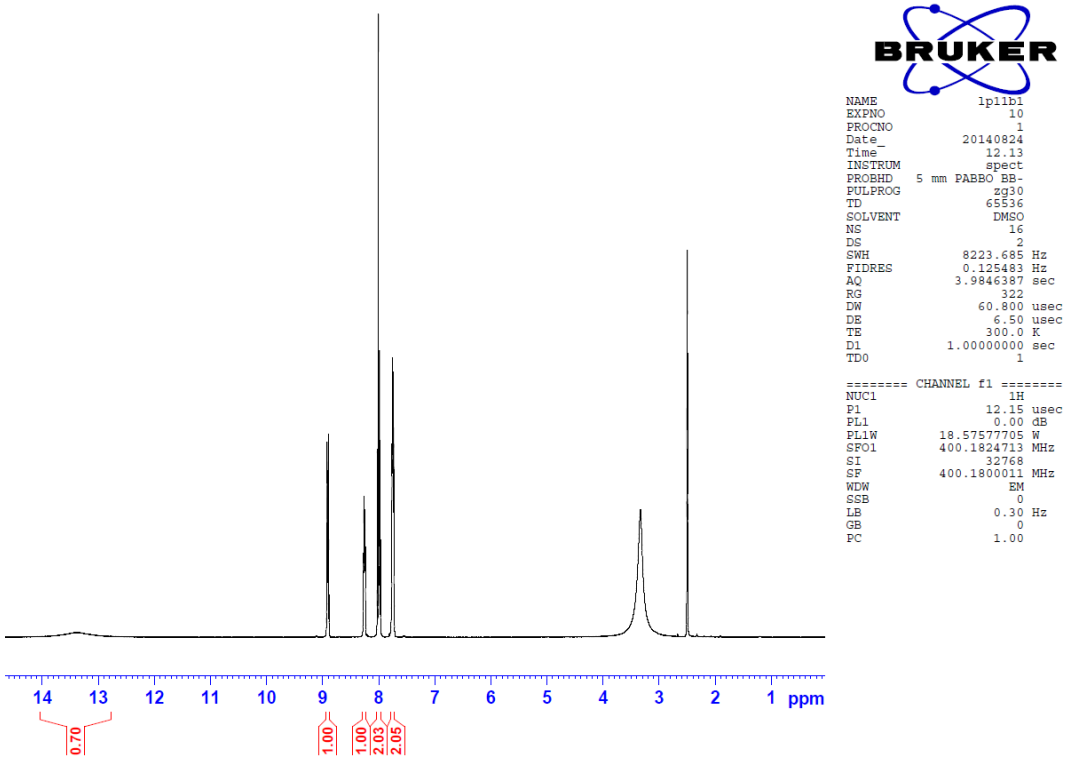

Figure 7.15 ^{1}H-NMR spectrum of compound **10**.

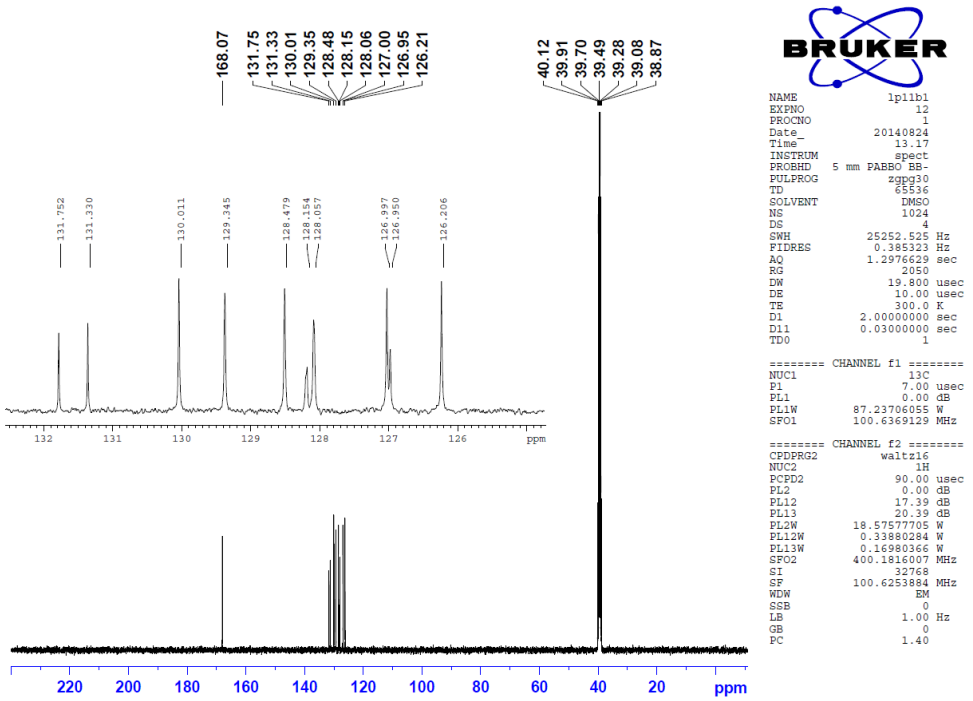

Figure 7.16 ^{13}C-NMR spectrum of compound **10**.

7.10 ethyl 4-bromo-1-naphthoate (11)

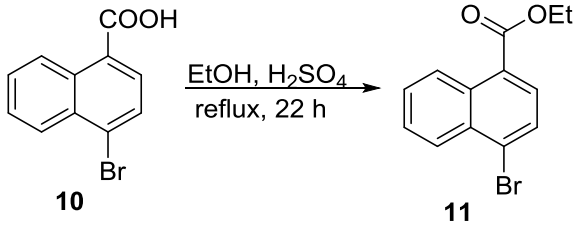

10 11

To a round bottom flask were added 4-bromo-1-naphthalenecarboxylic acid (9.2 g, 36.6 mmol, 1.0 eq.) ethanol (240 mL) and concentrated H_2SO_4 (98%, 3 mL). The mixture was heated to reflux and stirred for 26 h. The mixture was diluted with H_2O (100 mL) and washed with $NaHCO_3$ (2 M, 75 mL). After extracted with CH_2Cl_2 (3x200 mL), the organic layer was collected and dried over Na_2SO_4. The solvents were removed under vacuum to give the title compound as a pale yellow solid (9.7 g, 34.7 mmol) Yield: 95 %.

^{1}H-NMR (400 MHz, $CDCl_3$) δ: 8.98-8.94 (m, 1H), 8.36-8.34 (m, 1H), 7.99 (d, *J* = 7.9, 1H), 7.82 (d, *J* = 7.9 Hz, 1H), 7.69-7.61 (m, 2H), 4.47 (q, *J* = 7.1 Hz, 2H), 1.46 (t, *J* = 7.1 Hz, 3H).

^{13}C-NMR (100 MHz, $CDCl_3$) δ: 167.1, 132.4, 132.2, 129.9, 128.9, 128.5, 128.4, 127.7, 127.6, 127.5, 126.2, 61.3, 14.4.

MS (EI, CH_2Cl_2) m/z (rel%): 280/278 (M^+, 95/96), 252/249 (M^+-CH_2=CH_2, 15/15), 235/233 (M^+-OEt, 99/100), 207/205 (M^+-COOEt, 27/27), 126 (86), 115 (5), 99 (5), 75 (7), 63 (10).

The spectroscopic data were in accordance with the literature.[104]

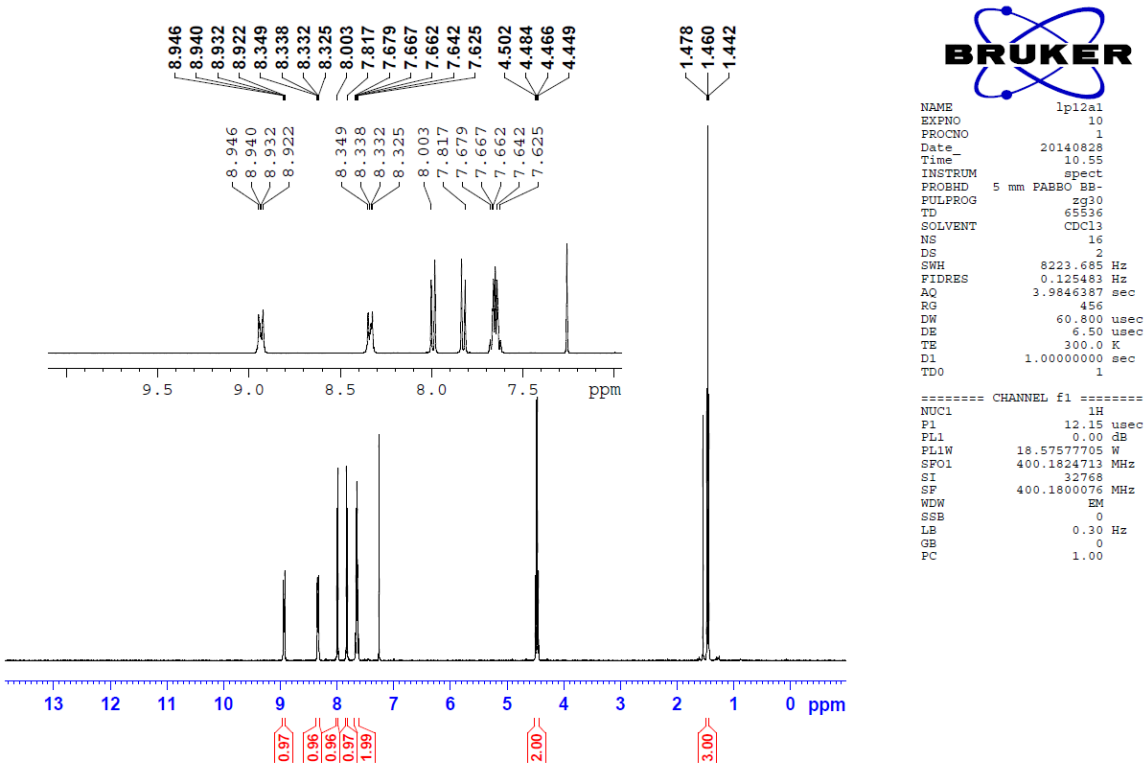

Figure 7.17 ^{1}H-NMR spectrum of compound **11**.

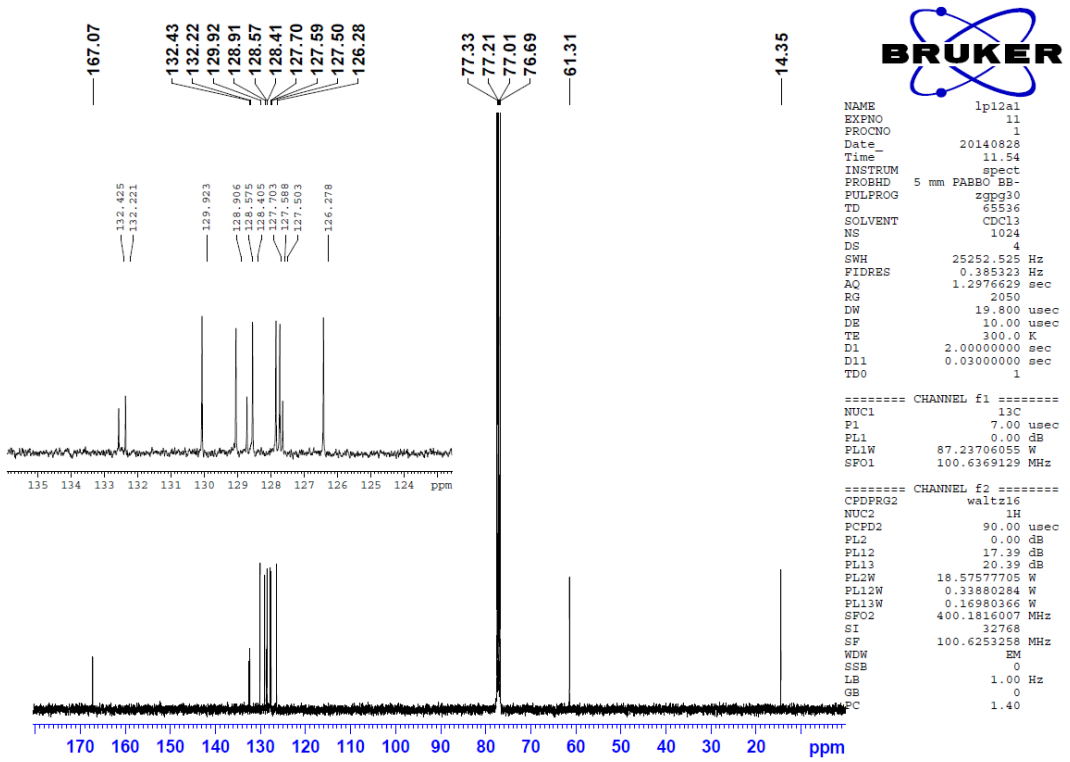

Figure 7.18 ^{13}C-NMR spectrum of compound **11**.

7.11 diethyl 1,1'-binaphthyl-4,4'-dicarboxylate (12)

Table 4.9 from **Chapter 4** is reproduced below as **Table 7.5**.

Table 7.5 Different scales of compound **12** synthesis.

Entry	Scale mmol	$PdCl_2(dppf)$ mol%	$B_2(pin)$ mmol	K_2CO_3 mmol	Solvent mL	Temperature °C	Reaction time h	Yield %
1	1.0	1	0.5 (0.5eq)	3.0	6.0	80	48	62
2	2.0	1.5	1.0 (0.5eq)	6.0	12.0	80	28	78
3	8.0	1.5	4.1 (0.51eq)	24.0	48.0	80	28	87
4	39.3	1.5	21.6 (0.54eq)	117.9	235.0	80	24	90

Entry 4 used as an example

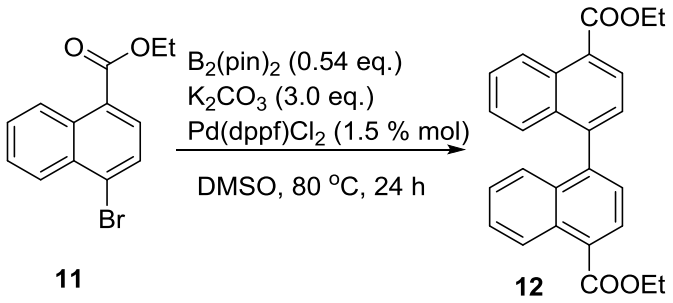

To a dry Schlenk flask (500 mL) with argon gas atmosphere were added ethyl 4-bromo-1-naphthoate (10.9 g, 39.3 mmol, 1.0 eq.), bis(pinacolato)diboron (5.5g, 21.63, 0.55 eq.), $PdCl_2(dppf)\cdot CH_2Cl_2$ complex (481.8 mg, 0.59 mmol, 1.5% mol), K_2CO_3 (16.3 g, 117.9 mmol, 3.0 eq.), and DMSO (235 mL). The light orange mixture was kept stirring at 80 °C for 24 h. The red mixture was cooled to room temperature and poured in ice to give a pink precipitate. The mixture was filtered and the pink solid was collected and dissolved in ethyl acetate (500 mL) and filtered with silica gel and the filtrate was dried over Na_2SO_4 and evaporated under vacuum. The crude solid was dissolved in hot ethyl acetate (300 mL) together with activated carbon. The hot mixture was filtered and the solvent was removed under vacuum to give titled compound as a pale yellow solid (7.0 g, 17.5 mmol). Yield: 90 %

^{1}H-NMR (600 MHz, $CDCl_3$) δ: 8.99 (d, *J* = 8.8 Hz, 2H), 8.27 (d, *J* = 7.4 Hz, 2H), 7.62-7.58 (m, 2H), 7.49 (d, *J* = 7.4 Hz, 2H), 7.38-7.35 (m, 2H), 7.35-7.31 (m, 2H), 4.5 (q, *J* = 7.3 Hz, 4H) 1.50 (t, *J* = 7.3 Hz, 6H).

^{13}C-NMR (150 MHz, $CDCl_3$) δ: 167.8, 143.0, 133.1, 131.5, 129.3, 128.0, 127.8, 127.1, 126.6, 126.3, 126.1, 61.4, 14.6.

MS (EI, CH_2Cl_2) m/z (rel%): 398 (M^+, 100), 353 (M^+-OEt, 27), 325 (M^+-HCOOEt, 12), 296 (16), 252 (39), 154 (6), 126 (12).

No reported NMR data in the the literature.

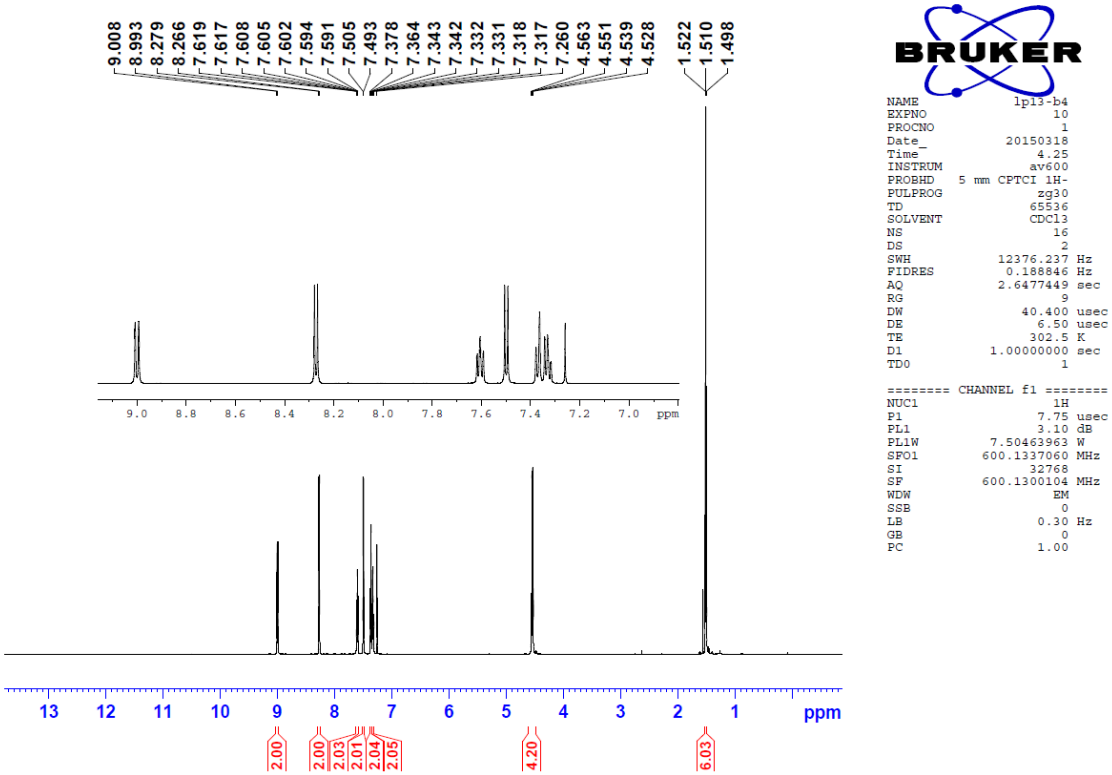

Figure 7.19 ^{1}H-NMR spectrum of compound **12**.

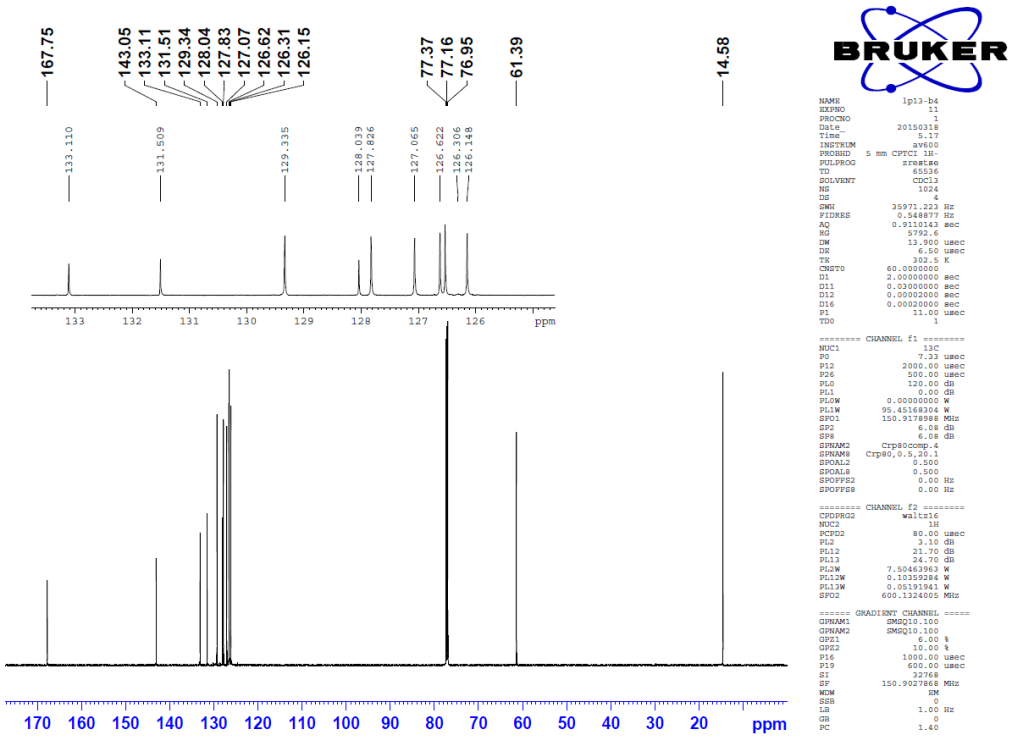

Figure 7.20 ^{13}C-NMR spectrum of compound **12**.

7.12 1,1'-binaphthalene (13)

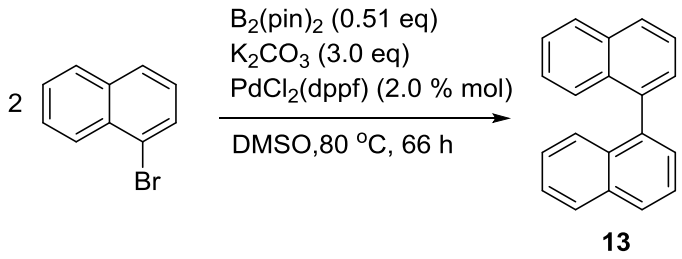

13

Procedure A:

To a dry Schlenk flask with argon atmosphere were added 1-bromonaphthalene (414 mg, 2.0 mmol, 1.0 eq.), bis(pinacolato)diboron (344 mg, 1.35 mmol, 1.3 eq.), $PdCl_2(dppf)$**.** CH_2Cl_2 complex (32.6 mg, 0.02 mmol, 4.0 % mol), K_2CO_3 (419.5 mg, 3.0 mmol, 3.0 eq.), and DMSO (12.0 mL). The light brown mixture was kept on stirring at 80°C for 66 h. The mixture was cooled to room temperature, diluted by water (50 mL) and extracted with CH_2Cl_2 (30 mL). This was washing with NaOH (aq, 20%, 15 mL) and H_2O (3X50 mL), and the organic phase were dried over Na_2SO_4. The solvent was removed and the crude solid was purified by silica gel chromatography (CH_2Cl_2: hexane =1:3 as eluent) to afford a pale yellow solid (229.0 mg, 0.63 mmol). Yield: 90 %.

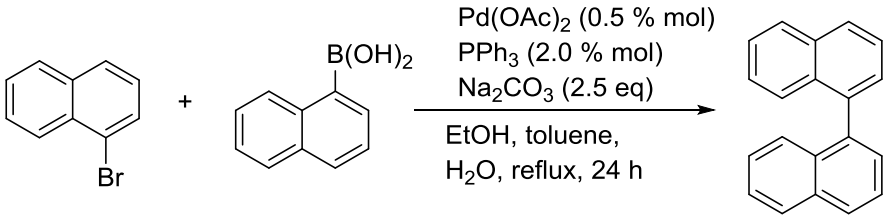

13

Procedure B:

To a dry Schlenk flask (250 mL) with argon gas atmosphere added 1-bromonaphthalene (8.54 g, 41.2 mmol, 1.0 eq.), 1-naphthylboronic acid (7.81 g, 45.4 mmol, 1.1 eq.), Pd $(OAc)_2$ (50.5 mg, 0.21 mol, 0.5% mol.), triphenylphosphine (220.3 mg, 0.84 mmol, 2.0 % mol), and Na_2CO_3 (2 M, 50 mL, 100 mmol, 2.5 eq.), ethanol (50 mL) and toluene (100 mL). The mixture was kept stirring at reflux for 24 h. The dark green reaction mixture was cooled to room temperature and diluted with 100 mL water and brine (200 mL).The mixture then extracted with ethyl acetate (3x200 mL). The organic layer was collected and dried over Na_2SO_4.The solvent was evaporated under reduced pressure. The crude solid was purified by silica gel chromatography (hexane → CH_2Cl_2: hexane =1:3 as eluent). The solvents were removed under vacuum to give the title compound as a white solid (8.21 g, 32.3 mmol).Yield: 78 %.

^{1}H-NMR (600 MHz, $CDCl_3$) δ: 7.97-7.93 (m, 4H), 7.57 (m, 2H), 7.51-7.46 (m, 4H), 7.40 (d, *J* = 8.4 Hz, 2H), 7.31-7.21(m, 2H).

^{13}C-NMR (150 MHz, $CDCl_3$) δ: 138.6, 133.7, 133.0, 128.3, 128.0, 127.9, 126.7, 126.1, 125.9, 125.5.

MS (EI, CH_2Cl_2) m/z (rel%): 254 (M^+, 100), 253 (M^+-H, 93),252 (73), 251 (7), 250 (19), 239 (15), 126 (25).

The spectroscopic data were in accordance with the literature.[105]

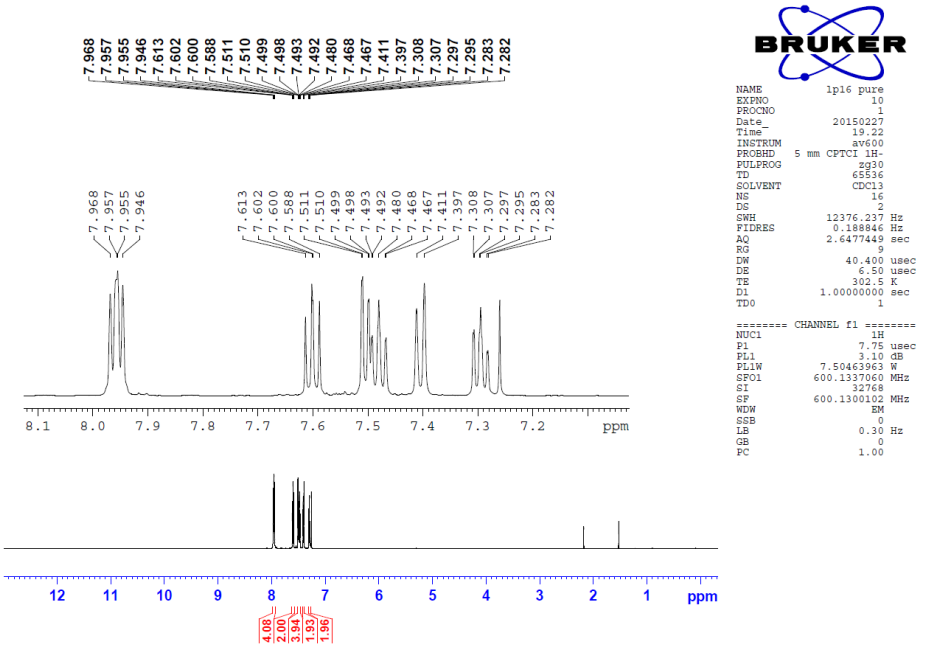

Figure 7.21 ^{1}H-NMR spectrum of compound **13**.

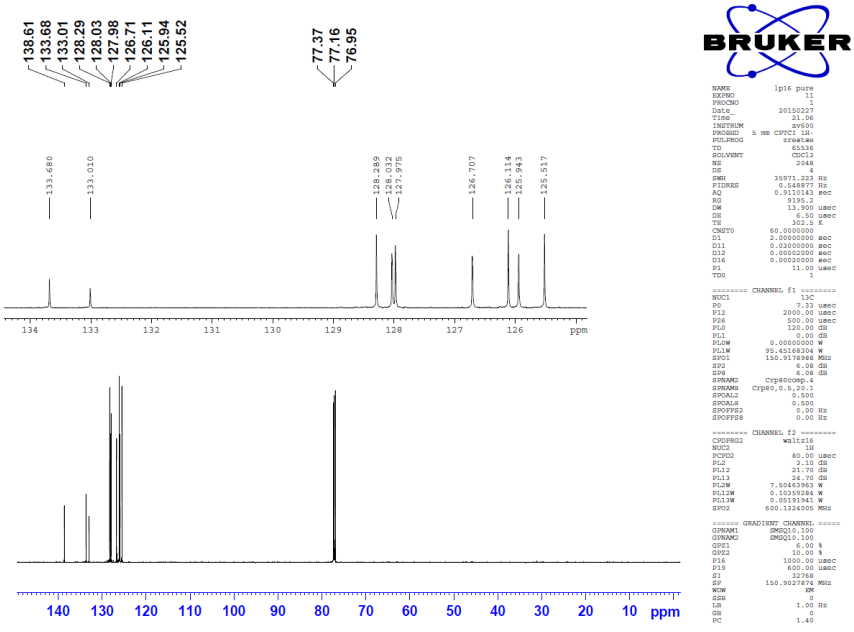

Figure 7.22 ^{13}C-NMR spectrum of compound **13**.

7.13 4,4′-dibromo-1,1'-binaphthalene (14)

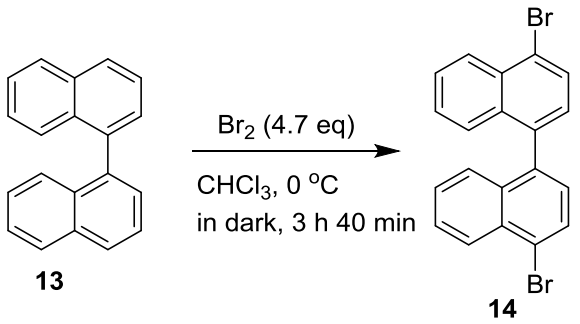

To a 100 mL round bottom flask with argon atmosphere was added 1,1'-binaphthalene (2.0 g, 7.9 mmol, 1.0 eq.) and $CHCl_3$ (60 mL). The solution was cooled to 0 ^oC and degased for 15 minutes. Aluminum foil was wrapped around the flask to shield from light and bromine (1.9 mL, 37.5 mmol, 4.7 eq.) was added dropwise for 30 minutes. And maintain the temperature at 0 ^oC while stirring for 3 h 40 min. The reaction mixture was washed with saturated Na_2SO_3 solution (100 mL) and extracted by CH_3Cl (3x60 mL). The organic layer was collected and dried over Na_2SO_4. The solvent was evaporated under reduce pressure to give a white solid. After recrystallized from chloroform the needle shape crystal was obtained. (2.97 g, 7.2 mmol) Yield: 91 %

^{1}H-NMR (600 MHz, $CDCl_3$) δ: 8.36 (d, *J* = 8.6 Hz, 2H), 7.9 (d, *J* = 7.4 Hz, 2H), 7.62-7.57 (m, 2H), 7.36-7.30 (m, 6H).

^{13}C-NMR (150 MHz, $CDCl_3$) δ: 137.8, 134.0, 132.1, 129.6, 128.3, 127.6, 127.5, 127.1, 127.0, 123.1.

MS (EI, CH_2Cl_2) m/z (rel%): 414/412/410 (M^+,38/75/40), 333/331 (M^+-Br,8/8), 252 (M^+-2Br, 100), 250 (38), 126 (50), 125 (32), 113 (7).

The spectroscopic data were in accordance with the literature.[106]

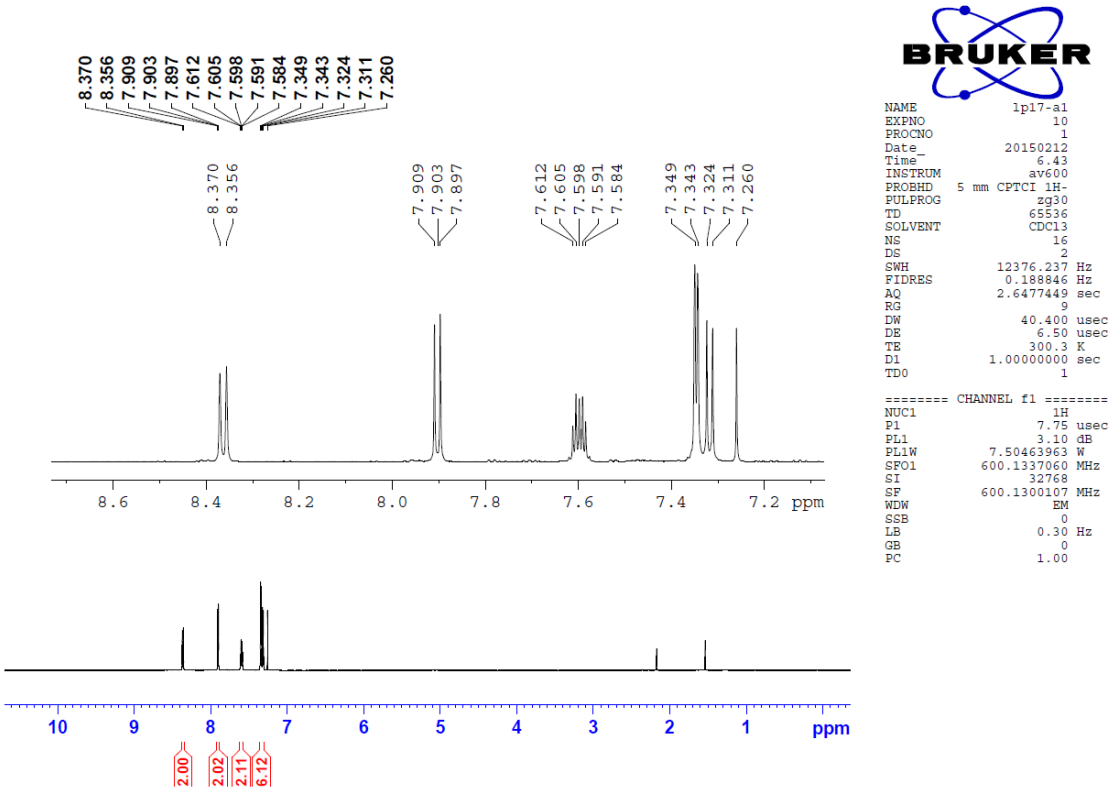

Figure 7.23 ^{1}H-NMR spectrum of compound **14**.

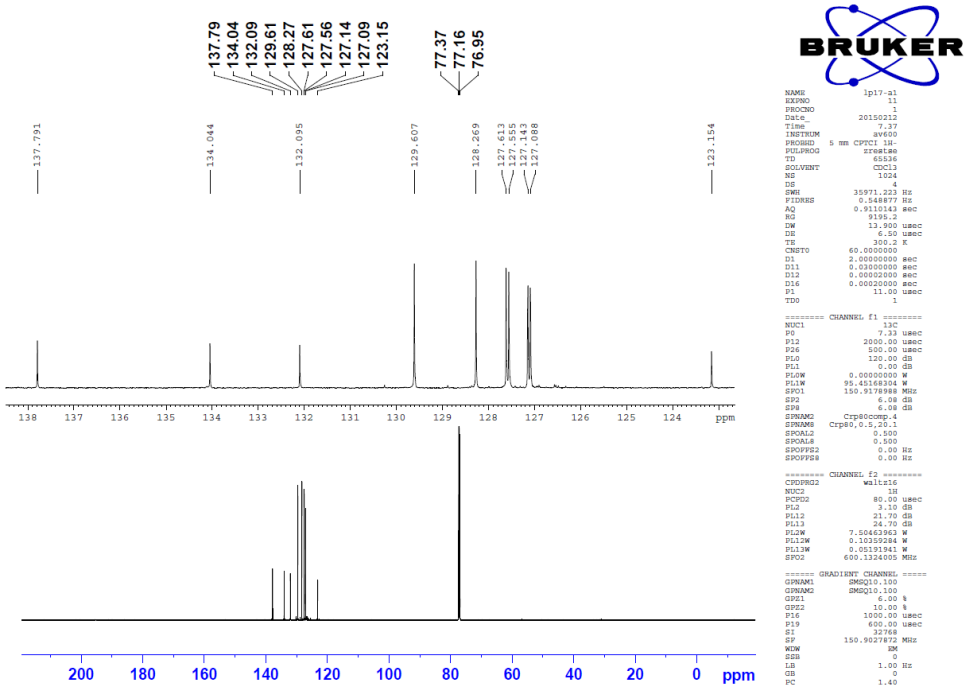

Figure 7.24 ^{13}C-NMR spectrum of compound **14**.

7.14 4,4′-dicyano-1,1′-binaphthyl (15)

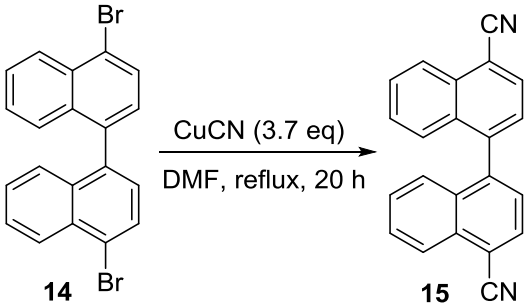

To a 100 mL round bottom flask with argon atmosphere was added 4,4′-dibromo-1,1'-binaphthalene (4.0 g, 9.68 mmol, 1.0 eq.), CuCN (3.2g, 35.8 mmol, 3.7 eq.) and DMF (80 mL). The mixture was refluxed for 20 h. Subsequently, the reaction mixture was cooled to room temperature and poured in to H_2O (200 mL) and ammonium hydroxide solution (28 %, 100 mL). The mixture was extracted by $CHCl_3$ (3x200 mL) and the organic phase washed with H_2O (3x200 mL). After the solvent was evaporated, the organic residue was purified by silica gel chromatography (CH_2Cl_2: hexane = 1:1). The tittle compound was obtained as a yellow solid (2.3g, 7.6 mmol). Yield: 78%

^{1}H-NMR (200 MHz, $CDCl_3$) δ: 8.39 (d, *J* = 8.5 Hz, 2H), 8.05 (d, *J* = 7.3 Hz, 2H), 7.78-7.68 (m, 2H), 7.53 (d, *J* = 7.3 Hz, 2H), 7.48-7.33 (m, 4H).

MS (EI, CH_2Cl_2) m/z (rel%): 304 (M^+, 100), 303 (80), 302 (47), 289 (26), 275 (14), 152 (11), 139 (8), 125 (12).

The spectroscopic data were in accordance with the literature.[95]

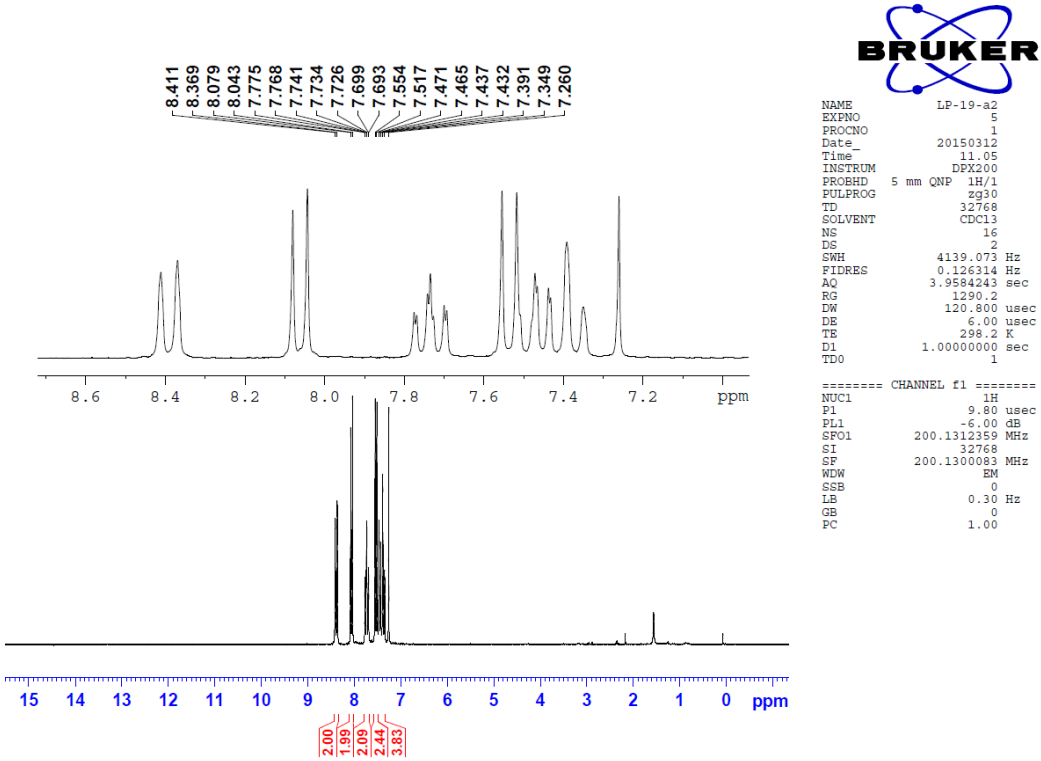

Figure 7.25 ^{1}H-NMR spectrum of compound **15**.

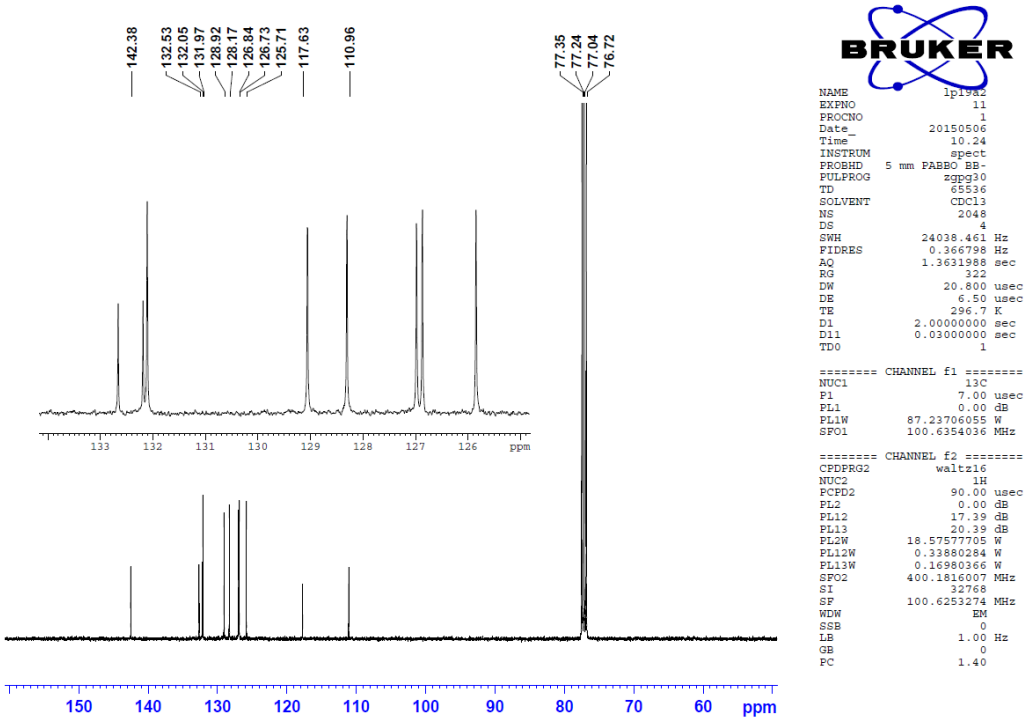

Figure 7.26 ^{1}H-NMR spectrum of compound **15**.

7.15 1,1'-binaphthyl-4,4'-dicarboxylic acid (2)

Procedure A [67]

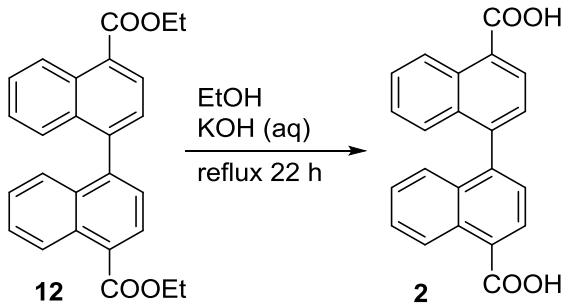

To a 500 mL round bottom flask diethyl 1,1'-binaphthyl-4,4'-dicarboxylate (7.0 g, 17.5 mmol, 1.0 eq.) H_2O (135 mL), ethanol (235 mL), and KOH (7.9 g, 140.3 mmol, 8.0 eq.) were added. The resulting mixture was heated at reflux for 5 h. Subsequently, the reaction mixture was cooled to room temperature, and diluted with H_2O (240 mL). The organic solvent was removed under vacuum, diluted with water to 900 mL and cooled to 0 ^oC. Concentrated HCl (aq, 37%) was added dropwise while stirring until pH was 0. The resulting precipitate was filtered under reduced pressure and the white cake washed with H_2O until the filtrate was neutral. The dried solid was collected and suspended in hot water (800 mL), and stirred for 1h. The water was filtered off and the solid was collected and dried in oven 110 ^oC for 24 h. The titled compound was obtained as a beige solid (5.3 g, 15.7 mmol).Yield: 88%

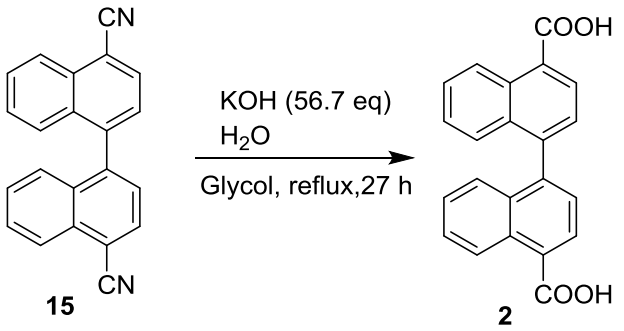

Procedure B[100]

Compound 15 (304 mg, 1.0 mmol, 1.0 eq.) was mixed with KOH (3.1 g, 56.7 mmol, 56.7 eq.), H_2O (0.6 mL), and glycol in a 100 mL flask. The mixture was heated at reflux for 27 h. Subsequently, the reaction mixture was cooled to room temperature and diluted with H_2O (100 mL). The mixture was acidified with HCl (37 %) to give brown precipitate. The resulting precipitate was filtered under reduced pressure and the white cake washed with H_2O until the filtrate was neutral. The water was filtered off and the solid was collected and dried in oven 110 ^oC for 24 h. The titled compound was obtained as a beige solid (256 mg, 0.75 mmol) Yield: 75 %

No reported NMR data in the literature.

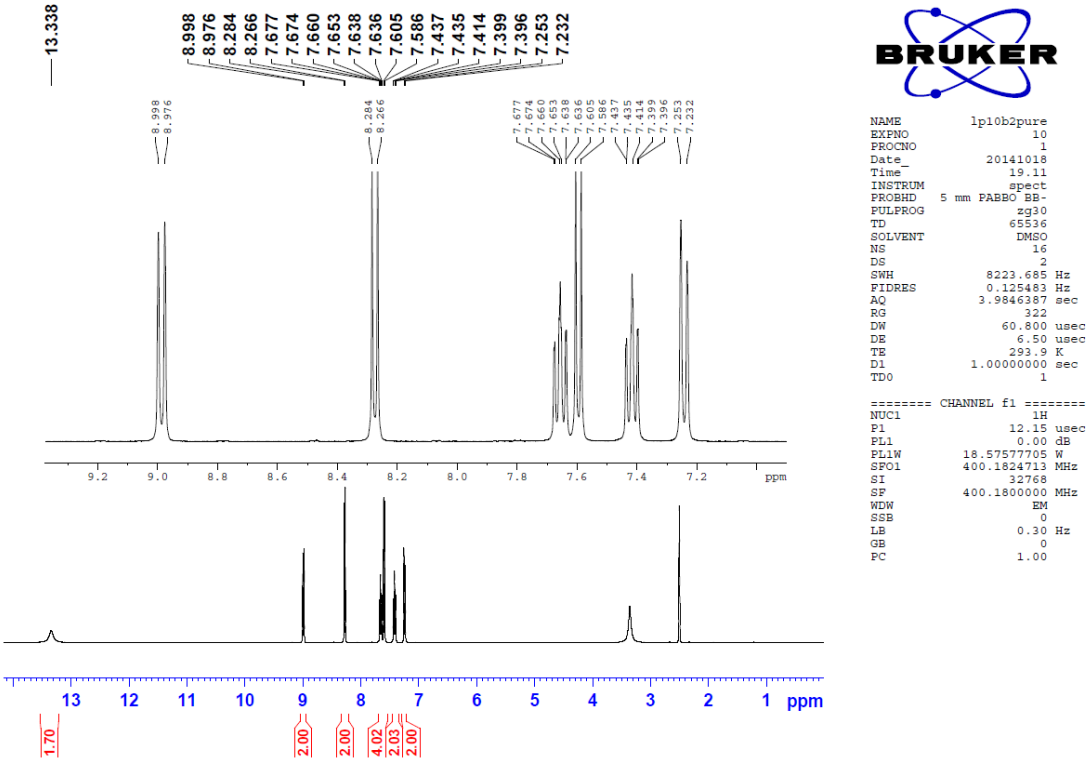

Figure 7.27 ^{1}H-NMR spectrum of compound **2**.

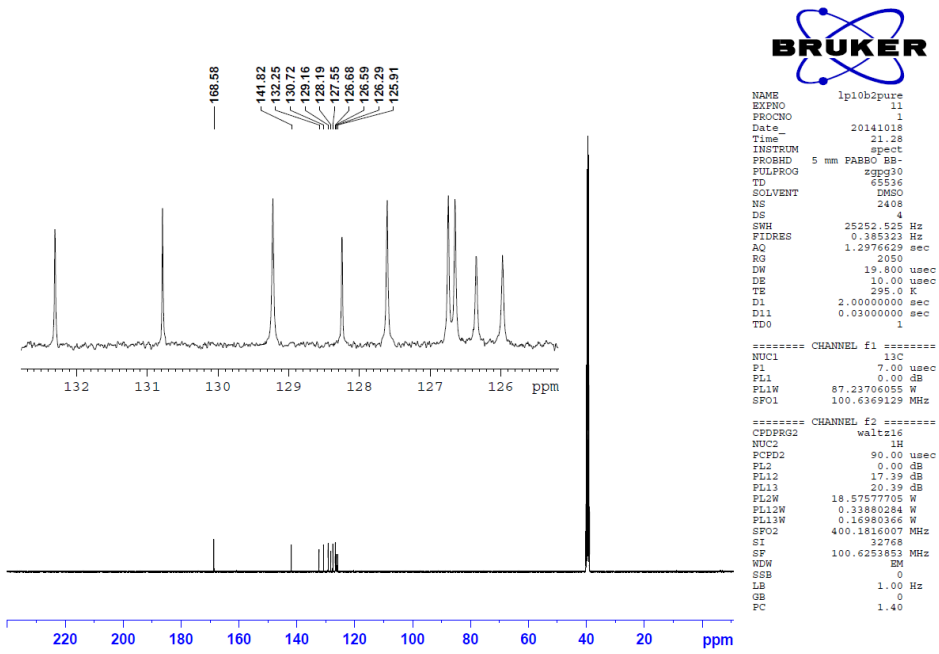

Figure 7.28 ^{13}C-NMR spectrum of compound **2**.

7.16 4,4'-dimethyl-1,1'-binaphthyl (16)

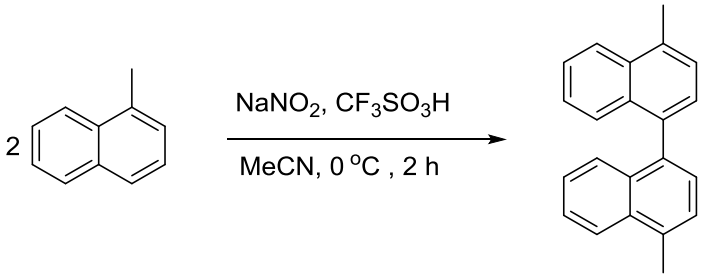

To an open flask containing acetonitrile (30 mL), added CF_3SO_3H (0.75 mL, 8.44 mmol, 2.0 eq.) and $NaNO_2$ (29.0 mg, 0.42 mmol, 0.1 eq.) with vigorous stirring at 0 °C (ice bath) and then 1-methylnaphthalene (600.0 mg, 4.22 mmol, 1.0 eq.) in acetonitrile (10 mL) was added thereto. The dark mixture turned green. After stirring at 0 °C for 2 h, the mixture was poured into ice water and then extracted with $CHCl_3$ (3x40 mL). The organic phase was separated and dried over Na_2SO_4. The solvent was removed and the crude solid was purified by silica gel chromatography (100 % hexane). The solvents were removed under reduce pressure to give the title compound as a white solid (547.0 mg, 1.93 mmol) Yield: 91 %

^{1}H-NMR (400 MHz, $CDCl_3$) δ: 8.10 (d, *J* = 8.5 Hz, 2H), 7.54-7.49 (m, 1H), 7.46-7.37 (m, 6H), 7.31-7.25 (m, 2 H), 2.81 (s, 6H).

^{13}C-NMR (100 MHz, $CDCl_3$) δ: 137.0, 133.9, 133.0, 132.6, 127.6, 127.3, 126.1, 125.5 (d, J=4.6 Hz, 2C), 124.2, 19.5.

MS (EI, CH_2Cl_2) m/z (rel%): 282 (M^+, 100), 267 (M^+-CH_3, 41), 266 (32), 252 (M^+-$2CH_3$, 31), 141 (6), 132 (10), 126 (14).

No reported NMR data in the literature.

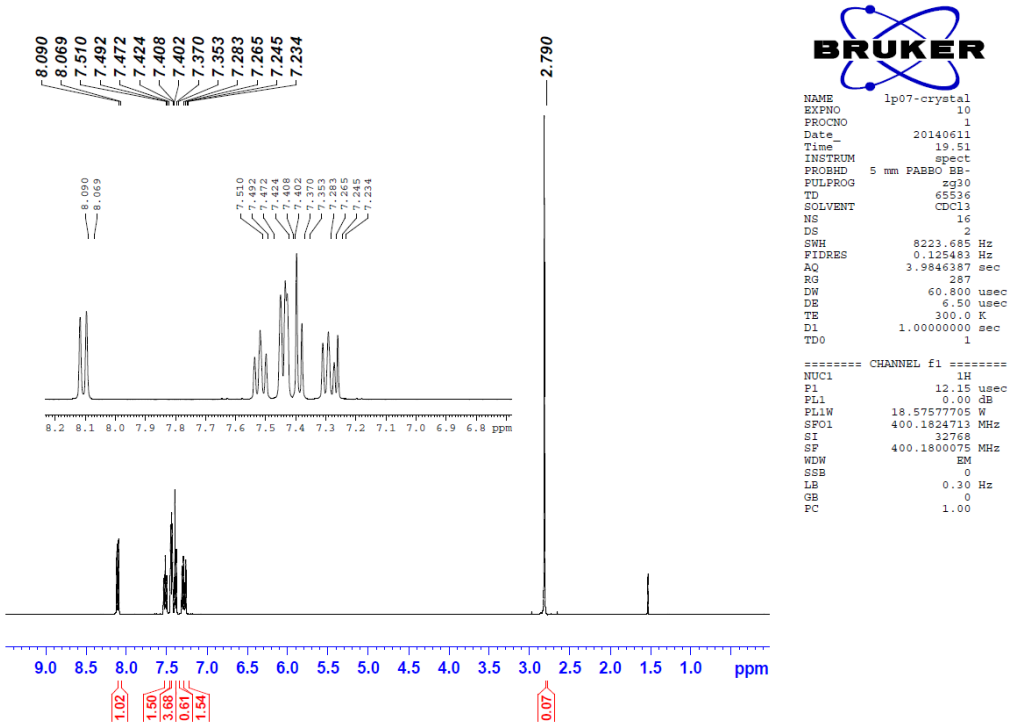

Figure 7.27 ^{1}H-NMR spectrum of compound **16**.

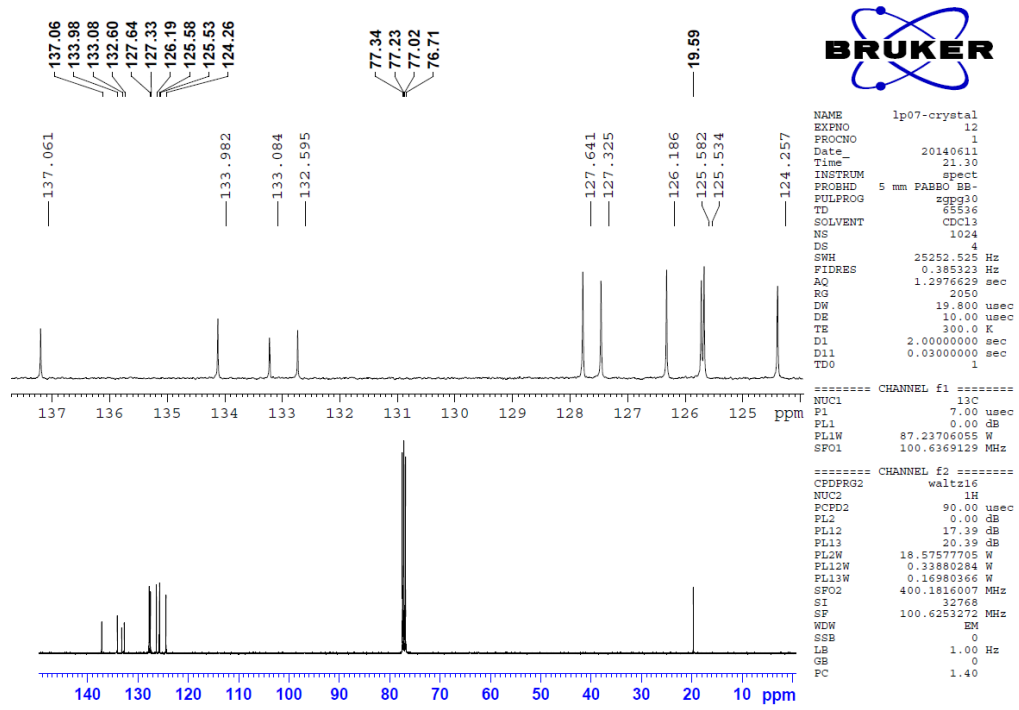

Figure 7.26 ^{1}H-NMR spectrum of compound **16**.

7.17 MOF synthesis

Single crystal synthesis

MOF- UiO-67-BNDC-1 single crystal synthesis batch 80%

Compound	Volume	mass mg	ratio
$ZrCl_4$	/	109	1.0
BNDC	/	30	0.2
H_2BPDC	/	86	0.3
35 % HCl	32 µL	/	3.0
DMF	10 mL	/	300
Benzoic acid	/	1582	30

Weight benzoic acid (1.582 g, 12.92 mmol, 30 eq) and dissolved in hot DMF (10 mL) at 80 ^oC. Then added $ZrCl_4$ (109,0 mg 0,43 mmol, 1,0 eq), H_2O (32 µL, 0.34 mmol, 0.8 eq). After the mixture became clear solution, added the BNDC linker (30,0 mg, 0.09 mmol, 0,2 eq) and H_2BPDC (86.0 mg, 0.34 mmol, 0.8 eq). Stirred until all the solid dissolved, and then transferred the mixture to reaction tube and static heating at 120 ^oC for 20 h 30 min to give white precipitate.

Washing

15 mL DMF (25 ^oC)

15 mL DMF (25 ^oC)

15 mL DMF (25 ^oC)

Followed by solvent exchange with THF three times (3x 15 mL)

The resulting white solid was dried in oven 60 ^oC overnight

MOF- UiO-67-BNDC-2 single crystal synthesis

Compound	Volume	mass mg	ratio
$ZrCl_4$	/	222.0	1.0
BNDC	/	335.0	1.0
35% HCl	45.7 µL	/	3.0
DMF	8 mL	/	500
Benzoic acid	/	3550	5

To a beaker added benzoic acid (3550 mg, 9.69 mmol, 30.0 eq) and dissolved in hot DMF (25 mL) at 80 ^{o}C. Then added $ZrCl_4$ (222,0 mg 0,32 mmol, 1,0 eq), 35% HCl (45 µL, 0.17 mmol, 0.5 eq). After the mixture became clear solution, added the BNDC linker (335,0 mg, 0.32 mmol, 1.0 eq). Stirred until all the solid dissolved, and then transferred the mixture to three glass tube and static heating at 120 ^{o}C, 130 ^{o}C, 140 ^{o}C for 2 days to give white precipitate.

The precipitate washed by DMF three times

10 mL DMF (25 ^{o}C)

10 mL DMF (25 ^{o}C) without stirring

10 mL DMF (25 ^{o}C)

Followed by solvent exchange with THF three times (3x 8 mL)

The resulting white solid was dried in oven 60 ^{o}C overnight

MOF- UiO-67-BNDC-3 single crystal synthesis single crystal formed

Compound	Volume	mass mg	ratio
$ZrCl_4$	/	125	1.0
BNDC	/	187	1.0
H_2O	15 µL	/	1.5
DMF	6.5 mL	/	150
4-nitrobenozic acid	/	2806	30

To a small vial added DMF 6.5 mL, and then dissolved ZrCl4 (130 mg, 0.55 mmol, 1.0 eq) in hot DMF. Followed by adding 4-nitrobenozic acid (2806 mg, 16.5 mmol, 30 eq) . Until all the solids were dissolved, the BNDC linker (187 mg, 0.55 mmol, 1.0 eq) was added thereto. Kept stirring until all solids were dissolved and the hot mixture was then transferred to a preheated glass tube (at 120 ^{o}C) immediately and covered the tube with a small glass vial. Keep the mixture at 120 ^{o}C oven for 65 h.

MOF- UiO-67-BNDC-6 single crystal synthesis

Compound	Volume	mass mg	ratio
$ZrCl_4$	/	112	1.0
BNDC	/	189	1.0
H_2O	15 µL	/	1.5
DMF	6.5 mL	/	150
Phenyl acetic acid	/	2283	30

To a small vial added DMF 6.5 mL, and then dissolved $ZrCl_4$ (112 mg, 0.56 mmol, 1.0 eq) in hot DMF. After that, added phenyl acetic acid (2283 mg, 16.8 mmol, 30 eq) to the mixture. Until all the solids were dissolved, the BNDC linker (189 mg, 0.56 mmol, 1.0 eq) was added thereto. Kept stirring until all solids were dissolved and the hot mixture was then transferred to a preheated glass tube (at 120 ^{o}C) immediately and covered the tube with a small glass vial. Keep the mixture at 120 ^{o}C oven for 65 h.
The precipitate washed by DMF three times

10 mL DMF (25 ^{o}C)

10 mL DMF (25 ^{o}C) without stirring

10 mL DMF (25 ^{o}C)

Followed by solvent exchange with THF three times (3x 10 mL)

MOF- UiO-67-BNDC-7 single crystal synthesis

Compound	Volume	mass mg	ratio
$ZrCl_4$	/	152	1.0
BNDC	/	241	1.0
H_2O	19 µL	/	1.5
DMF	8 mL	/	150
NBA	/	4.15	38

To a small vial added DMF 8 mL, and then dissolved $ZrCl_4$ (152 mg, 0.65 mmol, 1.0 eq) in hot DMF. Then, added 4-nitrobenozic acid (4150 mg, 24.8 mmol, 38 eq). Until all the solids were dissolved, the BNDC linker (241 mg, 0.70 mmol, 1.07 eq) was added thereto. Kept stirring until all solids were dissolved and the hot mixture was then transferred to a preheated glass tube (at 120 ^{o}C) immediately and covered the tube with a small glass vial. Keep the mixture at 120 ^{o}C oven for 2 days

MOF powder sample synthesis

MOF- UiO-67-BNDC-4

Compound	Volume	mass mg	ratio
$ZrCl_4$	/	588	1.0
BNDC	/	884	1.0
H_2O	140 µL	/	3.0
DMF	30 mL	/	150
Benzoic acid	/	3790	12

Weight benzoic acid (3,79 g, 31.03 mmol, 12,0 eq) and dissolved in hot DMF (30,0 mL) at 80 ^oC. Then added $ZrCl_4$ (588 mg 2.52 mmol, 1,0 eq), H2O (140 ul). After the mixture became clear solution, added the BNDC linker (884,0 mg, 0,69 mmol, 1,0 eq) Stirred until all the solid dissolved, and put it in the oven static heating at 120 ^oC for 2days to give white precipitate.

Washing

Decant the solvent and washed with DMF three times

25 mL at 25 ^oC

25 mL at 80 ^oC stirring for 1h

25 mL at 25 ^oC

washed with THF three times (10 mL x3)

The resulting white solid was dried oven (85 ^oC) overnight. XRD IS OK

50 mg sample dried in 200 ^oC for 24h checked XRD. It is ok

50 mg sample washed with 20 mL MeOH at 40oC for 3h, washed with MeOH two more times at RT, dried in oven at 200oC 06/03/2015

Water stability test

150 mg at 25 mL water 150 degree in autoclave overnight and divided into two portions, one used directly for XRD. 05/03/2015

The other washed with THF 3x25 mL and dried in oven 120 degree and run XRD

XRD result is good.

pH Stability test

The original sample 100 mg X2 was stirring in pH=4 and pH=10 buffer solution each for 0.5h and then washed with 15 mLx3 water. Water was removed by centrifugation. The sample was put on the XRD sample hold; let it dry in the air.

MOF- UiO-67-BNDC-5

Compound	Volume	mass mg	ratio
$ZrCl_4$	/	325	1.0
BNDC	/	474	1.0
H_2O	49 µL	/	2.0
DMF	16 mL	/	150
Benzoic acid	/	3369	20

To a beaker added benzoic acid (728 mg, 5.94 mmol, 10.0 eq) and dissolved in hot DMF (23 mL) at 80 ^oC. Then added $ZrCl_4$ (140,0 mg 0,59 mmol, 1,0 eq), H_2O (32 µL, 1.78 mmol, 3.0 eq). After the mixture became clear solution, added the BNDC linker (201 mg, 0.59 mmol, 1.0 eq). Stirred until all the solid dissolved, and then transferred the mixture to three glass tube and static heating at 110 ^oC (lp08) and 120 ^oC (lp09) for 2 days to give white precipitate.

Washing

Decant the solvent and washed with DMF three times

10 mL at 25 ^oC

10 mL at 80 ^oC stirring for 1h

10 mL at 25 ^oC

washed with THF three times (10 mL x3)

The resulting white solid was dried oven (60 ^oC) overnight.

Appendix

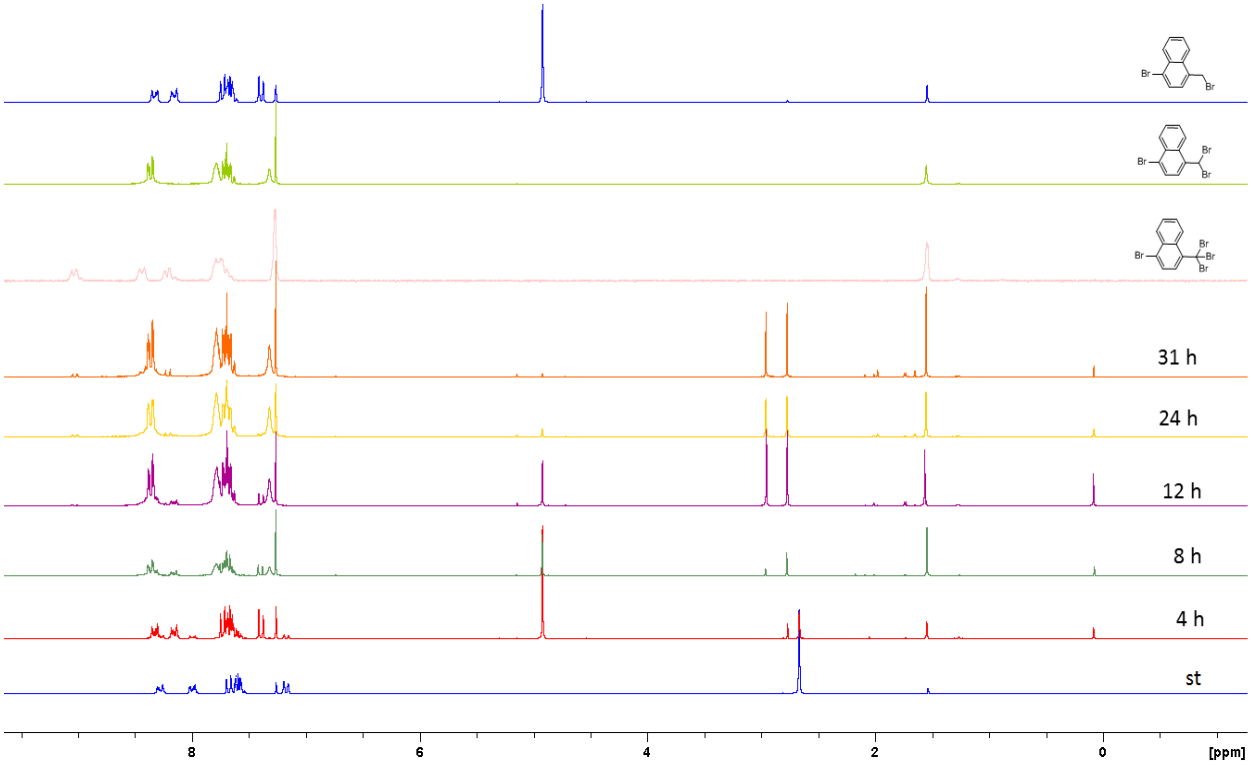

Appendix 1. Monitoring of bromination reaction (entry **1** in **table 4.4**) by Stacked ^{1}H NMR ($CDCl_3$, 200 MHz).

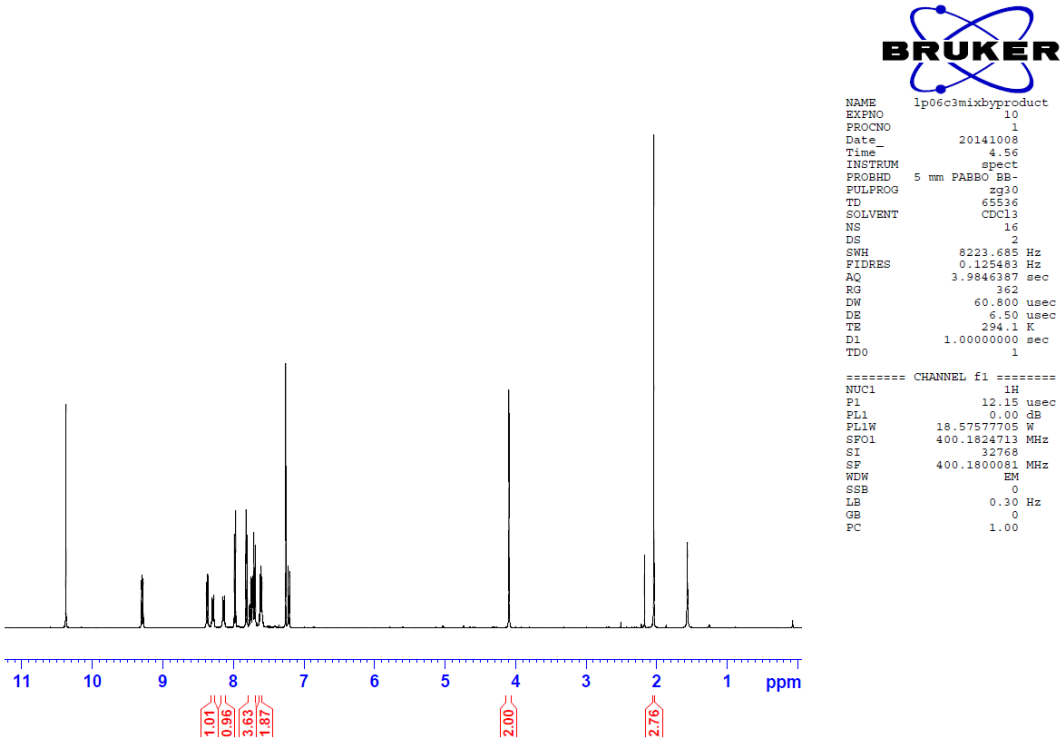

Appendix 2. 1H NMR of the acetal byproduct mixed with the product 7 (Synthesis of 4-bromo-1-naphthaldyhe (7) from compound 6)

BET plot		
V_m	349.19	[cm^3(STP) g^{-1}]
$a_{s,BET}$	1519.8	[m^2 g^{-1}]
C	10140	
Total pore volume(p/p_0=0.990)	0.6155	[cm^3 g^{-1}]
Average pore diameter	1.6198	[nm]
Langmuir plot		
V_m	388.55	[cm^3(STP) g^{-1}]
$a_{s,Lang}$	1691.2	[m^2 g^{-1}]
B	3.7322	
MP plot		
a_1	2003.8	[m^2 g^{-1}]
a_2	7.7398	[m^2 g^{-1}]
V_p	0.6386	[cm^3 g^{-1}]
$d_{p,peak}$	0.6	[nm]

Appendix 3. The table of N2 adsorption results.

Reference

(1) Zhou, H.-C.; Long, J. R.; Yaghi, O. M. *Chem. Rev.* 2012, *112*, 673.

(2) O'Keeffe, M. *Chem. Soc. Rev.* 2009, *38*, 1215.

(3) Li, H.; Eddaoudi, M.; O'Keeffe, M.; Yaghi, O. M. *Nature* 1999, *402*, 276.

(4) Batten, S. R., Champness, N. R., Chen, X-M., Garcia-Martinez, J., Kitagawa, S., Öhrström, L., O'Keeffe, M., Paik Suh, M., Reedijk, J. In *Pure Appl. Chem.* 2013; Vol. 85, p 1715.

(5) Abrahams, B. F.; Hardie, M. J.; Hoskins, B. F.; Robson, R.; Sutherland, E. E. *J. Chem. Soc., Chem. Commun.* 1994, 1049.

(6) Kitagawa, S.; Kitaura, R.; Noro, S.-i. *Angew. Chem., Int. Ed.* 2004, *43*, 2334.

(7) Cavka, J. H.; Jakobsen, S.; Olsbye, U.; Guillou, N.; Lamberti, C.; Bordiga, S.; Lillerud, K. P. *J. Am. Chem. Soc.* 2008, *130*, 13850.

(8) Biswas, S.; Zhang, J.; Li, Z.; Liu, Y.-Y.; Grzywa, M.; Sun, L.; Volkmer, D.; Van Der Voort, P. *Dalton Trans.* 2013, *42*, 4730.

(9) Czaja, A. U.; Trukhan, N.; Muller, U. *Chem. Soc. Rev.* 2009, *38*, 1284.

(10) Ulrich Schubert, N. H. In *Synthesis of Inorganic Materials*; Wiley-VCH: 2012, p 265.

(11) Stock, N.; Biswas, S. *Chem. Rev.* 2012, *112*, 933.

(12) Lee, Y.-R.; Kim, J.; Ahn, W.-S. *Korean J. Chem. Eng.* 2013, *30*, 1667.

(13) Øien, S. *Synthesis and characterization of modified UiO-67 metal-organic frameworks. Masteroppgave, University of Oslo* 2012.

(14) Tsuruoka, T.; Furukawa, S.; Takashima, Y.; Yoshida, K.; Isoda, S.; Kitagawa, S. *Angew. Chem., Int. Ed.* 2009, *48*, 4739.

(15) Schaate, A.; Roy, P.; Godt, A.; Lippke, J.; Waltz, F.; Wiebcke, M.; Behrens, P. *Chem.-Eur. J.* 2011, *17*, 6643.

(16) Nilsen, M. H., Jakobsen, S., Lamberti, C., Bonino, F., Gianolio, D.,Bordiga, S.; Olsbye, U., Lillerud, K. P. ; In *34th Annual BZA conference* Edinburgh, 2011.

(17) Hong-Cai Zhou, S. K. *Chem. Soc. Rev.* 2014, *43*, 5412.

(18) Ma, L.; Abney, C.; Lin, W. *Chem. Soc. Rev.* 2009, *38*, 1248.

(19) Sumida, K.; Rogow, D. L.; Mason, J. A.; McDonald, T. M.; Bloch, E. D.; Herm, Z. R.; Bae, T. H.; Long, J. R. *Chem. Rev.* 2012, *112*, 724.

(20) Kreno, L. E.; Leong, K.; Farha, O. K.; Allendorf, M.; Van Duyne, R. P.; Hupp, J. T. *Chem. Rev.* 2012, *112*, 1105.

(21) Loiseau, T.; Serre, C.; Huguenard, C.; Fink, G.; Taulelle, F.; Henry, M.; Bataille, T.; Férey, G. *Chem. Eur. J.* 2004, *10*, 1373.

(22) van den Berg, A. W. C.; Arean, C. O. *Chem. Commun.* 2008, 668.

(23) Murray, L. J.; Dinca, M.; Long, J. R. *Chem. Soc. Rev.* 2009, *38*, 1294.

(24) Rowsell, J. L. C.; Millward, A. R.; Park, K. S.; Yaghi, O. M. *J. Am. Chem. Soc.* 2004, *126*, 5666.

(25) Latroche, M.; Surblé, S.; Serre, C.; Mellot-Draznieks, C.; Llewellyn, P. L.; Lee, J.-H.; Chang, J.-S.; Jhung, S. H.; Férey, G. *Angew. Chem., Int. Ed.* 2006, *45*, 8227.

(26) Wong-Foy, A. G.; Matzger, A. J.; Yaghi, O. M. *J. Am. Chem. Soc.* 2006, *128*, 3494.

(27) Chavan, S.; Vitillo, J. G.; Gianolio, D.; Zavorotynska, O.; Civalleri, B.; Jakobsen, S.; Nilsen, M. H.; Valenzano, L.; Lamberti, C.; Lillerud, K. P.; Bordiga, S. *Phys. Chem. Chem. Phys.* 2012, *14*, 1614.

(28) Pirngruber, G. D.; Llewellyn, P. L. In *Metal-Organic Frameworks*; Wiley-VCH Verlag GmbH & Co. KGaA: 2011, p 99.

(29) Couck, S.; Denayer, J. F. M.; Baron, G. V.; Rémy, T.; Gascon, J.; Kapteijn, F. *J. Am. Chem. Soc.* 2009, *131*, 6326.

(30) He, Y.; Zhou, W.; Qian, G.; Chen, B. *Chem. Soc. Rev.* 2014, *43*, 5657.

(31) Zhang, T.; Lin, W. *Chem. Soc. Rev.* 2014, *43*, 5982.

(32) Horcajada, P.; Surble, S.; Serre, C.; Hong, D.-Y.; Seo, Y.-K.; Chang, J.-S.; Greneche, J.-M.; Margiolaki, I.; Ferey, G. *Chem. Commun.* 2007, 2820.

(33) Serre, C.; Millange, F.; Thouvenot, C.; Noguès, M.; Marsolier, G.; Louër, D.; Férey, G. *J. Am. Chem. Soc.* 2002, *124*, 13519.

(34) Øien, S.; Agostini, G.; Svelle, S.; Borfecchia, E.; Lomachenko, K. A.; Mino, L.; Gallo, E.; Bordiga, S.; Olsbye, U.; Lillerud, K. P.; Lamberti, C. *Chem. Mater.* 2015, *27*, 1042.

(35) Zhang, W.; Huang, H.; Liu, D.; Yang, Q.; Xiao, Y.; Ma, Q.; Zhong, C. *Microporous Mesoporous Mater.* 2013, *171*, 118.

(36) Horcajada, P.; Gref, R.; Baati, T.; Allan, P. K.; Maurin, G.; Couvreur, P.; Férey, G.; Morris, R. E.; Serre, C. *Chem. Rev.* 2012, *112*, 1232.

(37) Henninger, S. K.; Jeremias, F.; Kummer, H.; Janiak, C. *Eur. J. Inorg. Chem.* 2012, *2012*, 2625.

(38) Ricco, R.; Malfatti, L.; Takahashi, M.; Hill, A. J.; Falcaro, P. *J. Mater. Chem. A* 2013, *1*, 13033.

(39) R E Dinnebier, S. J. L. B. *Powder Diffraction theory and practice*; The Royal Society of Chemistry, 2008.

(40) Vitalij K. Pecharsky, P. Y. Z. *Fundamentals of Powder Diffraction and Structural Characterization of Materials 2nd*; Springer 2009.

(41) He, B. B. *Two-dimensional X-ray Diffraction*; Wiley, 2009.

(42) Coats, A. W.; Redfern, J. P. *Analyst* 1963, *88*, 906.

(43) T. Hatakeyama, F. X. Q.; Wiley: 1999, p 45.

(44) Vermoortele, F.; Bueken, B.; Le Bars, G.; Van de Voorde, B.; Vandichel, M.; Houthoofd, K.; Vimont, A.; Daturi, M.; Waroquier, M.; Van Speybroeck, V.; Kirschhock, C.; De Vos, D. E. *J. Am. Chem. Soc.* 2013, *135*, 11465.

(45) F. Rouquerol, J. R., K.S.W. Sing, P. Llewellyn and G. Maurin In *Adsorption by Powders and Porous Solids Principles, Methodology and Applications Second edition*; Elsevier: 2014.

(46) Putkham, A., Newcastle University, 2010

(47) Langmuir, I. *J. Am. Chem. Soc.* 1916, *38*, 2221.

(48) Langmuir, I. *J. Am. Chem. Soc.* 1918, *40*, 1361.

(49) Masel, R. I. In *Principles of Adsorption and Reaction on Solid Surfaces*; John Wiley & Sons: 1996.

(50) Walton, K. S.; Snurr, R. Q. *J. Am. Chem. Soc.* 2007, *129*, 8552.

(51) Rouquerol, J.; Llewellyn, P.; Rouquerol, F. In *Stud. Surf. Sci. Catal.*; P.L. Llewellyn, F. R.-R. J. R., Seaton, N., Eds.; Elsevier: 2007; Vol. Volume 160, p 49.

(52) Egerton, R. F. *Physical Principles of Electron Microscopy An Introduction to TEM, SEM, and AEM*; Springer, 2005.

(53) Bordiga, S.; Bonino, F.; Lillerud, K. P.; Lamberti, C. *Chem. Soc. Rev.* 2010, *39*, 4885.

(54) Chavan, S.; Vitillo, J. G.; Uddin, M. J.; Bonino, F.; Lamberti, C.; Groppo, E.; Lillerud, K.-P.; Bordiga, S. *Chem. Mater.* 2010, *22*, 4602.

(55) Kandiah, M.; Nilsen, M. H.; Usseglio, S.; Jakobsen, S.; Olsbye, U.; Tilset, M.; Larabi, C.; Quadrelli, E. A.; Bonino, F.; Lillerud, K. P. *Chem. Mater.* 2010, *22*, 6632.

(56) Kandiah, M.; Usseglio, S.; Svelle, S.; Olsbye, U.; Lillerud, K. P.; Tilset, M. *J. Mater. Chem.* 2010, *20*, 9848.

(57) Valenzano, L.; Civalleri, B.; Chavan, S.; Bordiga, S.; Nilsen, M. H.; Jakobsen, S.; Lillerud, K. P.; Lamberti, C. *Chem. Mater.* 2011, *23*, 1700.

(58) Jakobsen, S.; Gianolio, D.; Wragg, D. S.; Nilsen, M. H.; Emerich, H.; Bordiga, S.; Lamberti, C.; Olsbye, U.; Tilset, M.; Lillerud, K. P. *Phys. Rev. B* 2012, *86*, 125429.

(59) Shearer, G.; Forselv, S.; Chavan, S.; Bordiga, S.; Mathisen, K.; Bjørgen, M.; Svelle, S.; Lillerud, K. *Top. Catal.* 2013, *56*, 770.

(60) Yaghi, O. M.; O'Keeffe, M.; Ockwig, N. W.; Chae, H. K.; Eddaoudi, M.; Kim, J. *Nature* 2003, *423*, 705.
(61) Wang, B.; Huang, H.; Lv, X.-L.; Xie, Y.; Li, M.; Li, J.-R. *Inorg. Chem.* 2014, *53*, 9254.
(62) Jasuja, H.; Walton, K. S. *The Journal of Physical Chemistry C* 2013, *117*, 7062.
(63) Brunel, J. M. *Chem. Rev.* 2005, *105*, 857.
(64) Ngo, H. L.; Hu, A.; Lin, W. *J. Mol. Catal. A: Chem.* 2004, *215*, 177.
(65) Morocco, A. P. *Critical Care Clinics* 2005, *21*, 691.
(66) Chow, H.-F.; Ng, M.-K. *Tetrahedron: Asymmetry* 1996, *7*, 2251.
(67) Tanaka, K.; Oda, S.; Nishihote, S.; Hirayama, D.; Urbanczyk-Lipkowska, Z. *Tetrahedron: Asymmetry* 2009, *20*, 2612.
(68) Shin, H. N. K., Chi Sik; Cho, Young Jun; Kwon, Hyuck Joo; Kim, Bong Ok; Kim, Sung Min; Yoon, Seung Soo *PCT Int. Appl. (2010), WO 2010114263 A2 20101007* 2010.
(69) Kim, J. I.; Schuster, G. B. *J. Am. Chem. Soc.* 1992, *114*, 9309.
(70) Meyers, A. I.; Lutomski, K. A. *J. Am. Chem. Soc.* 1982, *104*, 879.
(71) Hellwinkel, D.; Bohnet, S. *Chem. Ber.* 1987, *120*, 1151.
(72) Seki, M.; Yamada, S.-I.; Kuroda, T.; Imashiro, R.; Shimizu, T. *Synthesis* 2000, 1677.
(73) Bongui, J.-B.; Elomri, A.; Cahard, D.; Tillequin, F.; ccedil; ois; Pfeiffer, B.; Pierr; eacute; Alain; Seguin, E. *Chemical and Pharmaceutical Bulletin* 2005, *53*, 1540.
(74) Demir, A. S.; Reis, Ö. *Tetrahedron* 2004, *60*, 3803.
(75) de la Mare, P. B. D.; Newman, P. A. *Journal of the Chemical Society, Perkin Transactions 2* 1984, 231.
(76) http://science.csustan.edu/almy/3012/Sn1Sn2.htm.
(77) Diaz, C. J.; Haffner, C. D.; Speake, J. D.; Zhang, C.; Mills, W. Y.; Spearing, P. K.; Cowan, D. J.; Green, G. M.; Smithkline Beecham Corporation, USA . 2008, p 149pp.
(78) Nising, C. F.; Schmid, U. K.; Nieger, M.; Bräse, S. *The Journal of Organic Chemistry* 2004, *69*, 6830.
(79) Nelson, T. D.; Crouch, R. D. *Org. React. (Hoboken, NJ, U. S.)* 2004, *63*, No pp. given.
(80) Magano, J.; Dunetz, J. R. *Chem. Rev.* 2011, *111*, 2177.
(81) Kolotuchin, S. V.; Meyers, A. I. *The Journal of Organic Chemistry* 1999, *64*, 7921.
(82) Kürti, L.; Czakó, B. *Strategic Applications of Named Reactions in Organic Synthesis* Elsevier, 2005.
(83) Chen, H.; Luzy, J.-P.; Gresh, N.; Garbay, C. *Eur. J. Org. Chem.* 2006, *2006*, 2329.
(84) http://www.ilpi.com/msds/ref/ccl4.html.
(85) Wang, Z. *Comprehensive Organic Name Reactions and Reagents, 3 Volume Set*; Wiley-Interscience, 2009.
(86) Tang, J.; Zhu, J.; Shen, Z.; Zhang, Y. *Tetrahedron Lett.* 2007, *48*, 1919.
(87) Kulangiappar, K.; Anbu Kulandainathan, M.; Raju, T. *Ind. Eng. Chem. Res.* 2010, *49*, 6670.
(88) Pinto-Bazurco Mendieta, M. A. E.; Negri, M.; Hu, Q.; Hille, U. E.; Jagusch, C.; Jahn-Hoffmann, K.; Müller-Vieira, U.; Schmidt, D.; Lauterbach, T.; Hartmann, R. W. *Archiv der Pharmazie* 2008, *341*, 597.
(89) Matt, C.; Wagner, A.; Mioskowski, C. *The Journal of Organic Chemistry* 1997, *62*, 234.
(90) Suguro, Y.; Matsuda, H.; Mitsubishi Kasei Corp., Japan . 1992, p 4 pp.
(91) Park, B. R.; Kim, K. H.; Kim, T. H.; Kim, J. N. *Tetrahedron Lett.* 2011, *52*, 4405.
(92) Park, J. K.; Lee, K. H.; Park, J. S.; Seo, J. H.; Kim, Y. K.; Yoon, S. S. *Mol. Cryst. Liq. Cryst.* 2010, *531*, 55.
(93) Wu, N.; Li, X.; Xu, X.; Wang, Y.; Xu, Y.; Chen, X. *Lett. Org. Chem.* 2010, *7*, 11.
(94) Guo, W.; Faggi, E.; Sebastián, R. M.; Vallribera, A.; Pleixats, R.; Shafir, A. *The Journal of Organic Chemistry* 2013, *78*, 8169.
(95) Kelber, J.; Achard, M.-F.; Garreau-de Bonneval, B.; Bock, H. *Chem. Eur. J.* 2011, *17*, 8145.

(96) Stephens, C. E.; Patrick, D. A.; Chen, H.; Tidwell, R. R.; Boykin, D. W. *Journal of Labelled Compounds and Radiopharmaceuticals* 2001, *44*, 197.

(97) Maligres, P. E.; Waters, M. S.; Fleitz, F.; Askin, D. *Tetrahedron Lett.* 1999, *40*, 8193.

(98) Sundermeier, M.; Zapf, A.; Beller, M.; Sans, J. *Tetrahedron Lett.* 2001, *42*, 6707.

(99) Smith, M. B. *March's Advanced Organic Chemistry : Reactions, Mechanisms, and Structure.*; 7th ed.; John Wiley & Sons, 2013.

(100) Chen, J.-C.; Chiang, C.-J.; Liu, Y.-C. *Synthetic Metals* 2010, *160*, 1953.

(101) Liu, H.; Kondo, S.-i.; Takeda, N.; Unno, M. *J. Am. Chem. Soc.* 2008, *130*, 10074.

(102) Hohlweg, M.; Schmidt, H. W. *Makromol. Chem.* 1989, *190*, 1587.

(103) Bret, G.; Harling, S. J.; Herbal, K.; Langlade, N.; Loft, M.; Negus, A.; Sanganee, M.; Shanahan, S.; Strachan, J. B.; Turner, P. G.; Whiting, M. P. *Org. Process Res. Dev.* 2011, *15*, 112.

(104) Cramer, J. R.; Ning, Y.; Shen, C.; Nuermaimaiti, A.; Besenbacher, F.; Linderoth, T. R.; Gothelf, K. V. *Eur. J. Org. Chem.* 2013, *2013*, 2813.

(105) Viswanathan, G. S.; Wang, M.; Li, C.-J. *Angew. Chem., Int. Ed.* 2002, *41*, 2138.

(106) Faggi, E.; Sebastián, R. M.; Pleixats, R.; Vallribera, A.; Shafir, A.; Rodríguez-Gimeno, A.; Ramírez de Arellano, C. *J. Am. Chem. Soc.* 2010, *132*, 17980.